VILNIUS UNIVERSITY
CENTER FOR PHYSICAL SCIENCES AND TECHNOLOGY

Abdullah Khan

Assessment of Human Exposure to Traffic-Related Microplastics and Black Carbon in Urban Microenvironments

DOCTORAL DISSERTATION

Natural Sciences,
Physics (N 002)

VILNIUS 2025

The dissertation was prepared between 2021 and 2025 at the SRI Center for Physical Sciences and Technology.

Academic supervisor – Dr. Steigvilė Byčenkienė (Center for Physical Sciences and Technology; Natural Sciences, Physics - N 002).

This doctoral dissertation will be defended in a public meeting of the Dissertation Defense Panel:

Chairperson – Dr. Galina Lujanienė (Center for Physical Sciences and Technology; Natural Sciences, Physics - N 002),

Members:

Dr. Rita Plukienė (Center for Physical Sciences and Technology; Natural Sciences; Physics - N 002),

Assoc. Prof. Dr. Vaida Šerevičienė (Vilnius Gediminas Technical University; Technological Sciences, Environmental Engineering - T 004),

Assoc. Prof. Dr. Vaida Vasiliauskienė (Vilnius Gediminas Technical University; Natural Sciences, Physics - N 002),

Prof. Dr. Tareq Hussein (University of Helsinki / University of Jordan; Natural Sciences, Physics - N 002).

The dissertation will be defended at a public/closed meeting of the Dissertation Defense Panel at 11 a.m. on September 18, 2025, in meeting room D401 at the Center for Physical Sciences and Technology.

Address: Saulėtekio av. 3, Room No. D401, Vilnius, Lithuania.
Tel.+37052648884; e-mail: office@ftmc.lt

The text of this dissertation can be accessed at the libraries of Vilnius University, as well as on the website of Vilnius University:
https://www.vu.lt/naujienos/ivykiu-kalendorius

VILNIAUS UNIVERSITETAS
FIZINIŲ IR TECHNOLOGIJOS MOKSLŲ CENTRAS

Abdullah Khan

Transporto sukeliamo oro užterštumo mikroplastiku ir juodąja anglimi poveikio žmogui vertinimas miesto mikroaplinkose

DAKTARO DISERTACIJA

Gamtos mokslai,
Fizika (N 002)

VILNIUS 2025

Disertacija rengta 2021-2025 metais VMTI Fizinių ir technologijos mokslų centre.

Mokslinė vadovė – dr. Steigvilė Byčenkienė (Fizinių ir technologijos mokslų centras; gamtos mokslai, fizika – N 002).

Gynimo taryba:

Pirmininkė – dr. Galina Lujanienė (Fizinių ir technologijos mokslų centras; gamtos mokslai, fizika – N 002).

Nariai:

dr. Rita Plukienė (Fizinių ir technologijos mokslų centras; gamtos mokslai, fizika – N 002),

doc. dr. Vaida Vasiliauskienė (Vilniaus Gedimino technikos universitetas; gamtos mokslai, fizika – N 002),

doc. dr. Vaida Šerevičienė (Vilniaus Gedimino technikos universitetas; technologijos mokslai, aplinkos inžinerija – T 004),

prof. dr. Tareq Hussein (Helsinkio universitetas / Jordanijos universitetas; gamtos mokslai, fizika – N 002).

Disertacija ginama viešame Gynimo tarybos posėdyje 2025 m. rugsėjo mėn. 18 d. 11:00 val. Fizinių ir technologijos mokslų centro auditorijoje D401.

Adresas: Saulėtekio al. 3, D401,Vilnius, Lietuva.
Tel. +37052648884 ; el. paštas office@ftmc.lt

Disertaciją galima peržiūrėti VU bibliotekoje ir VU interneto svetainėje adresu: *https://www.vu.lt/naujienos/ivykiu-kalendorius*

CONTENTS

ABBREVIATIONS

μ-FTIR	Micro-Fourier Transform Infrared Spectrometer
AAQD	European Union's Ambient Air Quality Directive
APS	Aerodynamic Particle Sizer
BC	Black Carbon
BCe	Equivalent Black Carbon
COPD	Chronic Obstructive Pulmonary Disease
CPC	Condensation Particle Counter
DMA	Differential Mobility Analyzer
Dp	Particle Diameter
DPF	Diesel Particulate Filters
EC	Elemental Carbon
ESP	Electrostatic Precipitators
FTMC	Centre for Physical Sciences and Technology
UGI	Urban Green Infrastructure
GPF	Gasoline Particulate Filters
HEPA	High-efficiency Particulate Air
HVAC	Heating, Ventilation, and Air Conditioning
MERV-13	Minimum Efficiency Reporting Value filters
VOCs	Volatile organic compounds
WHO	World Health Organization
MPs	Microplastics
NAAQS	National Ambient Air Quality Standards
NPF	New Particle Formation
OC	Organic Carbon
PAHs	Polycyclic Aromatic Hydrocarbons
PM	Particulate Matter
PNC	Particle Number Concentration
SMPS™	Scanning Mobility Particle Sizer™
TEM	Transmission Electron Microscopy Analysis
ToF	Time-of-Flight
TWP	Tire Wear Particle
TWRP	Tire Wear Road Wear Particle

U.S. EPA	US Environmental Protection Agency
UFPs	Ultrafine particles
IAQ	Indoor Air Quality
MPPD	Multiple Path Particle Dosimetry Model
HRT	Human Respiratory Tract
URT	Upper Respiratory Tract
TB	Tracheobronchial Region
AL	Alveolar Region
IRI	Inhalation Risk Index
TV	Tidal Volume
BF	Breathing Frequency
GSD	Geometric Standard Deviation
MDD	Minute Deposition Dose
IR	Inhalation Rate

INTRODUCTION

Relevance

Air pollution is a leading environmental health threat, with particulate matter (PM) a major contributor to respiratory and cardiovascular diseases (de Bont et al., 2022). It is estimated that seven million premature deaths occur each year due to air pollution (Chen et al., 2024). A key driver of this global health burden is the deteriorating air quality conditions in urban areas, where approximately 90 % of the population is exposed to pollutant concentrations that exceed the air quality guidelines set by the World Health Organization (WHO) (Chen et al., 2024; Karthick Raja Namasivayam et al., 2024). In urban environments, particulate pollution arises from various sources, broadly categorized into exhaust and non-exhaust emissions. Exhaust emissions like black carbon (BC) are primarily produced through the incomplete combustion of fossil fuels and biomass burning, affecting the global climate by absorbing solar radiation and having profound health implications (Chowdhury et al., 2022; Sharma et al., 2024). In contrast, non-exhaust emissions include particles generated from brake wear, tire abrasion, road surface erosion, and the resuspension of road dust (Baensch-Baltruschat et al., 2020). These particles are increasingly recognized as airborne microplastics (MPs) due to their synthetic polymer composition, smaller size, and environmental durability (Sangkham et al., 2022). Airborne MPs are of particular concern due to the potential inhalation, which can lead to serious health issues like respiratory diseases and neurological symptoms (Winiarska et al., 2024). It is estimated that approximately six million tons of MPs from tire wear and road wear infiltrate the urban atmosphere annually, positioning this source as one of the most significant contributors of airborne MPs pollution in urban environments (Lee et al., 2024; Liao et al., 2021).

Ambient air quality assessments rely on fixed-site or background monitoring stations to estimate population exposure. However, fixed-site measures often fail to capture the dynamics of personal exposure

in different microenvironments. Because the air pollution levels in these microenvironments can vary substantially over short temporal and spatial distances. Therefore, individuals are not uniformly exposed to ambient concentrations; instead, their inhaled dose is influenced by proximity to emission sources, duration of exposure, and the time spent in specific microenvironments. Urban residents typically spend almost 90 % of their daily time in indoor spaces, with an additional 4–7 % in the vehicle microenvironments (Matz et al., 2018). Despite their significance, these microenvironments are frequently underrepresented in health risk exposure studies, which often rely on background monitoring data or temporally averaged metrics that fail to reflect the high variability in personal exposure.

Urban Green Infrastructure (UGI) has attracted considerable attention as a promising tool for mitigating air pollution, especially in densely populated urban areas with high traffic volumes (Kwak et al., 2019). UGIs such as green walls, street trees, and roadside hedges are advocated for their ability to improve air quality by trapping PM, reducing pollutant dispersion, and enhancing microclimatic conditions (Lafortezza et al., 2018). Despite increasing interest in UGI, its effectiveness in lowering individual exposure to PM remains underrepresented, particularly from non-exhaust sources. Moreover, the ability of UGI to filter or disperse PM of varying sizes and shapes is still insufficiently studied, with some evidence suggesting that its benefits may be limited or context-dependent. Given the growing significance of non-exhaust emissions in urban environments, evaluating the effectiveness of UGI in addressing both exhaust and non-exhaust particulate exposure represents a critical gap for further research.

Problem formulation

Substantial research has been conducted on PM exposure in urban environments, and several critical gaps remain in the current understanding of personal exposure dynamics. First, there is limited integration of the dual contributions of exhaust and non-exhaust

emissions to urban particulate pollution. Many studies focus on exhaust emissions, neglecting non-exhaust emission sources such as brake wear, tire wear, and road dust. Which is becoming an increasingly significant source as vehicle fleets transition to cleaner technologies. Second, most exposure assessments continue to rely on ambient air quality monitoring or broad-scale exposure estimates, which fail to account for the spatial and temporal variability in personal exposure due to factors such as proximity to roadside hotspots and individual mobility patterns through different microenvironments. Third, the effectiveness of UGI in mitigating PM exposure, especially in the context of non-exhaust emissions, is still under-explored, despite its potential to reduce pollution from exhaust emissions. This study seeks to bridge these gaps by considering both exhaust and non-exhaust emission sources, integrating personal exposure data across various urban microenvironments, and evaluating the role of UGI as a sustainable, nature-based pollution mitigation strategy.

The Main Study Aim

This study aims to investigate personal exposure to particulate pollution from traffic-related exhaust and non-exhaust sources in urban environments.

It will focus on roadside emission hotspots, the mitigation role of UGI, and daily activity patterns, specifically during commuting and office hours.

Tasks

1. To evaluate the abundance and characteristics of MPs near the busy street, identifying potential sources that contribute to non-exhaust particulate pollution.
2. To evaluate the effectiveness of UGI in mitigating airborne MP pollution and reducing personal exposure.
3. To assess personal exposure to exhaust-derived BC and PM during daily activities, focusing on commuting and time spent in a mechanically ventilated, energy-efficient office building.

Scientific Novelty

This is the first study to provide direct, seasonally and spatially resolved field evidence of traffic-related airborne MP capture by UGI in Northern Europe. By evaluating a *Thuja occidentalis* hedge near a busy street, the study quantifies the real-time mitigation potential of non-exhaust MPs—an overlooked but critical aspect of urban air pollution management.

Defensive Statements

1. The airborne MPs near urban roads are mainly fragment-shaped, black, and primarily composed of polyethylene. Seasonal factors and proximity to non-exhaust traffic emissions significantly affect their abundance and distribution.
2. The effectiveness of *Thuja occidentalis* in mitigating non-exhaust airborne MPs is seasonally dependent and size-selective, with higher removal efficiencies observed for fragment-shaped particles and MPs in the 50–100 µm range.
3. In urban environments, commuting, which usually accounts for less than 10 % of daily time, contributes up to 80 % of an individual's total daily exposure to PMs.
4. Vehicular exhaust is recognized as the primary source of BC during commuting, representing 66 % of the total BC mass and significantly contributing to increased pulmonary deposition doses, especially during peak morning traffic hours.

Author Contribution

The author of this work actively took part in the mobile measurement campaign in Vilnius. The author handled data processing, formal analysis, validation, and visualization, preparing the original manuscript, submitting the findings to a scientific journal, and presenting the scientific results at national and international conferences.

List of Publications

1) Khan, A., Araminienė, V., Uogintė, I., Varnagirytė-Kabašinskienė, I., Černiauskas, V., Gudynaitė-Franckevičienė, V., ... & Byčenkienė, S. (2025). Evaluating the role of urban green infrastructure in combating traffic-related microplastic pollution. *Science of The Total Environment*, *983*, 179688; https://doi.org/10.1016/j.scitotenv.2025.179688.

2) Khan, A., Davulienė, L., Šemčuk, S., Kandrotaitė, K., Minderytė, A., Davtalab, M., ... & Byčenkienė, S. (2024). Integrated personal exposure and deposition of black carbon on human lungs. Air Quality, Atmosphere & Health, 17(1), 35-50; https://doi.org/10.1007/s11869-023-01428-8.

3) Davulienė, L., Khan, A., Šemčuk, S., Minderytė, A., Davtalab, M., Kandrotaitė, K., ... & Byčenkienė, S. (2022). Evaluation of work-related personal exposure to aerosol particles. Toxics, 10(7), 405; https://doi.org/10.3390/toxics10070405.

4) Byčenkienė, S., Khan, A., & Bimbaitė, V. (2022). Impact of $PM_{2.5}$ and PM_{10} emissions on changes of their concentration levels in Lithuania: A case study. Atmosphere, 13(11), 1793; https://doi.org/10.3390/atmos13111793.

Other Publications

1. Byčenkienė, S., Gill, T., Khan, A., Kalinauskaitė, A., Ulevicius, V., & Plauškaitė, K. (2023).Estimation of carbonaceous aerosol sources under extremely cold weather conditions in an urban environment. Atmosphere, 14(2),310; https://doi.org/10.3390/atmos14020310.

2. Afzaal, M., Mazhar, I., Rasheed, R., Sharif, F., Khan, W. U. D., Bashir, N., ... & Khan, A. (2022). Industrial chemicals as micropollutants in the environment. In Environmental Micropollutants (pp. 13-44). Elsevier; https://doi.org/10.1016/B978-0-323-90555-8.00003-9.

List of Conferences

1. Khan, A., Araminienė, V., Uogintė, I., Varnagirytė-Kabašinskienė, I., Černiauskas, V., Gudynaitė-Franckevičienė, V., Džiugys, A., Davulienė, L., Misiulis, E., Davtalab, M., Byčenkienė, S., Where Microplastics Meet Pedestrians: Evaluating green infrastructures' role in reducing transport-related pollution, 68th International Conference Open Readings, May 13–16, 2025, Vilnius, Lithuania (Oral).

2. Khan, A., Araminienė, V., Uogintė, I., Davulienė, L., Burbulytė, A., Varnagirytė-Kabašinskienė, I., Černiauskas, V., Gudynaitė-Franckevičienė, V., Džiugys, A., Misiulis, E., Davtalab, M., Byčenkienė, S., Integrating green infrastructure to address microplastic pollution in urban areas, 15th FTMC Annual Scientific Conference, March 20–21, 2025, Vilnius, Lithuania (Oral).

3. Khan, A., Araminienė, V., Uogintė, I., Davulienė, L., Burbulytė, A., Varnagirytė-Kabašinskienė, I., Černiauskas, V., Gudynaitė-Franckevičienė, V., Džiugys, A., Misiulis, E., Byčenkienė, S., The role and potential of green infrastructure in filtering transport-generated microplastics, 14th FizTech, October 15–17, 2024, Vilnius, Lithuania (Oral).

4. Khan, A., Araminienė, V., Uogintė, I., Davulienė, L., Varnagirytė-Kabašinskienė, I., Gudynaitė-Franckevičienė, V., Džiugys, A., Misiulis, E., Byčenkienė, S., Mitigating transport-induced microplastics through green infrastructure: A sustainable solution, European Aerosol Conference (EAC 2024), August 25–30, 2024, Tampere, Finland (Poster).

5. Khan, A., Araminienė, V., Uogintė, I., Davulienė, L., Varnagirytė-Kabašinskienė, I., Gudynaitė-Franckevičienė, V., Džiugys, A., Misiulis, E., Byčenkienė, S., Evaluating the role of green infrastructure in reducing transport-related microplastics for strengthening urban environmental health,

67th International Conference Open Readings, April 23–26, 2024, Vilnius, Lithuania (Poster).

6. Khan, A., Davulienė, L., Šemčuk, S., Kandrotaitė, K., Minderytė, A., Davtalab, M., Uogintė, I, Skapas, M., Dudoitis, V., Byčenkienė, S., Integrated personal exposure and deposition of black carbon on human lungs, 13th FizTech, October 18–19, 2023, Vilnius, Lithuania (Oral).

7. Khan, A., Davulienė, L., Šemčuk, S., Kandrotaitė, K., Minderytė, A., Davtalab, M., Uogintė, I., Skapas, M., Dudoitis, V., Byčenkienė, S., Personal exposure to black carbon and its deposition on human lungs in different micro-environments, during commuting and in the office, European Aerosol Conference (EAC 2023), September 3–8, 2023, Malaga, Spain (Poster).

8. Khan, A., Davulienė, L., Šemčuk, S., Kandrotaitė, K., Minderytė, A., Davtalab, M., Uogintė, I., Skapas, M., Dudoitis, V., Pauraitė, J., Garbarienė, I., Byčenkienė, S., Personal exposure and deposition of black carbon on human lungs in Vilnius, Lithuania, Open Readings 2023, April 18–21, 2023, Vilnius, Lithuania (Poster).

9. Khan, A., Davulienė, L., Šemčuk, S., Kandrotaitė, K., Minderytė, A., Davtalab, M., Uogintė, I., Skapas, M., Dudoitis, V., Pauraitė, J., Garbarienė, I., Byčenkienė, S., Lung deposition and personal exposure to black carbon during commuting and in the office, NOSA Symposium, March 13–15, 2023, Oslo Science Park, Norway (Oral).

10. Khan, A., Davulienė, L., Šemčuk, S., Kandrotaitė, K., Minderytė, A., Davtalab, M., Uogintė, I., Skapas, M., Dudoitis, V., Pauraitė, J., Garbarienė, I., Byčenkienė, S., Personal exposure and deposition of black carbon on human lungs, 12th FizTech, October 19–20, 2022, Vilnius, Lithuania (Poster).

11. Khan, A., Davulienė, L., Šemčuk, S., Kandrotaitė, K., Minderytė, A., Davtalab, M., Uogintė, I., Dudoitis, V., Skapas,

M., Pauritė, J., Garbarienė, I., Andriejauskienė, J., Byčenkienė, S., Concentration and source apportionment of black carbon in various microenvironments, Vilnius, Lithuania, 11th International Aerosol Conference (IAC 2022), September 4–9, 2022, Athens, Greece (Poster).

12. Khan, A., Afzaal, M., Byčenkienė, S., Gill, T., Bilal, M., Concentrations of airborne PM_{10} and bounded lead in major bus terminals of Lahore and Peshawar, Pakistan, 65th International Conference Open Readings, March 15–18, 2022, Vilnius, Lithuania (Poster).

1. LITERATURE REVIEW

The literature review examines current knowledge on the sources, characteristics, and health impacts of both exhaust and non-exhaust particulate pollution. Atmospheric aerosols are complex mixtures of solid and liquid particles suspended in the air, originating from a range of natural and anthropogenic sources. Among these, BC and airborne MPs have emerged as significant contributors to urban particulate pollution, representing two distinct yet complementary facets of aerosol science.

1.1 Airborne particulate matter

Airborne PM constitutes a substantial portion of the atmospheric aerosol particles, which differ in size, composition, sources, and can arise from both exhaust and non-exhaust emissions (Fussell et al., 2022). Exhaust emissions primarily result from the incomplete combustion of fossil fuels in transportation and industrial processes, generating fine particles such as BC, which are strongly associated with adverse health and climate effects (Nawab et al., 2024). In contrast, non-exhaust emissions are generated from mechanical processes, including tire wear, brake wear, and the resuspension of road dust. These particles are identified as airborne MPs—synthetic polymer particles produced from the friction between the road surface and the tire (Z. Gao et al., 2022). Airborne MPs fall under the category of non-exhaust PM, contribute to the complexity of urban aerosols, and pose a growing concern due to their persistence, inhalation potential, and uncertain long-term health effects (Gehrke et al., 2023).

BC represents a significant portion of fine PM ($PM_{2.5}$) and poses serious health risks, including premature mortality, alongside environmental effects such as global climate warming (Chowdhury et al., 2022; Eklund et al., 2014; Sharma et al., 2024). BC is a collective term encompassing a wider range of carbonaceous aerosols produced by incomplete combustion, ranging from charred plant residues (CPRS) to well-graphitized soot. Unlike carbon black (CB), BC lacks

a universally accepted chemical definition and may be referred to as soot, elemental carbon, or graphitic carbon. Different definitions are employed, some based on chemical and physical properties (e.g., light absorption) and others on measurement techniques (Janssen et al., 2011). In 2001, (Watson & Valberg, 2001) define BC as "soot carbon" and "an impure form of near-elemental carbon with a graphite-like structure, produced in flaming combustion and internal combustion engines". Equivalent black carbon (eBC) is "the quantity of strongly light-absorbing carbon with the exact optical properties of soot carbon that would produce the same signal in an optical instrument (e.g., the aethalometer) as the sample". In its recently published report to Congress on BC, BC is the "carbonaceous fraction of PM that absorbs all wavelengths of solar radiation" (and hence the appropriateness of the name "black") (Watson & Valberg, 2001).

MPs have been recognized as emerging pollutants in recent years due to their widespread presence in various environmental compartments. These synthetic polymer particles of 1 µm to 5 mm sizes are released into the environment through multiple pathways (Sridharan et al., 2021). MP can be found in various ecosystems like water, soil, and air. However, their occurrence in urban environments has severe public health implications, especially where there are extensive traffic emissions. TWPs are among the prime sources of MPs in the atmosphere and contribute significantly to urban pollution. TWPs are typically dark or black rod-like particles with a diameter of less than 1 µm to over 100 µm, and therefore can be suspended in the atmosphere for a longer time (Wagner et al., 2018).

Understanding the relationship between exhaust and non-exhaust contributions to airborne particulate pollution is essential for comprehensive air quality assessment and mitigation strategies. As climate change, urbanization, and industrialization increased, particulate pollution has become a primary environmental and health concern with worldwide implications (Khomenko et al., 2021). While some PM, such as sulfate particles, cool the air, others, such as BC,

add to global warming as they absorb solar radiation (Cai et al., 2019). Nonetheless, apart from their role in the earth's energy balance, aerosols pose a risk to human health. Fine and ultrafine particles enter the respiratory tract, depositing along airways and even entering the bloodstream, where they cause inflammatory responses linked to respiratory disease, cardiovascular disease, and systemic oxidative stress (Schraufnagel, 2020). In densely urban areas with high pollution burdens, exposure to PM exacerbates morbidity and mortality, particularly affecting vulnerable populations. While scientists and policymakers turn to sustainable solutions in air regulation, understanding the complex relationship between aerosol dynamics and human exposure is the priority. In a time defined by environmental health crises, particulate pollution response is a scientific and global obligation.

1.1.1. Definition and classification of PM

The U.S. Environmental Protection Agency (EPA) classifies PM among the six criteria air pollutants that are regulated under the Clean Air Act's National Ambient Air Quality Standards (NAAQS) (Johnson & Graham, 2005). PM is a heterogeneous mixture of solid particles and liquid droplets that can be suspended in the air for long periods, affecting the global and regional climate patterns, and is a major contributor to the global disease burden (Khomenko et al., 2021).

PM is primarily classified based on its aerodynamic diameter into several classes: nanoparticles (<50 nm), ultrafine particles (<100 nm), fine particles (<1.0 μm), and coarse particles (1.0 μm –100 μm). Ultrafine particles are further classified into nucleation mode (below 30 nm) and Aitken mode (30 nm to 100 nm) (Toledano et al., 2009). PM can further be classified based on chemical makeup, i.e., a wide range of organic (e.g., polycyclic aromatic hydrocarbons (PAHs), volatile organic compounds (VOCs), e.g., metals, nitrates, sulfates, carbonaceous particles, and biological (e.g., pollen, bacteria, fungal) matter (Toledano et al., 2009). Based on the source composition, e.g.,

anthropogenic and natural. Anthropogenic sources are primarily due to human activities, such as transportation emissions (e.g., automobiles), industrial activities (e.g., manufacturing, construction), power generation, biomass burning (e.g., wood, agricultural residues), and waste burning. Emissions from anthropogenic sources significantly contribute to urban air pollution (Wong et al., 2022). On the other hand, natural sources consist of wildfires, which release a great deal of PM into the atmosphere; dust storms, common in arid regions; and volcanic eruptions, which release fine ash particles into the atmosphere. Even though natural sources contribute to periodic air pollution events, anthropogenic sources are the main contributors to high and persistent PM levels in urban areas (Zhang et al., 2021). PMs are released into the air in two ways: they may be directly emitted (primary) or formed from gas-to-particle conversion processes (secondary). Secondary particles form from processes involving nucleation, condensation, and chemical processes on surfaces or in liquid phases. Nucleation mode aerosols are most likely to form through homogeneous nucleation, when gases condense onto tiny particles (Calvo et al., 2013; Nie et al., 2025). In contrast, Aitken and accumulation mode particles develop as these freshly formed particles collide, merge (coagulate), and grow further through condensation. Ultrafine particles can also enter the atmosphere directly from combustion sources like fossil fuel and biomass burning, coal combustion (Yli-Juuti et al., 2011). Secondary formation processes involving sulfur and nitrogen oxides produce ammonium nitrate and sulfate in the particle phase. At the same time, oxidation of organic gaseous precursors also contributes to particle formation. Coarse particles are primarily produced by mechanical processes like the resuspension of particles due to winds blowing over the surface, sea spray, volcanic eruptions, and other natural emissions (Nie et al., 2025).

PM lifetime and size distribution depend on the meteorological conditions lasting from a few days to weeks in the atmospheric boundary layer. PM undergoes various physical and chemical

processes during dispersion in the atmosphere, where it comes into contact with atmospheric gases, water vapor, and other particles. The process is called aerosol aging. Aging of aerosols can influence particle size distribution, chemical composition, and characteristics, which will impact their transport, deposition, and possible health impacts (Riemer et al., 2010). There are two main removal mechanisms of PM from the air: wet and dry deposition. Wet deposition is the most significant sink for atmospheric aerosol particles, where particles are washed out by precipitation and removed by clouds, while larger particles settle and deposit under the effect of gravity, called dry deposition, which is less significant on a global scale (Liu et al., 2024). Particles in larger sizes sink more quickly, while finer particles can remain suspended for longer time frames, even days to weeks. Wet removal mechanisms (e.g., precipitation) and dry deposition (e.g., gravity settling) purify the air but will not remove fine and ultrafine particles from the atmosphere completely (Speak et al., 2012) (Fig. 1).
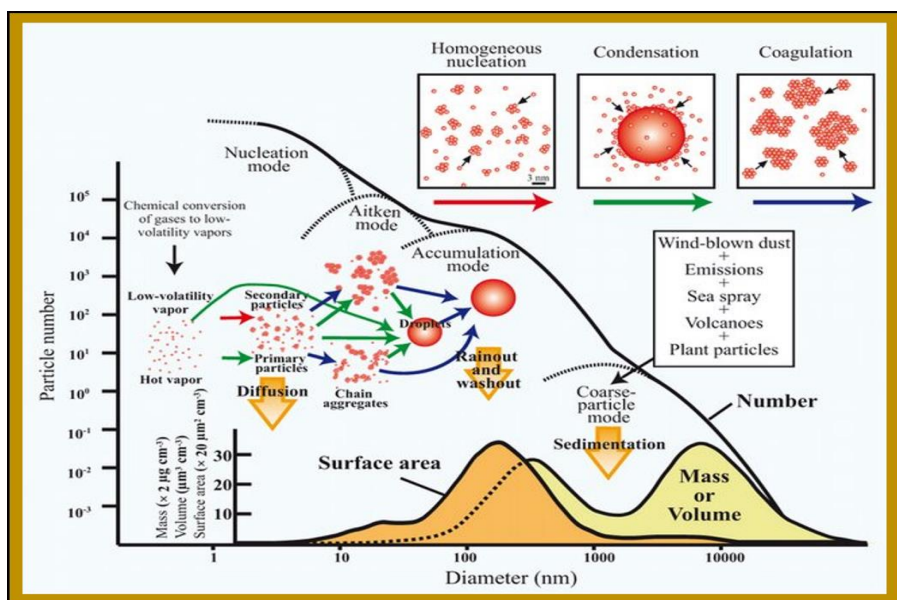
Fig. 1. Schematic representation of atmospheric aerosol size distribution, sources, formation mechanisms, and removal processes across different modes.

24

1.1.2. Overview of exhaust and non-exhaust emission sources of PM

1.1.2.1. Exhaust emission sources

Exhaust emission sources are primarily the result of combustion processes in engines, power plants, and industrial facilities. These sources release fine PM that includes BC, organic carbon (OC), heavy metals, and other pollutants (Palle et al., 2021). The main exhaust sources include vehicular emissions: road traffic, particularly diesel vehicles, is a major source of fine particles. Industrial combustion: power plants, industrial boilers, and factories release fine PM while burning fossil fuels. Residential heating: wood stoves, fireplaces, and coal furnaces in homes contribute to particulate pollution, especially in colder months. Exhaust emissions tend to produce fine particles ($PM_{2.5}$ and $PM_{0.1}$) that are small enough to be inhaled deeply into the lungs, contributing to significant health risks, including respiratory diseases, cardiovascular diseases, and cancer (Sharma et al., 2024).

Among the exhaust emission sources, BC is one of the most significant pollutants because of its smaller size and potential for negative health impacts. BC in rural and urban ambient air originates from various anthropogenic and natural sources, often forming a complex mixture of materials. Anthropogenic sources include (stationary and mobile) diesel and gasoline engines (especially older diesel engines), fossil fuel-based power plants, industrial and commercial boilers, and residential heating systems such as oil furnaces, fireplaces, and woodstoves in developed countries. In developing countries, simple cookstoves and open fires contribute significantly. Additionally, biomass burning from agricultural activities and forest fires also releases BC into the atmosphere (Janssen et al., 2011; Long et al., 2013). In many developed countries, BC emissions from both mobile and stationary sources are declining due to stricter engine emission standards, the use of cleaner fuels, and $PM_{2.5}$ control technologies like fabric filters, electrostatic precipitators, and diesel particulate filters (Butt et al., 2017).

1.1.2.2. Non-exhaust emission sources

Non-exhaust emission sources of particulate pollution are primarily generated from the abrasion between tires and road surfaces (Ly & El-Sayegh, 2023). Non-exhaust emissions, especially traffic-related MPs, contribute significantly to urban air pollution. While emission regulations have reduced exhaust pollutants, non-exhaust sources remain a significant challenge. Other sources, like urban construction activities, also contribute to non-exhaust particulate emissions (Luo et al., 2022). Primary MPs are manufactured for commerce in cosmetics, personal care products, and biomedical applications. These include microbeads found in exfoliating products and MP additives in industrial operations. Secondary MPs are derived from the fragmentation and breakdown of bigger plastic materials via mechanical abrasion, photodegradation, oxidative processes, and biological degradation (Sridharan et al., 2021).

The degradation of vehicle tires through friction between the road surface and vehicle tires generates smaller particles called tire wear particles (TWPs), which contribute significantly to urban PM pollution. The most prevalent airborne MP source in urban environments is tire and road wear particles (TRWPs), which result from tire wear and roadside dust. Tire wear particles (TWPs), a sub-fraction of TRWPs, are made of synthetic rubber and other polymer additives. TWPs are dispersed in the environment through wind activities, traffic behaviors, and deposition processes in the atmosphere (Ly & El-Sayegh, 2023; Sommer et al., 2018). The global road traffic has been estimated to contribute approximately 6 million metric tons of TRWPs annually. The United States accounted for about 1.120 million metric tons of TWPs in 2010, and Europe accounted for an estimated 1.327 million metric tons in 2014. Current studies have indicated that TRWPs contribute 0.8 % to 8.5 % of $PM_{2.5}$ and around 10 % of PM_{10} in the atmosphere, making them one of the major contributors to PM (Gehrke et al., 2023; González-Flórez et al., 2023).

1.2. Health and environmental impacts of particulate pollution

1.2.1. Health effects of BC and MPs

Air pollution is responsible for approximately 7 million deaths annually from both indoor and outdoor (Khomenko et al., 2021). Poor air in urban environments is a major contributor to these deaths, where nearly 9 out of every 10 people living in areas that fail to meet WHO air quality guidelines (Shaddick et al., 2020). Particulate air pollution is a critical public health concern, particularly in enclosed environments like buildings and transport. Fine particle exposure, particularly with a diameter less than 2.5 µm, permeates our blood, lungs, and even organs and triggers a series of long-term illnesses from COPD and asthma to heart disease and premature death (Oliveira et al., 2019). With every breath we inhale, in bad air, polluted by transportation and industrial emissions, we expose ourselves to the harmful effects of toxic pollutants in the air (Salma et al., 2015).

BC particles occur predominantly in the fine and ultrafine fractions, which average between the $PM_{2.5}$ (≤ 2.5 µm) and the $PM_{0.1}$ (≤ 100 nm) size fractions and therefore are inhalable and penetrate deep within the human respiratory system. BC's particle size distribution and chemical composition are influenced by combustion and fuel; ultrafine particles of BC are produced during biomass burning and diesel combustion, and larger aggregates are produced via industrial processing and coal combustion (Chauhan et al., 2024). In addition, BC distribution can also be affected by its ability to coagulate with other aerosols. BC is purely composed of elemental carbon (EC); in rare cases, it may also have organic carbon (OC), ions, and trace metals such as lead, arsenic, and cadmium (Abdel-Shafy & Mansour, 2016; Johansson et al., 2016). Since the structure is porous and the surface area is larger, BC is an efficient carrier of toxic chemicals such as polycyclic aromatic hydrocarbons (PAHs) and heavy metals, which are adsorbed at the surface of BC. Their presence in BC is of concern in particular, since these compounds are mutagenic and carcinogenic, and can additionally increase the toxicity of BC (Niranjan & Thakur,

2017). Studies have indicated that BC can adsorb enormous amounts of up to 80 %–90 % of PAHs and PCBs from the atmosphere, leading to prolonged environmental and health effects (Brugge et al., 2007). BC is not just a single pollutant but also a carrier of toxic materials, which adds to its overall toxicity. Exposure to BC is well established in epidemiological research, contributing to respiratory, cardiovascular, and systemic impacts. Given its nanometer size, BC can penetrate the alveolar region of the lungs and induce oxidative stress and inflammatory processes by forming reactive oxygen species (ROS) (Bouza et al., 2022; Brugge et al., 2007). Chronic exposure has been implicated in asthma, bronchitis, lung cancer, and the risk of cardiovascular disease (Faria et al., 2022). To determine such risks, the WHO classified diesel exhaust as carcinogenic in 2012, and the European Union has subsequently advocated an airborne BC public health standard. Research has established that BC reduction could provide more significant health benefits than $PM_{2.5}$ reduction, with the evidence suggesting that a reduction in BC by one unit would extend life by four to nine times more than a similar reduction in $PM_{2.5}$ (Oxley et al., 2015). BC remains a global concern, combining public health risks with environmental and global climate concerns. Its ability to infiltrate deep into the respiratory system and carry harmful pollutants enhances its impact, disproportionately affecting urban populations and vulnerable subgroups. While control technologies and technologies have reduced emissions in some sectors, biomass combustion, wildfires, and incomplete combustion persist. Reduction of BC pollution must occur synergistically—coupling air quality improvement, public health interventions, and climate change mitigation efforts—to derive lasting benefits for humans and the environment.

Airborne MPs are an emerging contaminant and have various pathways of entering the human body, including inhalation, oral consumption of MPs through food and water, and dermal exposure. Among these direct exposure pathways, inhalation can be harmful to

our lung health (Nawab et al., 2024). The toxicological potential of airborne MPs relies on their physicochemical properties, such as size, shape, and polymer type. Due to their increased surface area-to-volume ratio, nanoparticles are more reactive and thus impose a larger impact on biological systems as they can penetrate deeper into our lungs (Salma et al., 2015). The biological activity of MPs also mainly depends on their shape. Microfibers, which are typically found in synthetic textiles and tire tread wear, can be deposited in the human respiratory or gastrointestinal tract for a long time and can even lead to inflammation (Ozdemir, 2019). Research has determined that chronic exposure to airborne MPs via inhalation has been linked with lung inflammation, oxidative stress, and cellular damage. Besides, MPs have also been suggested as possible vectors of heavy metals, harmful chemicals, and POPs that have the capability of increasing the potential for causing damage to human health (Abdel-Shafy & Mansour, 2016; Nawab et al., 2024). People who live in urban centers, especially near busy roads, are more vulnerable to the high concentration of MPs. Chronic respiratory exposure to airborne MPs has been linked to most of the studies with adverse respiratory effects, such as impaired lung function and increased susceptibility to respiratory infections (Torres-Agullo et al., 2021).

Despite the improvements brought about by technology in emission control devices and initiatives to restrict ambient air pollution, the fight against PM is far from over. Stricter air quality regulations, global environmental policies, and public health policies are required, but they must be complemented by strong enforcement and mutual commitment to cleaner air.

1.3. Personal exposure in urban microenvironments

A microenvironment is generally defined as a small, relatively homogenous area where human activities occur. This includes indoor environments (homes, offices), transportation (cars, buses, subways), and specific outdoor locations (near busy roads, parks). Personal

exposure to PM in these microenvironments does not occur uniformly across all spaces and times; instead, it is strongly influenced by the specific microenvironments individuals occupy throughout the day (Davuliene et al., 2022). Recognizing and quantifying exposure at the microenvironmental level is crucial, as these exposures can dominate an individual's daily particle dose and contribute significantly to health risks (J. Gao et al., 2022).

Studies have shown that people spend approximately 90 % of their time indoors, with 4–6 % of that time in vehicles, making these microenvironments significant contributors to overall exposure (Pruss-Ustun et al., 2017). Due to factors such as poor ventilation systems, indoor pollution sources, and the infiltration of outdoor pollutants, the concentration of fine particles (PM$_{2.5}$) and ultrafine particles (UFPs, <100 nm) in these environments can be substantially elevated (Rawat & Kumar, 2023). Similarly, enclosed buildings designed for energy efficiency may reduce ventilation rates to below 0.5 air changes per hour (ACH), increasing indoor pollutant accumulation and exacerbating exposure risks (Rawat & Kumar, 2023).

The widespread adoption of energy-efficient buildings, designed with close structures and advanced insulation, has significantly improved energy conservation but also reduced natural ventilation, contributing to the accumulation of indoor pollutants. Maintaining indoor air quality (IAQ) in these environments is largely dependent on Heating, Ventilation, and Air Conditioning (HVAC) systems equipped with high-efficiency filters, which can achieve up to 90 % removal efficiency for fine PM (PM$_{2.5}$) (Jones et al., 2021). Indoor PM primarily originates from two sources: indoor-generated pollutants and outdoor-penetrating particles. Indoor sources, such as cooking activities (particularly frying and grilling), release significant amounts of ultrafine particles (UFPs), with concentrations reaching 1–10 million particles/cm³ in unventilated kitchens (Manigrasso et al., 2015). Similarly, tobacco smoke in poorly ventilated spaces can generate PM$_{2.5}$ concentrations exceeding 300 µg/m³, which poses a

substantial health risk. Indoor activities like vacuuming and sweeping can also resuspend settled dust, increasing PM_{10} concentrations by 50–100 µg/m³ (Manigrasso et al., 2015). Outdoor pollutants, such as vehicle emissions and industrial pollution, infiltrate buildings, although modern enclosed buildings can reduce $PM_{2.5}$ infiltration by 30–50 % compared to conventional structures, minimizing exposure to outdoor air pollution (Jones et al., 2021).

In vehicles, the enclosed cabin environment, combined with external pollution sources, results in significant exposure to air pollution, with ventilation mode playing a critical role in determining exposure levels. Recirculation mode, which reuses indoor air, can reduce the infiltration of $PM_{2.5}$ by 40–60 %, offering protection from outdoor pollutant exposure, but it can also lead to the accumulation of carbon dioxide (CO_2) and indoor pollution if not periodically refreshed (Wang et al., 2024). In contrast, fresh air intake mode helps dilute indoor pollution concentrations but brings in traffic-related aerosol particles, increasing $PM_{2.5}$ concentrations by 70 % from nearby traffic (Wang et al., 2024). The duration of exposure is also critical, with commuters potentially inhaling 10–20 % of their daily $PM_{2.5}$ intake while inside the vehicle, especially during long commutes or heavy traffic, where indoor-vehicle concentrations can reach 50–100 µg/m³ (Deevi & Lu, 2024).

1.3.1. Importance of microenvironmental exposure

Traditional exposure assessments often rely on background ambient monitoring stations, and numerous studies have demonstrated that these monitors poorly represent personal exposures, especially for short-lived pollutants like BC. However, microenvironmental measurements capture the variability in particle concentrations that individuals experience, leading to a more accurate estimation of exposure doses. Understanding particle exposure within specific microenvironments enables better identification of major sources of pollution. For example, indoor microenvironments are often

dominated by indoor-generated particles (cooking, smoking, candles), whereas vehicular emissions heavily influence near-road outdoor microenvironments. This knowledge is essential for targeted intervention strategies (e.g., improved ventilation, air purification, behavioral changes) that are more effective than broad ambient-level regulations alone. Microenvironmental settings often expose individuals to high short-term particle concentrations (peaks) that might not be captured in daily or weekly averages (Kousis et al., 2022). Acute exposure to high particle loads, even for short durations, has been linked to adverse cardiovascular and respiratory outcomes. Thus, understanding temporal spikes in particle concentrations within microenvironments is important for linking exposure events to acute health effects, an area increasingly emphasized in epidemiological research (Sadrizadeh et al., 2022).

Children, the elderly, and people in certain professions—vulnerable groups—spend more time in potentially highly polluting microenvironments (e.g., schools near traffic, industrial workplaces, underground metro systems). To safeguard vulnerable populations from disproportionately high particle doses, it is essential to evaluate microenvironmental exposure (Faria et al., 2022). Microenvironmental exposure assessment is crucial for accurately characterizing individual exposures to particle pollution. It bridges the gap between ambient measurements and personal health risks, highlighting the crucial role of pollutant sources and short-term concentration spikes.

1.3.2. Time–activity patterns of urban residents

Unlike ambient air quality data, which provides general pollution levels in specific locations, time–activity patterns offer insight into how people move through and interact with various microenvironments throughout the day, each with distinct air quality characteristics (Dias & Tchepel, 2018). In urban settings, residents often transition between indoor environments (homes, offices, transit systems) and outdoor spaces (streets, parks, commercial areas). These

environments differ significantly in pollutant concentrations, especially in the case of traffic-related pollutants such as BC and $PM_{2.5}$. For example, individuals who spend a large portion of their day commuting, particularly by walking, cycling, or using public transport, are more likely to be exposed to higher levels of black carbon, as these routes often run alongside high-traffic roads where exhaust emissions are concentrated.

Moreover, certain groups such as outdoor workers, street vendors, delivery personnel, and school children (during commutes or outdoor play) may experience disproportionately high exposure due to their specific time–activity profiles (Faria et al., 2022). On the other hand, individuals spending most of their time indoors in well-ventilated or filtered environments might encounter lower pollution levels. However, indoor air quality can also be compromised by infiltration of outdoor pollutants and indoor sources.

Therefore, understanding urban residents' time–activity patterns is essential in personal exposure assessment. Incorporating these patterns allows for a more accurate estimation of personal exposure. It helps identify vulnerable populations, ultimately supporting targeted interventions to mitigate health risks associated with urban air pollution.

1.3.3. Challenges in assessing real-world exposure levels

Evaluation of personal exposure to urban air pollution in different microenvironments is confronted with several practical challenges. First, concentrations can vary widely spatially and temporally because of traffic patterns, climatic conditions, and urban infrastructure. Fixed site monitoring stations cannot record these microenvironmental patterns and may misrepresent individual exposure levels. Secondly, individuals move through various microenvironments (e.g., in homes and outdoors, and in cars) and other enclosed spaces (e.g., office buildings, dwellings, and schools) with pollution levels and emission sources. Reliable assessment thus

demands complete tracking of activity patterns and duration of time in particular microenvironments. Finally, indoor exposures that account for a significant portion of total exposure are neglected because of outdoor measurements, even though there may be indoor sources of pollution. Personal monitor use presents additional challenges. While portable or body-mounted sensors give more reliable data than stationary monitors, they are costly and may operate for only a limited duration of time. Low-cost monitoring sensors may not be precise enough and lack enough sensitivity, particularly in various environments. Integrating information from various sources (including personal and background monitor stations) requires modeling and considerable computational power. These are some of the complexities in assessing the real-world exposure level in urban microenvironments.

1.4. PM deposition in the human respiratory system

The respiratory system is particularly vulnerable to fine and ultrafine particles, which can penetrate deep into the lungs and even translocate to other organs in the human biological system. Understanding the mechanisms, influencing factors, and modeling of PM deposition is essential for risk assessment. Several factors that involve size, shape, density of particles, and individual breathing patterns are important in assessing the deposition mechanism (Pichelstorfer et al., 2013). Other physiological properties, such as age and sex, also influence deposition patterns. Generally, women tend to have increased particle deposition in the conducting airways compared to men, whereas men experience deeper penetration of particles into the lung's air spaces, which are the most sensitive regions of the human lungs. Similarly, children and older adults are more vulnerable to inhaled aerosols because their airway and lung structure and function differ from those of healthy, normal lungs (Sturm, 2012).

The human respiratory tract is commonly divided into three regions for deposition analysis: the nasopharyngeal (head), tracheobronchial (TB region), and alveolar (AL) regions (Fig. 2).

Particle size is an important parameter in deposition mechanism, coarse particles (PM$_{10}$) tend to settle in the upper respiratory tract (URT) compared to finer particles (PM$_{2.5}$) and ultrafine particles (UFPs) that penetrate deeper into the lungs (Lindén et al., 2023).

Larger particles in the size range of 5 µm to 20 µm deposit in the upper respiratory airway via inertial impaction, largely in regions such as the nasal areas or at bifurcations where there is a rapid change in airflow direction. These particles do not lose velocity because of their increased inertia and thereby directly impact the airway interfaces (Lindén et al., 2023; Londahl et al., 2014). Sedimentation is largely responsible for depositing smaller particles (PM$_{2.5}$ µm) in the lower respiratory airway, the bronchioles, and the alveoli. Gravitational settling disengages particles from the air stream in regions where the airflow is slower (Darquenne, 2014). Deposition through diffusion is dominant for ultrafine particles (usually less than 0.1 µm). These particles experience random motion (Brownian motion) that facilitates them to hit and settle on the airway and alveolar surfaces (Sturm, 2012).

The deposited aerosol dose in the respiratory system is usually assessed through mathematical modeling, experimental methods, and complex computer simulations. Various tools are used to calculate deposited aerosol dose in the respiratory system, such as the ICRP model (International Commission on Radiological Protection), the MPPD (Multiple-Path Particle Dosimetry) model, and computational fluid dynamics (CFD) simulations (Corley et al., 2021; Darquenne, 2014; Davuliene et al., 2022). However, the use of specific methodologies depends on the aim of the study and available resources. The present study favored the MPPD model since it simulates aerosol transport and deposition in multiple airway generations. This model considers various variables, including breathing mode (oral and nasal breathing modes), anatomical differences (age and gender), and deposition mechanisms such as impaction, sedimentation, and diffusion. The use of the MPPD model

is common in inhalation toxicology, therapeutic aerosol studies, and risk assessments of air exposure (Miller et al., 2016).
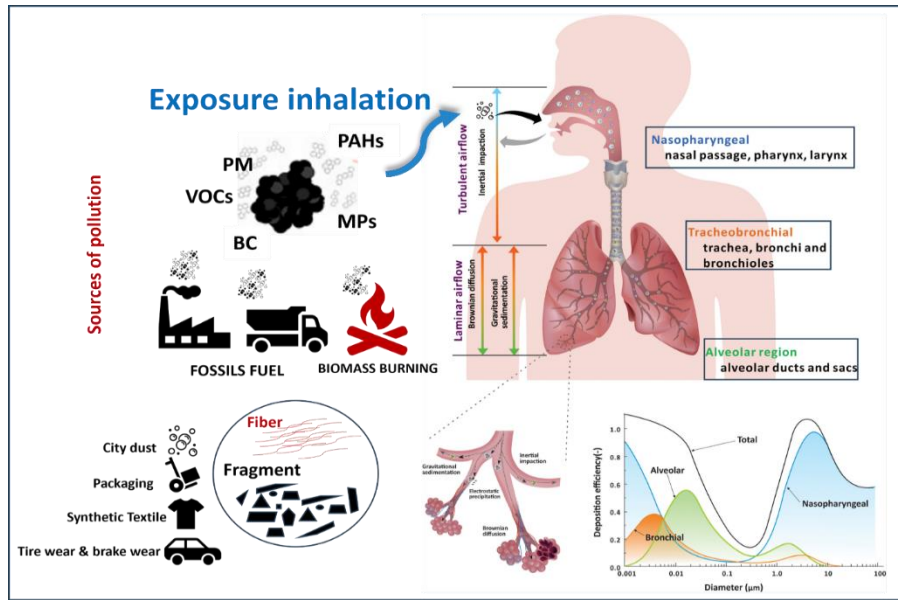
Fig. 2. Personal exposure and deposition of PM in the human respiratory system.

1.5. Role of urban green infrastructure in air pollution mitigation

1.5.1. Concept and types of urban green infrastructure

UGI refers to a network of natural and semi-natural spaces within urban areas designed to provide environmental, social, and economic benefits (Fig. 3). It is a green strategy to make cities more sustainable and resilient by integrating nature into urban spaces. UGI is a novel planning concept widely accepted as a green strategy in sustainable climate-risk management (SCRM) for improving urban environmental health (Lafortezza et al., 2018). The UGI is receiving more attention due to its importance for cities' life, whether developed, developing, or soon to be developed (Lafortezza et al., 2018). Urban parks and green spaces offer social, mental, and environmental benefits. Examples

include city parks, community gardens, and nature reserves. Green walls covered with plants can improve air quality, enhance insulation, and add aesthetic value to urban spaces. Green roofs are covered with vegetation and soil, often used to reduce heat islands, manage stormwater, and improve air quality. Urban forest areas within cities or urban fringes provide biodiversity, recreational opportunities, and carbon sequestration. Ecological corridors and green networks connect natural areas within and between urban areas, enabling wildlife movement and helping conserve biodiversity. Trees and green streets provide shade, improve air quality, and reduce the heat island effect. Green streets may also include permeable pavement and other sustainable design elements. Rain gardens and bioswales are designed to manage rainwater runoff by allowing water to soak into the ground, often planted with native vegetation. Green walls and fences provide aesthetic and functional benefits by enhancing privacy, soundproofing, and biodiversity (Redondo-Bermudez et al., 2021).

1.5.2. Mechanisms of particle capture and dispersion reduction

Urban vegetation captures airborne particles through dry deposition, where particles settle on leaves and surfaces due to gravitational settling and physical interception (Capotorti et al., 2020). UGI primarily removes PM through stomatal uptake and deposition on leaf surfaces. Several factors influence the effectiveness of PM removal: Leaf morphology, density, and surface roughness significantly affect PM capture. Plants with coarse-textured leaves and large surface areas are more efficient in trapping PM. The most extensively studied UGI type, with evidence showing that dense tree canopies significantly reduce PM concentrations. Trees with high leaf density and multi-layered canopies, such as needle-leaved species, capture more pollutants. To maximize PM removal, vegetation should be strategically placed near pollution sources like roads and industrial zones. The green roofs and walls concept is an effective alternative, particularly for reducing pollution levels near roads. Roadside plants,

hedges, and bushes also filter motor vehicle emissions, reducing the amount of PM that pedestrians are exposed to, specifically in hotspot areas (Sebastiani et al., 2021; Selmi et al., 2016).
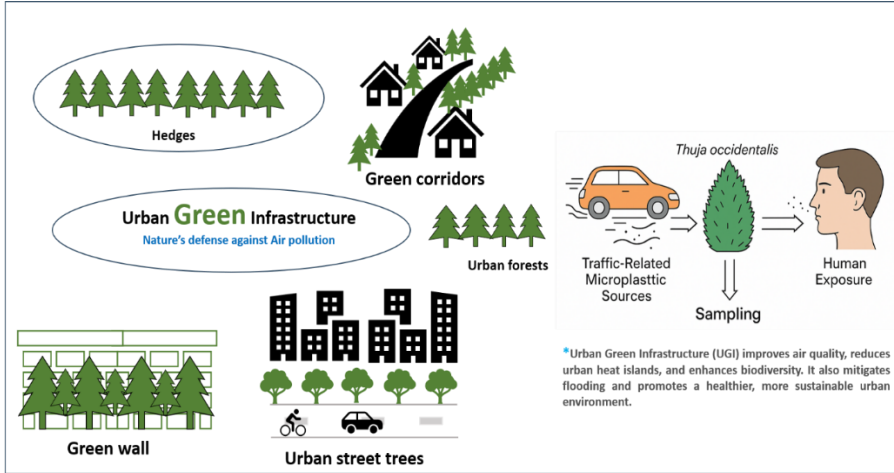
Fig. 3. Effectiveness of urban green infrastructure in mitigating traffic-related MPs pollution.

1.5.3. Urban green infrastructure in the context of traffic-related air pollution control

UGI acts as a natural air filter, capturing airborne PM, gases (e.g., NO_2), and volatile organic compounds (VOCs) through leaf surfaces and plant canopies. Tall trees with low-hanging branches can improve vertical dispersion of pollutants away from pedestrian level near busy roads. Strategically placed green barriers (e.g., hedgerows) effectively intercept emissions at the source, particularly from traffic-related emissions. Vehicle exhaust emissions, including BC and PM, are significantly mitigated by vegetation with high leaf surface area and waxy or hairy texture. Non-exhaust emissions—such as brake dust, tire wear particles, road surface abrasion, and resuspended road dust—are increasingly dominant in PM pollution. UGI can trap non-exhaust PM at ground level, particularly through low-height vegetation like grasses, shrubs, and roadside hedges.

Recently, many studies have shown significant evidence on the effectiveness of UGI in removing particle pollution from the air for a healthier environment. In this regard, several studies have been reported in the United Kingdom where vegetation has reduced PM_{10} levels in 25 % of UK cities by 2 % to 10 % (McDonald et al., 2007). $PM_{2.5}$ dropped from 35.54 µg/m^3 to 28.81 µg/m^3 when Mediterranean cypress dense planting was implemented (Ozdemir, 2019). Silver birch trees in Lancaster reduced particle pollution from commuter traffic by as much as 50 % (Maher et al., 2013). The UGI in the municipality of Ferrara (Italy) removed about 19.8 Mg of PM_{10} from the air (Muresan et al., 2022). Strasbourg's public trees eliminate about 7 % of the PM_{10} particulate released into the city's environment (Selmi et al., 2016). In Naples, southern Italy, the UGI annually removed 1,148 Mg of PM_{10} (Sebastiani et al., 2021). Based on the evidence, UGI is a potential tool for mitigating traffic-related pollution from exhaust and non-exhaust emission sources.

1.5.4. Knowledge gaps: limited understanding of urban green infrastructure effectiveness for MPs

Research on UGI's role in mitigating airborne MPs is limited, with most studies concentrating on its effectiveness in capturing PM, leaving a significant gap in understanding its capacity to intercept MPs specifically in roadside environments. The potential for resuspension of captured MPs from plant surfaces back into the atmosphere under varying environmental conditions, such as wind and rain, is poorly understood, posing questions about the long-term effectiveness of UGI in MP retention. There is insufficient data on the seasonal variability of UGI's effectiveness in capturing MPs. There is a lack of standardized methodologies for measuring the deposition of MPs on vegetation, making it challenging to compare results across different studies and to develop best practices for UGI design aimed at MP mitigation. The interaction between UGI and other urban elements, such as non-exhaust traffic emissions, in influencing the distribution

and deposition of airborne MPs has not been comprehensively analyzed. Finally, integrating UGI strategies into urban planning for airborne MP mitigation lacks a robust evidence base.

1.6 Chapter conclusions

Rapid urbanization and population growth have intensified pressure on urban air quality. Mitigating air pollution has proven to be more challenging because air quality levels have worsened in major cities across the globe. Exposure to harmful exhaust-related pollutants, particularly BC, has not reduced uniformly and remains elevated in densely populated urban areas. In parallel, a new class of non-exhaust emissions, such as MPs from tire wear, brake wear, and road dust resuspension, has emerged as an additional and poorly understood threat to urban air quality. Short-term pollution peaks and continuous exposure in indoor and transport-related microenvironments—where exhaust and non-exhaust particles frequently accumulate—remain significant yet inadequately addressed health concerns, particularly for vulnerable populations and low-income communities.

Existing monitoring networks focus on ambient concentrations at fixed sites, neglecting individual-level exposure variability. Many epidemiological studies assume exposure based on general outdoor levels, ignoring different microenvironments. There is a major research gap in understanding BC exposure in different environments, due to limited measurements, technical challenges with portable sensors, lack of standard protocols, and poor integration of personal mobility and exposure data. This leads to exposure misrepresentation and potentially underestimates health risks, especially for individuals commuting through heavily polluted corridors.

UGI offers a promising, nature-based, sustainable approach to mitigating airborne particulate pollution. Vegetation barriers can capture airborne particulate pollution from traffic-related exhaust and non-exhaust emissions near busy streets in urban areas. Besides improving air quality, UGI provides co-benefits such as cooling urban heat islands, enhancing biodiversity, and improving social well-being.

Addressing future air quality challenges requires a shift toward a holistic approach that simultaneously targets traditional exhaust and newly recognized non-exhaust pollutants.

2. MATERIALS AND METHODS

2.1. Microplastics in roadside environments and the role of urban green infrastructure

2.1.1 Site selection

Kaunas (54.8985°N, 23.9036°E), Lithuania's second-largest city, is situated at the confluence of the Nemunas and Neris rivers (Fig. 4). The city functions as a key center for scientific research, cultural activities, transportation, and industrial development. As of 2023, Kaunas had an estimated population of approximately 319,800 residents, with a population density of 1,938 inhabitants per square kilometer, according to the official Lithuanian State Data Agency (2023), which provides data on population size and composition (accessed March 7, 2025, from https://osp.stat.gov.lt/en/lietuvos-gyventojai-2023/salies-gyventojai/gyventoju-skaicius-ir   sudetis). Forested areas represent the dominant component of the semi-natural landscape, accounting for 51 % of land cover. However, within a 3 km radius of the city, urban infrastructure—including buildings, roads, and other impermeable surfaces—covers approximately 96 % of the land. Broadening the scope to a 15-km radius, the land use pattern shifts, with cropland occupying 44 % and forests 28 % of the area. At a larger spatial scale of 80 km, croplands dominate with 57 % coverage, while forested areas comprise around 30 % of the landscape (Grazuleviciute-Vileniske et al., 2015). Primary sources of ambient air pollution in Kaunas include vehicular emissions, particularly from tire and brake wear, degradation of road markings, resuspended road dust, and emissions from industrial activities. The city experiences a humid continental climate, marked by distinct seasonal fluctuations. Annual temperature ranges typically span from -6.7°C in winter to 23.3°C in summer, with occasional extremes falling below -17.2°C or exceeding 28.9°C (retrieved March 7, 2025, from https://www.meteo.lt/en/).
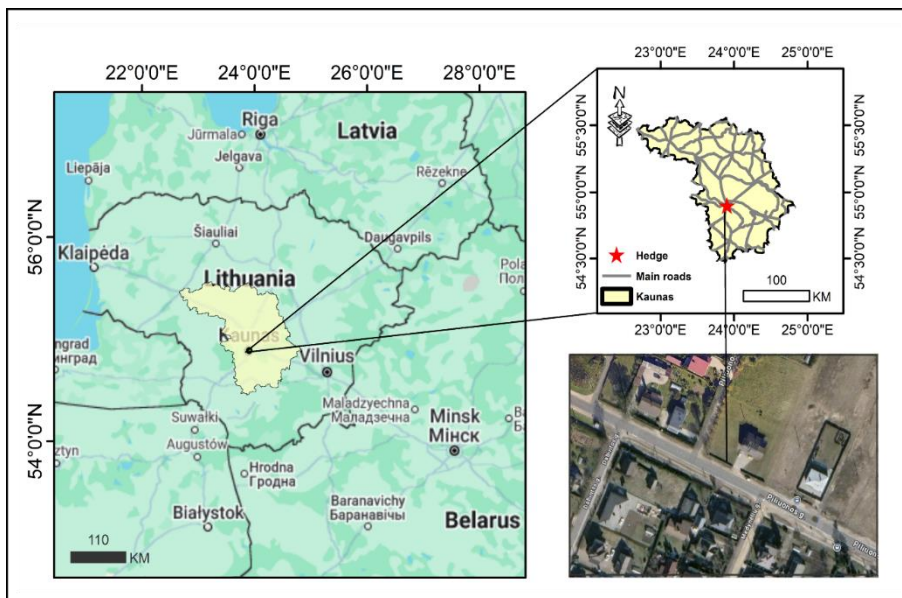
Fig. 4. Study area map located in Kaunas, Lithuania.

2.1.2 Airborne microplastic sampling design

A field study was conducted in Kaunas, Lithuania (coordinates: 54°51'00.7"N, 24°01'46.5"E), where a *Thuja occidentalis* hedge—measuring approximately 0.6 meters in width, 1.5 meters in height, and 19 meters in length—was selected as a representative example of urban green infrastructure for assessing airborne MP deposition (Fig. 5). The hedge is located between a roadway and adjacent residential buildings and was purposefully chosen to explore its effectiveness in mitigating MP pollution originating from traffic emissions. To evaluate the spatial distribution of deposited MPs, passive sampling was carried out using 8 cm diameter glass fiber filters housed in Petri dishes. These samplers were deployed at four distinct distances relative to the hedge: (i) -1 meter, positioned directly adjacent to the road to capture the highest expected MP concentrations from traffic; (ii) 0 meters, placed at ground level beneath the hedge canopy; (iii) +1 meter, located one meter behind the hedge; and (iv) +2 meters, positioned two meters behind the hedge, representing a zone further removed from the

43

emission source. Each filter was exposed on the ground for 24 hours during sampling campaigns, remaining undisturbed to allow the deposition of airborne particulates.

Sampling was performed across four seasons to capture seasonal variability: summer (June 2023), autumn (October 2023), winter (February 2024), and spring (March 2024). A total of 22 samples were collected during the study. Four samples were obtained at each distance for each seasonal campaign, resulting in 16 samples collected in the presence of the hedge. Additionally, four comparative samples were collected in spring 2024 at the exact four distances, but in an open area without the hedge, to serve as a reference for evaluating the hedge's impact on MP deposition.

To further investigate the vertical distribution of MP particles within the hedge, two supplementary samples were taken from different heights inside the hedge structure: one at mid-height (0.75 m) and the other at the top (1.5 m). Upon completion of the sampling, filters were carefully sealed to avoid contamination and particle loss, then transported to the laboratory for detailed analysis.
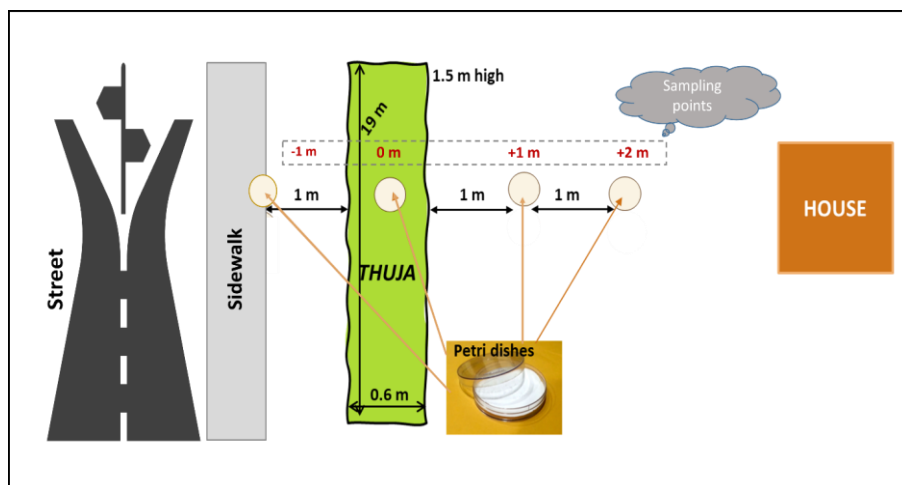
Fig. 5. Investigating MP deposition through passive sampling at four locations along the street.

2.1.3 Laboratory analysis

Particles captured on the glass fibers were washed gently into separate pre-cleaned glass beakers using distilled water. Samples were digested with chemicals to eliminate potential organic contaminants through a solution of 30 % hydrogen peroxide (H_2O_2) (Sigma-Aldrich, Germany) for 24 hours. To isolate MPs from other waste, a density separation method was used using a saturated zinc chloride ($ZnCl_2$) solution with a density of 1.6 to 1.8 g/cm³ (Crutchett & Bornt, 2024; Konechnaya et al., 2020; Rodrigues et al., 2020). The samples were positioned in a separation funnel containing the $ZnCl_2$ solution and left undisturbed for hours so that particles with lower densities—typically MPs—rose to the surface, while denser non-plastic garbage settled at the bottom. Subsequently, the floating fraction was filtered through glass fiber filters ("Branchia," diameter 50 mm, pore size 1.6 μm). The filters were then oven-dried at 60°C for 24 hours to condition them for MP analysis. The samples were dried and characterized using a digital optical microscope with a 200x magnification objective. Individual particles were assessed and classified based on morphological attributes, including size, shape, and color. The length of the longest axis of each particle was measured through "Motic Images Plus 3.0" image analysis software. Size categorizing was conducted through the subsequent ranges: <20 μm, 20–50 μm, 50–100 μm, 100–250 μm, 250–500 μm, 500–2000 μm, and >2000 μm. Based on structural characteristics, particles were further categorized into two broad morphological categories—fibers and fragments. Color was also observed, with the particles grouped into black, brown, white, blue, red, yellow, and others. For verification of the polymeric nature of the suspected MP particles, a sub-sample was placed on an aluminum oxide (Al_2O_3) filter for micro-Fourier transform infrared (μ-FTIR) spectroscopic analysis, performed on a LUMOS II spectrometer (Bruker, Germany). Spectra were captured 4000–1200 cm^1 using a scan time of 4. Each particle's spectral signature was compared against the instrument's reference library. Any particle was considered as MP

when its similarity to a reference polymer in the spectrum was found above a 70 % similarity level.

2.1.4. Quality control and assurance

To avoid any contamination, strict measures were followed in the course of the study. After each 24 hours of passive sampling, Petri dishes were airtight-sealed and covered with aluminum foil before being transported to the laboratory for further investigation. Sample preparation and extraction were all conducted under a laminar-flow cabinet environment, with a sterile particle-free work environment. All glassware was pre-washed before using ultrapure Milli-Q grade water to prevent potential carryover contamination. The staff members further restricted the addition of synthetic microfibers by maintaining stringent handling techniques, for instance, wearing only lab coats made entirely of pure cotton and sterile nitrile gloves during the experimental procedure. Furthermore, procedural blanks were also analyzed concurrently with the environmental samples to verify the absence of background contamination and the reproducibility of the analytical methods. These general steps were critical in verifying the recovered MP concentration data's replicability, validity, and accuracy.

2.1.5. MPs removal efficiency by the hedge

The removal efficiency (RE) of each size and shape class was estimated with equation (1);

$$RE\ (\%) = \frac{C\ (pre\ hedge) - C\ (post\ hedge)}{C\ (before\ hedge)} \times 100 \quad (1)$$

where RE is the percentage reduction in MP concentration; C (pre-hedge) is the concentration at -1 meter (sited immediately adjacent to the traffic source), and C (post-hedge) is the concentration at +1 meter (sited immediately behind the hedge, i.e., the ambient environment). This experimental design enabled direct spatial comparison of MP concentrations so that the ability of the hedge to

filter particles could be assessed based on particle shape and size distribution.

2.1.6. Statistical analysis

MP concentration data were visualized across seasonal variations using OriginPro 2025 (OriginLab Corporation, Northampton, MA, USA), generating precise and informative graphical outputs. To evaluate the association between MP number concentrations at varying distances from the roadway and their corresponding physicochemical properties, a Mantel test was applied via the Chiplot online platform (https://www.chiplot.online/). Furthermore, Pearson correlation analysis was employed to investigate the statistical relationships among key variables across the different sampling locations.

2.1.7. Inhalation risk index of microplastics

This study used the Inhalation Risk Index (IRI) to predict health risks from inhaling MPs in an urban environment. The IRI considers three factors: the airborne particle concentration, the toxicity of polymers, and deposition fraction in the human respiratory system. Since there are no established reference doses (RfDs) for airborne MPs until now, using the IRI allows for an effective way to place relative risks in different environments into context and to contrast the effect of roadside vegetation like *Thuja occidentalis* to reduce exposure. The IRI data were calculated from two locations along a road: -1 m (roadways) and +2m (behind the hedge), across different seasons (summer, autumn, winter, spring). The intention was to estimate the potential health risks of the MPs' chemical composition (polymer types) and morphology (fragments and fibers). Each polymer in the sample was also assigned a hazard score (on a scale of 1 to 10) based on the toxicity, derived from published research on the biological effects of the polymers. A deposition factor was also used to represent

how easily a particular polymer will likely be deposited in the human respiratory tract. Deposition fraction was calculated using the MPPD model. Higher deposition factors indicate a higher likelihood of particles settling in the lungs or other areas of the respiratory system. The IRI was calculated using the following formula 2:

$$IRI = (Particle\ Count)_{(Fragment\ and\ Fiber)} \times (Hazard\ Score)_{(\ polymer)} \times (Deposition\ Factor)_{(TD)} \quad (2)$$

Where particle count (particles/cm^2/day), hazard score (varies from polymer to polymer), and total deposition fraction in the human respiratory tract. The risk reduction (RR) by the *Thuja occidentalis* hedge was calculated by comparing the IRI values for the roadside (–1 m) and behind the hedge (+2 m). This approach allows us to understand how much the hedge has reduced the exposure to MPs. Risk reduction was performed using the following equation 3:

$$RR = \frac{IRI\ (Roadside) - IRI\ (Behind\ Hedge)}{IRI\ (Roadside)} \quad (3)$$

2.2. Black carbon in urban microenvironments

2.2.1 Study locations

The study examines personal exposure to PM and BC during office hours and commuting to and from the office, aiming to determine the deposition dose. The research was conducted in Vilnius, Lithuania's capital city, with a population of approximately 600,000. Vilnius, one of the biggest cities in the Baltic region, is home to reputable universities and research facilities, giving it a significant intellectual presence. Its membership in the EU makes access to several European research networks and funding possibilities possible. Vilnius has spatially varying air pollution, just like most capital cities. The city has a medium continental climate with warm summers and chilly winters. January is the coldest month (average temperature -4°C) and July is the warmest (average temperature 17°C), with an average

yearly temperature of 6.6°C. There is 688 mm of precipitation on average every year. Lithuania experienced an average temperature of 1.5°C in March 2022, with a positive anomaly of 0.8°C. The predominant wind direction was south. The measuring campaign had a maximum temperature of 17.7°C and a minimum temperature of -14.5°C. During the campaign, there was very little precipitation—an average of about 1.9 mm. Predetermined routes were taken for mobile measurements, traveling through residential and commercial districts as well as locations close to main and local roadways, both from home and between offices (Fig. 6). Three routes were selected for commuting: FTMC1-Home, FTMC1-FTMC2, and Home-FTMC1. The average air pollution level for the measurement days was calculated to assess whether the selected days represented typical conditions for the cold season. On the roof of the Centre for Physical Sciences and Technology (FTMC1, http://vilniusair.ftmc.lt, www.ftmc.lt, accessed on May 29, 2025), measurement equipment was set up at the reference urban background site. The site is 6–7 kilometers northeast of the city center and is protected by a wooded area from a busy street with 8400 daily traffic and a smaller street with 6200 daily traffic (https://portal.sisp.lt/portal/home/viewed on 29 May 2025).
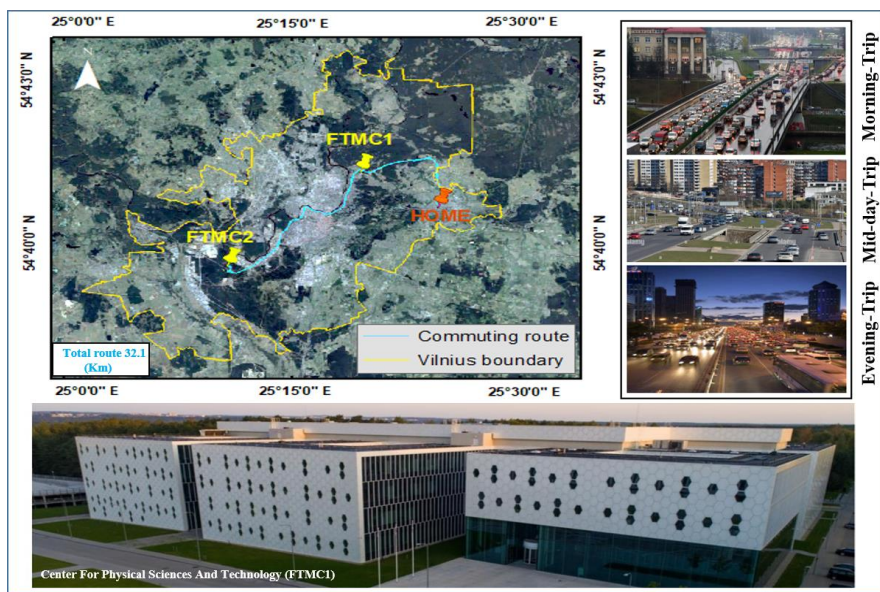
Fig. 6. Map of the study location in Vilnius, Lithuania, showing the home site, sub-office (Center for Physical Sciences and Technology FTMC2), fixed sample site (Center for Physical Sciences and Technology FTMC1), and mobile monitoring route (light blue).

2.2.2. Mobile measurements

Measurements of PMs (10, 2.5, 1 μm) and BC concentrations were made comprehensively between March 17 and 18, 2022, during the cold season. Around 8:00 AM and 6:00 PM (Lithuanian local time, UTC +2), the 15-kilometer commuting route from home to FTMC1 and FTMC1 to home was completed simultaneously during rush hours. While a 17.1 km commute between offices FTMC1 and FTMC2 was completed during midday. The URAD Monitor (A3 version 9, SC MAGNASCI SRL, Dumbravita, Romania) was used to track the mass concentrations of PM_1, $PM_{2.5}$, and PM_{10} as well as the air temperature, atmospheric pressure, and humidity along the routes. A mobile micro-aethalometer (microAeth® MA200, AethLabs, San Francisco, CA, USA) was used to measure BC mass concentration. The device's viability was verified by comparing the micro-aethalometer's findings with simultaneous BC measurements made at a fixed location

(FTMC1). Next, reference data from the urban background location (FTMC1) was combined with the verified mobile data. The spatial distribution of BC concentrations was shown on a map after results from each route were smoothed and transformed into shapefiles (point vectors) using ArcGIS version 10.6 software. For each sampling campaign, spatial interpolation was conducted using the Inverse Distance Weighting (IDW) technique. This method operates on the principle that data points closer to the location of interest exert a greater influence on the estimated value than those farther away. IDW offers two configuration modes: a fixed and variable search radius. In this research, the interpolation was carried out using the variable search radius approach, with the number of influencing points set to 12. Consequently, the search radius is dynamically adjusted for each interpolation point based on the distance required to include twelve neighbouring data points. A 2020 VW Tiguan equipped with an activated carbon cabin air filter (Valeo product code FP 26 009, part number: 5Q0-819-669) was used for the field measurements. During the measurement, the ventilation system was configured to draw air from the outside.

2.2.3. Fixed-site measurements

An aethalometer draws aerosol-laden air through a spot on a filter tape at a regulated flow rate to continually collect and analyze aerosol particles. Sensitive detectors monitor the intensity of light transmitted through an unexposed area of the tape, which serves as a reference, while the tape is simultaneously lit by light. Light passing through the filter spot gradually reduces as optically absorbing material accumulates over it. The concentration is calculated by dividing the amount of material collected by the drop in light intensity from one measurement to the next by the known air-flow volume. A 7-wavelength dual-spot Aethalometer® (Magee Scientific, model AE33, λ: 370, 450, 520, 590, 660, 880, 950 nm) was used to measure the BC mass concentration in real time at an urban background location

(FTMC1) between March 1 and March 31, 2022. A 2.5 µm impactor was used with the AE33 setup to account for variations in particle size distributions. The flow rate was set at 1.9 L/min, and the sampling time base was one minute. The light absorption coefficient at 880 nm was used to quantify BC, the main light absorber at this wavelength (Pauraite et al., 2021; Weingartner et al., 2003). The BC mass concentration is determined automatically from the aethalometer's output by utilizing the absorption coefficient and the mass absorption cross-section (7.77 m²/g) stated by the manufacturer. Shorter wavelengths cause an increase in absorption, which suggests the presence of "brown" carbonaceous material, usually from emissions from burning biomass. A wide-range Scanning Mobility Particle Sizer (SMPS, TSI model 3938W50) was used to measure the aerosol particle size distribution, which ranged from 10 to 430 nm. The system incorporates a Differential Mobility Analyzer (DMA, TSI Model 3083) to determine particle size and a Condensation Particle Counter (CPC, TSI Model 3750) to quantify particle number concentrations. Each scanning mobility particle sizer (SMPS) measurement cycle was completed in 4 and 30 seconds, with measurements conducted at five-minute intervals. Aerosol sampling and sheath air flow rates were 1.0 L/min and 10.0 L/min, respectively. Particle diffusion loss and multiple charge corrections were made using aerosol instrument manager software (SMPS version 11.3.0). The Aerodynamic Particle Sizer (APS) model TSI 3321 was programmed to make 4- and 50-second automatic sampling cycles every 5 minutes. This provided continuous data collection and effective representation of particle concentration with time. The APS was very reliable in solid particle counting with efficiencies of between 85 % to 99 % for the particles ranging from 0.8 µm to 10 µm. The AE33 and MA200 equipment variability was examined using inter-comparison data from 14 hours of simultaneous measurements (5-minute resolution) at the FTMC urban background location. According to a regression analysis (shown by the grey line), slope correction was insignificant, and the MA200

data must be adjusted by an intercept value of -189 ng/m³ to match the reference line (Fig. 7). R Studio was used to do correlation analysis [http://www.rstudio.com]. GPS and BC data were combined throughout the journey to determine hotspot areas and calculate mean personal exposure to BC.
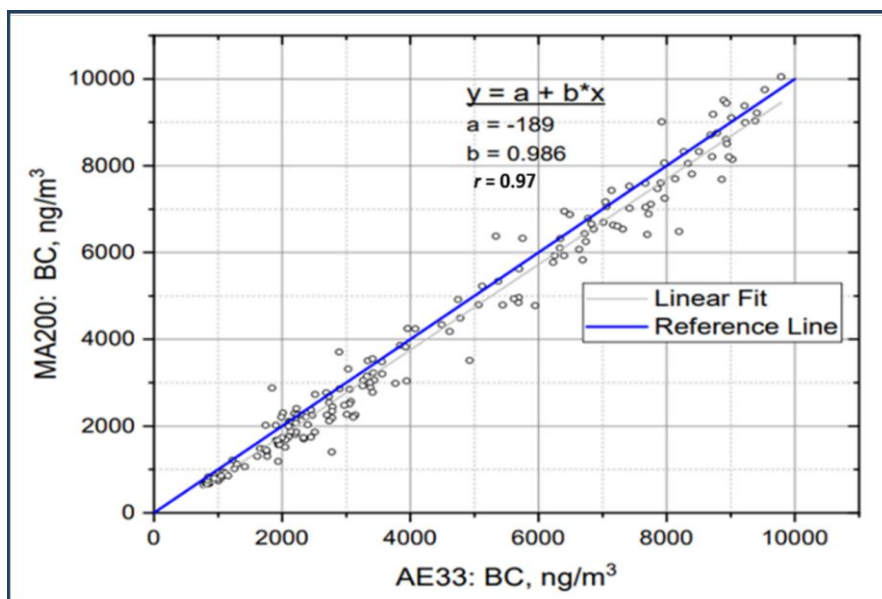
Fig. 7. Inter-comparison of the MA200 BC data with AE33 at urban background site (FTMC1).

2.2.4. Source apportionment of black carbon

The Aethalometer model is a widely utilized method for source apportionment of BC based on multi-wavelength optical absorption measurements, typically distinguishing between fossil fuel (traffic) and biomass burning sources. The source apportionment technique is based on observing distinct absorption spectra across various wavelengths of light for individual particles. A correction method was developed by (Sandradewi et al., 2008) to minimize biases such as "shadow", multiple scattering, and other effects causing measurement biases. Then, the Aethalometer model was applied to allocate BC mass

concentrations between biomass burning (BC_{bb}) and fossil fuel combustion (BC_{ff}). This model relies on absorption measurements at selected wavelengths (470 nm and 880 nm) and employs the absorption Ångström exponent (AAE) to distinguish between these two sources:

$$b_{abs}, BC_{ff} (880 \text{ nm}) = b_{abs} (470 \text{ nm}) - (470/880) * AAE_{ff)} /((470/880) * AAE_{bb} - (470/880) * AAE_{ff}) \qquad (4)$$

$$b_{abs}, BC_{ff} (880 \text{ nm}) = b_{abs} (470 \text{ nm}) - (470/880) * AAE_{bb)} /((470/880) * AAE_{ff} - (470/880) * AAE_{bb}) \qquad (5)$$

In this study, the absorption Ångström exponent (AAE) values were determined based on findings from previous research conducted by (Minderytė et al., 2022; Pauraite et al., 2021; Zotter et al., 2017). Specifically, the values selected are as follows: the AAE for fossil fuels (AAE_{ff}) is 0.9, the AAE for biomass burning (AAE_{bb}) is 1.68, and the AAE for BC (AAE_{BC}) is 1.43. Additionally, the Wavelength Dependence Analysis (WDA) method proposed by (Wang et al., 2016) was employed to assess the AAE of brown carbon (BrC):

$$b_{abs}, BC (370 \text{ nm}) = b_{abs}(880 \text{ nm}) - (880/370) * AAE_{BC} \qquad (6)$$

This method assumes that light absorption at 370 nm could be related to both BC and BrC light absorption, while light absorption at 880 nm represents only BC.

2.3. Personal exposure estimation methods

2.3.1. Multiple-path particle dosimetry model (MPPD v.3.04)

To calculate the risk of exposure to particulate pollution, the Multiple-Path Particle Dosimetry (MPPD) model (version 3.04) was applied. It simulates inhaled particle deposition within the regions of the human respiratory system, i.e., the head, tracheobronchial (TB), and pulmonary regions. Deposition fraction (DF) is the fraction of deposited particles of a certain size to the total inhaled number. The

DF is controlled by three primary deposition mechanisms: diffusion, impaction, and sedimentation. The model applies three general inputs: airway morphometry, breathing properties, and environmental exposure parameters.

(i) Airway Morphometry:

The MPPD offers eight geometry choices for lung geometry corresponding to anatomical development based on age. The lung is a complex, asymmetrical branching structure; thus, air flow and deposition patterns can drastically differ (Miller et al., 2016). The "Yeh/Schum symmetric model" was used for the analysis because it properly models the structure of the lung, which has three lobes on the right and two on the left. Functional residual capacity (FRC) and upper respiratory tract (URT) volume were also set accordingly.

(ii) Inhalation Properties:

Taking into consideration particle characteristics such as density, shape (aspect ratio), and size, particle diameter was included here, which was entered as either the Count Median Diameter (CMD) or the Mass Median Aerodynamic Diameter (MMAD). Concerning a monodisperse aerosol distribution, MMAD values of 1 μm, 2.5 μm, and 10 μm were used for PM_1, $PM_{2.5}$, and PM_{10}, respectively.

(iii) Exposure Conditions

Two kinds of exposures are available in the software: constant and variable. Due to the pattern of continuous exposure experienced by residents in many everyday environments, the constant mode of exposure was selected. Input in this type included body position, tidal volume (TV), breathing frequency (BF), and other variables such as inspiration and pause times. The posture was set as upright. Among several patterns of breathing—nasal, oral, mixed oronasal, and endotracheal—the nasal pathway was utilized for simulations.

In the present study, the model was used to calculate the DF of PM and BC using the average mass concentrations presented in Table 1.

Table 1. Mean size segregated PM mass concentration in-cabin during trips in Vilnius used in model input.

| Routes	Date and time	PM_{10} $\mu g/m^3$	$PM_{2.5}$ $\mu g/m^3$	PM_1 $\mu g/m^3$	BC $\mu g/m^3$
FTMC1 FTMC	17-03 midday	5.2	3.9	2.6	1.67
FTMC1-Home	17-03 evening	12.2	11.1	8.5	2.42
Home-FTMC1	18-03 morning	21.6	19.4	15.3	7.14
Office FTMC1	18-03 working hours	1.7	1.6	1.3	0.08

The International Commission on Radiological Protection (ICRP) has established specific guidelines to simulate the deposition of particles in the human respiratory tract. These guidelines assume an upright body orientation and standard gravitational acceleration of 981.0 cm/s². Key respiratory parameters include a functional residual capacity volume of 3300 mL and a tidal volume of 625 mL, with an inspiratory fraction of 0.5. The model assumes no pause fraction during breathing, indicating continuous airflow. The scenario focuses on nasal breathing, which is typical for assessing respiratory deposition. The breathing frequency was 19 L/min calculated for a 33 year old sedentary man (Fig. 8). Other parameters include a mass median aerodynamic diameter (MMAD) of 10, 2.5, and 1 for (PM_{10}, $PM_{2.5}$, and PM_1) and GSD values were used presented in (Table. 2) To minimize error and bias in the deposition fraction measurements of airborne MPs, a narrow size distribution is correctly represented by a GSD value of 1.13, establishing a balance between theoretical precision and practical feasibility. These parameters ensure accurate simulation of particle behavior and deposition in the respiratory

system, aiding in the assessment of inhalation risks and protective measures (Londahl et al., 2014).

Table 2. Geometric standard deviation values for PM deposition in the MPPD model.

		PM$_{10}$	PM$_{2.5}$	PM$_1$
Routes	Date and time	**GSD values**		
FTMC1-FTMC2	17-03 midday	1.5	1.44	1.21
FTMC1-HOME	17-03 evening	1.48	1.51	1.21
FTMC1-HOME*	18-03 morning	1.46	1.44	1.22
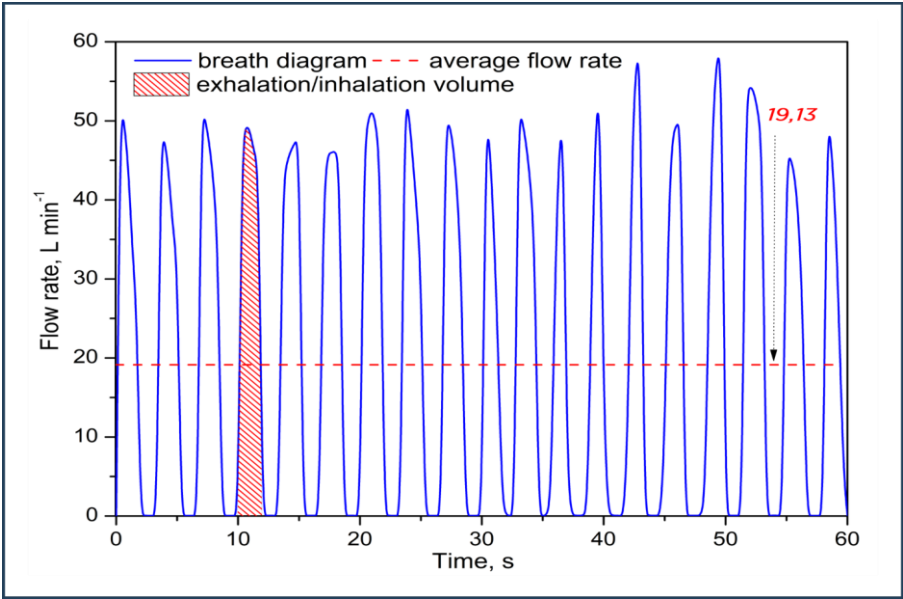
Fig. 8. Flow rate of exhaled air of a 33-year-old male during the laboratory experiment.

2.3.2. Measurement setup for deposition dose evaluation

The experimental arrangement used to assess the indoor deposition of BC mass concentration within the human respiratory tract is illustrated in Fig. 9. This configuration was developed at the Department of Environmental Research (FTMC1) specifically for this study, based on the design outlined by (Madueno et al., 2019). In this investigation, a 3M 6200 respirator (Fig. 9B) was employed for both inhalation and exhalation, featuring a customized modification that connected the outlet valve to a tube leading to the mixing chamber (Fig. 9C). The mixing chamber was implemented to prevent pressure disturbances caused by air resistance and to maintain a stable airflow required for BC measurements using a micro-aethalometer. A dryer (Fig. 9E) filled with silica gel was employed to remove moisture from the exhaled air before BC measurement with the AethLab MA200 micro-aethalometer (Fig. 9F). Additionally, a flowmeter (Fig. 9D, TSI model 4000 series) was used to measure exhaled airflow. At the same time, the Aethalometer Model AE33 (Fig. 9A) quantified BC concentration in inhaled air. It was assumed that BC mass losses within the experimental setup were negligible. However, due to the high relative humidity (~100 %) within the respiratory tract, the optical properties of BC particles may undergo restructuring, potentially introducing measurement uncertainties even under dry conditions (Radney et al., 2014). The volume of inhaled and exhaled air during a breath cycle (V) was determined using the recorded exhaled airflow rate (Fr, L/min) over the exhalation period (t_1 to t_2, min) as described by (Madueno et al., 2019). The inhaled volume of the 33-year-old sedentary male was 1.2 ± 0.1 L per breath cycle. Additionally, concentrations of O_2 and CO_2 were monitored using a QED Geotech G110 (UK) gas analyzer (Rostami et al., 2018). The inhaled air contained 19.7 % O_2 and 0.0 % CO_2, while the exhaled air contained 16.7 % O_2 and 3.0 % CO_2.
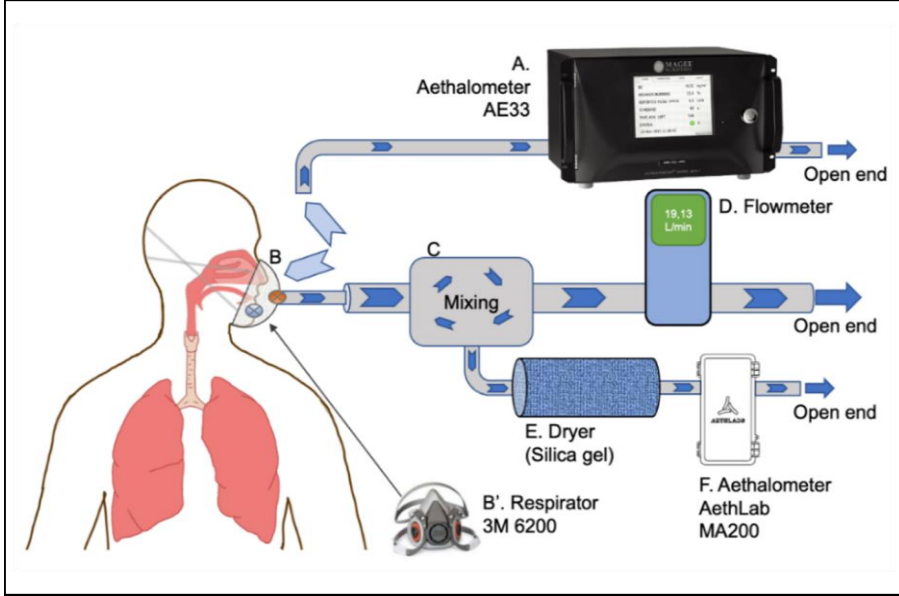
Fig. 9. The experimental setup for indoor respiratory tract deposition of BC measurements.

2.3.3. Deposition dose of PM and BC

A general approach to estimate the dose of aerosol particle deposition in the human respiratory system involves utilizing measured aerosol mass concentrations in the ambient air. This method has seen increasing application in research focused on aerosol-associated contaminants, including BC (Radney et al., 2014). One technique for calculating the respiratory minute deposition dose (MDD) of BC and PM, as proposed by (Londahl et al., 2014), is outlined below:

$$MDD_{(PM)} = DF \times MV \times \sum_i (PM_i \times \Delta t_i) \qquad (7)$$

$$MDD_{(BC)} = DF \times MV \times \sum_i (BC_i \times \Delta t_i) \qquad (8)$$

Here, MV denotes the minute ventilation, representing the volumetric airflow in the lungs (L/min), BC_i refers to the measured BC mass concentration, PM_i refers to the measured PM mass

concentration, and Δti corresponds to the duration of that interval (in minutes). The minute deposition dose (MDD) was determined by incorporating the exposure duration (in minutes), following the methodology proposed by (Londahl et al., 2014) to facilitate comparisons across varying exposure scenarios. In this study, the DF from the MPPD model was used to calculate the total deposition dose. Using a deposition fraction (DF) of 1 in calculating the deposition dose implies that 100 % of the inhaled particles are deposited in the respiratory tract. While this approach provides a conservative upper-bound estimate, it is generally unrealistic for most practical scenarios because not all inhaled particles are retained; many are exhaled. In practical applications and scientific research, employing a DF of 1 might be appropriate under specific conditions, such as worst-case scenario modelling to estimate the maximum potential exposure dose, or for particles that are highly adhesive or reactive and thus have a high likelihood of depositing upon contact with respiratory surfaces. However, omitting DF from dose-rate calculations or assuming DF = 1 introduces significant uncertainty. Actual DF values can vary widely, typically ranging from less than 0.1 to nearly 1, depending on the particle size and density (Londahl et al., 2014).

2.4. Lithuanian ambient air quality data

Lithuania, the southernmost and most populous among the three Baltic States, is notable for having been the first former Soviet republic to re-establish its independence, doing so on March 11, 1990. The country's major urban centers include the capital Vilnius (approximately 553,000 inhabitants), Kaunas (around 298,000), and Klaipėda (about 152,000 residents), with Šiauliai and Panevėžys also serving as key economic hubs. Lithuania experiences a humid climate influenced by maritime and continental systems, with average daytime temperatures ranging from -5°C in January to 20°C in July. Despite Lithuania being recognized as one of the European countries with relatively high air quality, ambient air pollution remains a concern

across national, municipal, and local scales. The European Union Directive 2008/50/EC emphasizes the critical need to address pollutant emissions directly at their sources and implement effective mitigation strategies at all governance levels to safeguard public health and the environment. The directive also underscores the necessity of establishing ambient air quality objectives per the latest World Health Organization (WHO) guidelines issued in 2021, alongside other relevant standards and programs. Access to reliable and objective data on pollutant concentrations and their temporal variations is essential to effectively regulate air pollutant emissions and support informed air quality management. In Lithuania, the Environmental Protection Agency (EPA) operates 15 automated air quality monitoring stations that measure the mass concentrations of fine ($PM_{2.5}$) and coarse (PM_{10}) particles. The data collected at these monitoring sites, accessible via the national environmental portal (www.gamta.lt), covers the period from 2005 to 2020 and provides a foundational basis for long-term air quality assessments (Fig. 10).
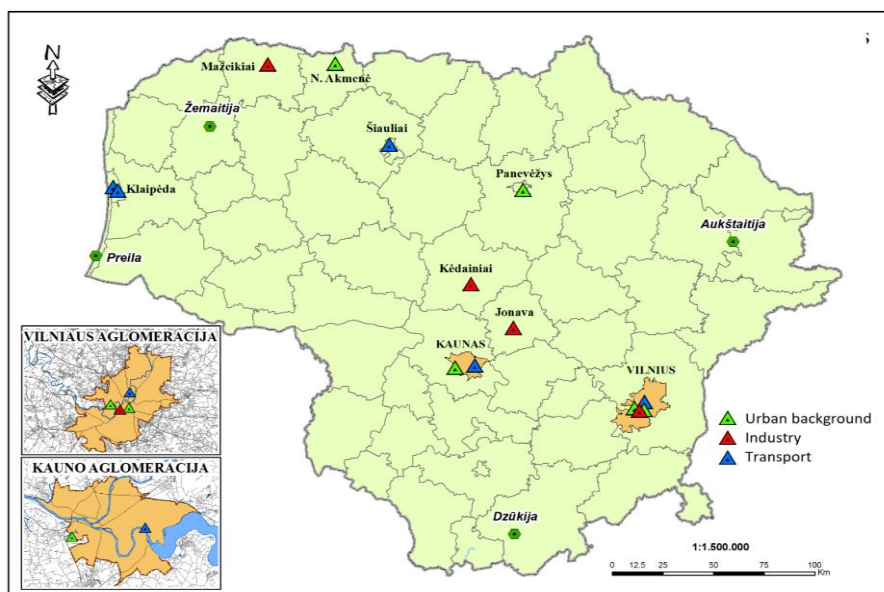
Fig. 10. EPA site network depicting traffic (blue), industry (red), and urban background (green).

Table 3. Summary of data sources, collection techniques, and their application in the research.

Data Type	Acquisition Method	Source	Tool/Model Used	Purpose in Study
BC concentration + PM concentrations	Field measurements	microAeth MA200 + uRADMonitor A4	-	Personal exposure assessment during commuting
BC concentration + PM concentrations	Background measurements	Aethalometer Model AE33 + APS (TSI 3321) + SMPS (TSI model 3938W50)	-	Personal exposure assessment in the office
BC concentration	Background measurements	Aethalometer Model AE33	AE model	Source apportionment of BC
Respiratory Deposition Estimates	Modelling	Derived from BC and PM data	MPPD model	Deposition dose and deposition fraction on the lungs
Commuting Route Distance & Time	Location tracker + Google Maps	GPS logging, Google Maps	-	Identifying the hotspot location during commuting
Microplastic Particle Counts, Size, Shape, and Color	Field sampling + lab analysis	Roadside passive samples	Optical microscope	Non-exhaust emissions Characterization

Microplastic Chemical Composition	Field sampling + lab analysis	Roadside passive samples	μFTIR	Non-exhaust emissions Characterization
Ambient PM and BC mass concentrations 2005-2020	National Environmental Portal	EPA monitoring stations	-	Lithuanian emission inventory

Given the variety of data sources and acquisition methods used in this study, Table 3 provides a structured overview. This table details the type of data collected, the acquisition method (e.g., field measurement, modeling, or publicly available sources), the original data source, any tools or models employed, and the specific purpose of each dataset in the research. This summary aims to clarify the methodological approach and improve transparency regarding the origin and application of the data used in the study.

3. RESULTS

## 3.1. Mitigation of microplastics by urban green infrastructure

3.1.1. Microplastic number concentration: an overview

A detailed overview of MP concentrations throughout the study campaign is presented in Fig. 11. During the experimental campaign (left panel), MPs were detected at all sampling points (-1, 0, +1, +2 meters) along the urban street environment across all seasons, with total MP concentrations ranging from 0.20 to 5.95 particles $cm^{-2} day^{-1}$. The highest MP concentration, 5.95 particles $cm^2 day^1$, was observed in spring at (- 1 m), followed by the same season inside the hedge (0 m), with 4.84 particles $cm^2 day^1$. In contrast, the lowest MP concentration was recorded in summer at a location behind the hedge (+2 m), with 0.20 particles $cm^2 day^1$. The seasonal variation in MP concentrations reflects the combined influence of meteorological conditions, emission sources activity, and atmospheric dynamics on MP dispersion (Hee et al., 2023; Lee et al., 2024). Specifically, during summer, a higher planetary boundary layer and enhanced vertical atmospheric mixing may facilitate greater vertical dispersion and dilution of airborne particles, leading to lower concentrations (Su et al., 2018). Additionally, reduced vehicle activity during holidays may reduce emissions, further influencing MP levels during the summer sampling campaign.

To understand the role of UGI in mitigating airborne MP pollution, the results from the spring season have been analyzed from both experimental (with hedge) and control (without hedge) environments (Fig. 11). For comparison purposes, we assume the (+1 meter) distance as a reference point to evaluate the hedge's ability in reducing MP pollution. This comparative approach provides valuable insights into the effectiveness of UGI, such as the *Thuja occidentalis* , in reducing the concentration of traffic-related MPs in urban street environments. The results from the spring season reveal distinct differences in MP concentration between experimental and control

environments. A pronounced difference was observed at (+1 m) behind the hedge, where the MP concentration in the experimental environment was recorded as 4.59 particles cm² day¹, significantly lower than the 9.2 particles cm² day¹ in the control environment. The 50.11 % reduction in the overall MP concentrations demonstrates the hedge's ability to limit the dispersion of MPs over a longer distance, clearly indicating its potential to improve air quality in areas downwind of traffic emissions. MP levels were higher, especially closer to the roadside (-1 m) than (+2 m), indicating that the hedge serves as an effective barrier in intercepting and trapping airborne MPs (Blanuša et al., 2020; Kumar et al., 2022; Redondo-Bermudez et al., 2021). The most notable reductions occurred further behind the hedge, suggesting that its impact extends beyond the immediate vicinity, providing a cleaner air quality buffer for surrounding areas. These findings reinforce the importance of integrating green infrastructure into urban planning as a sustainable solution for reducing traffic-related MP pollution and improving public health, especially in areas directly impacted by high vehicular emissions. A detailed explanation of the hedge's removal efficiency for MP size and shape throughout the entire campaign is provided in Section 3.1.2.6.
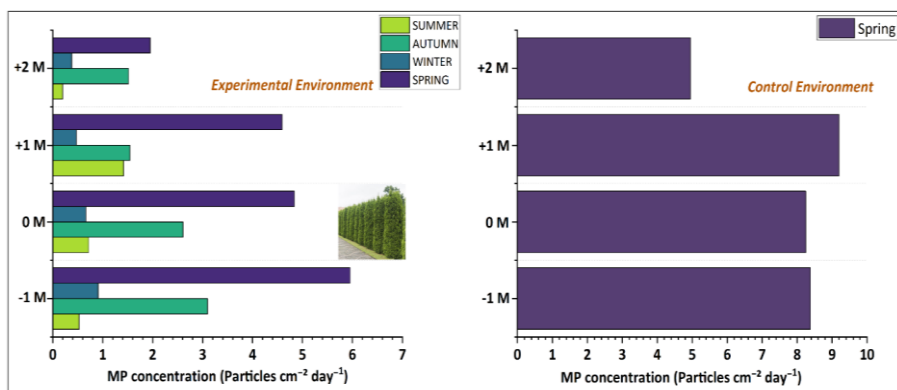
Fig. 11. MP concentration at varying distances from the road in the experimental environment (left panel) across all seasons and the control environment (right panel) during spring.

3.1.2. Physiochemical characteristics of MPs

3.1.2.1. Shape distribution

The shapes of MPs observed in the present study by optical microscopy were fragments and fibers. MP shapes distribution across different seasons and distances from a busy street throughout the study campaign reveals a total dominance of fragment particles. The highest average concentration of fragments was recorded in spring (98.25 %), while fibers were in the winter season (12.75 %) (Table 4). Furthermore, in spring, the fragment particles were dominant at all distances. At the same time, fibers were negligible (1-3 %) (Fig. 12). Winter exhibits a notable shift across all distances, with the highest concentration of fibers (22 %) observed at 0 meters. This observation suggests that colder temperatures and specific atmospheric conditions may influence the deposition behavior of fibers. Fibers can typically travel longer distances given their relatively larger aerodynamic diameter. However, their transport may be inhibited under particular environmental conditions, such as reduced turbulence and low dispersion of particles due to a lower atmospheric boundary layer associated with colder temperatures, leading to enhanced deposition in the local environment (Liu et al., 2022). These findings align with the previous study by (Xie et al., 2022), who reported that fragments were the dominant MP shape in urban environments, typically exceeding 85 % of the detected particles. Another study (Jiang et al., 2022) reported fragments constituting 99 % of the total MP in urban environments, while (Liao et al., 2021) found them to account for 83.5–94.2 %. This distribution is a characteristic of road surface and tire abrasion, where the wear and tear of tires against the road surface predominantly generates fragment-shaped particles. These particles are typically fragmented due to the continuous friction between tires and the road surface, producing smaller, more fragmented (irregular shape, hard, thick particles with sharp curved edges) than fibers (Tanaka & Takada, 2016). Fragments are more prevalent than fibers in road environments due to their primary sources, such as tire and road surface abrasion,

which generate abundant fragment particles (Jarlskog et al., 2021; Knight et al., 2020; Kole et al., 2017; Sommer et al., 2018).

Table 4. Average values of MP shape (fragment and fiber) in respective seasons.

Seasons	Fragment %	Fiber %
Summer	92.75	7.25
Autumn	94.25	5.75
Winter	87.25	12.75
Spring	98.25	1.75
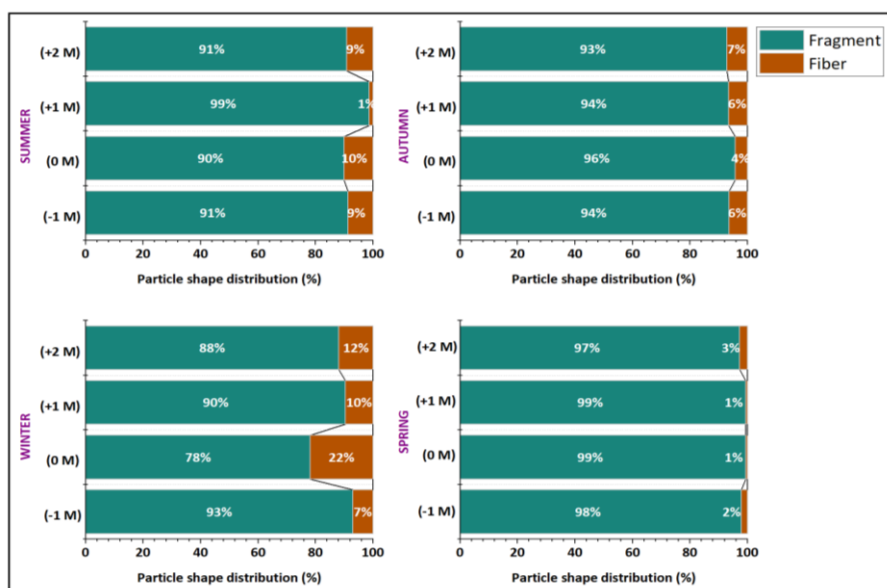
Fig. 12. Seasonal variation of MP shape distribution (fragments and fibers) at different distances from the street.
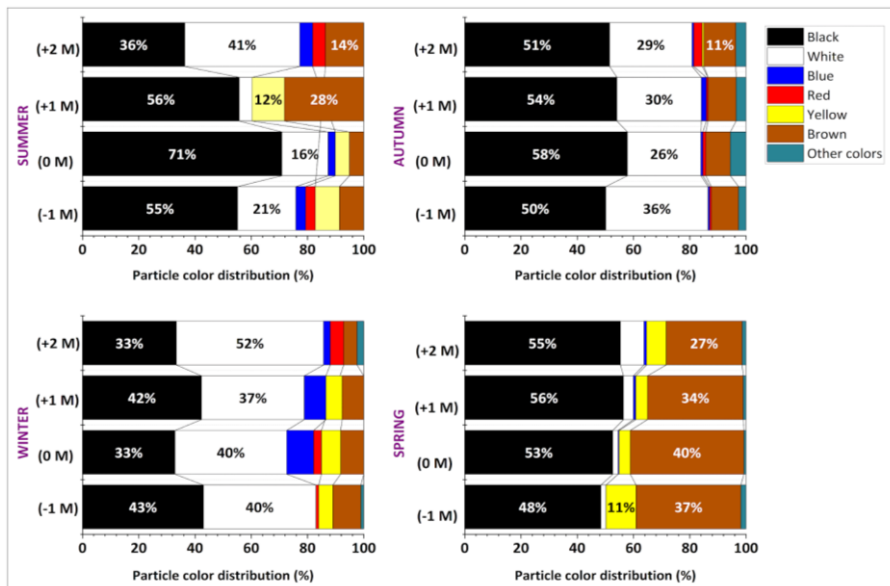
3.1.2.2. Color distribution

Color is a qualitative indicator of MPs' age and origin. During manufacturing, various colors are added to plastics to meet specific requirements and aesthetic needs, resulting in the diverse range of colors observed in urban environments (Khalid et al., 2020). The colored MP identified in roadside dust near urban streets likely originates from traffic-related activities and urban plastic waste. Other potential sources include atmospheric deposition, surface runoff, and human activities (Jahandari, 2023). Using an optical microscope, MP colors were identified in the filter samples and categorized into seven groups: white, yellow, red, brown, blue, black, and a mixed class labelled "other". The seasonal distribution of MP colors showed considerable variations across all distances (Fig. 13). Black was the most dominant color across all seasons, with the highest average concentration in spring (55.35 %), followed by white (42.16 %) in winter, and brown 26.98 % in spring. Blue, yellow, and red were less abundant in the study area (Table 5). During summer, the highest concentration of black color (71 %) was recorded inside the hedge (0 m) (Fig. 13). Winter showed a decline in black color (37.88 %). In contrast, white color peaked at 42.16 %, making it the most prevalent color in that season with the highest concentration (52 %) at +2 meters. Brown color reached its highest average concentration (26.98 %) in spring. Other colors, such as blue (4.92 %) and red (2.13 %), were most abundant in winter, while yellow peaked in spring at 6.98 % (Table 4). One of the major sources of black color in an urban environment is likely the wear and tear of vehicle tires. These particles often appear black due to the carbon black additives used in tire production, which provide strength, durability, and black color. Carbon black makes up between 22 % and 40 % of the weight of tires for light-duty vehicles (Kole et al., 2017). Consequently, the black color MP observed in the study area is likely a direct result of tire wear abrasion, a significant source of MP pollution in urban environments, particularly near roadways (Ballent et al., 2016). White and yellow are common colors

in thermoplastic road markings (TRMs), often selected for their high visibility and durability. TRMs are extensively used in highway and road construction, where the binder systems usually consist of a thermoplastic resin and a plasticizer or toughening agent, forming a solid, durable layer when applied to road surfaces (Mirabedini et al., 2020). Over time, traffic abrasion, weathering, and environmental exposure degrade these markings, releasing small MP particles into the surrounding environment. The seasonal variation in the color distribution of MPs highlights the dynamic and multifaceted nature of MP pollution sources in urban environments. The presence of other colors suggests the contribution of additional sources (e.g., roadside dust, textiles), environmental factors (weathering, resuspension, precipitation), and human activities (Zhang et al., 2021). These findings emphasize the complex relationship of multiple sources—traffic-related wear, plastic waste, and the degradation of urban infrastructure—driving MP contamination in urban areas.

Table 5. Average values of MP color distribution (%) in respective seasons.

Seasons	Black	White	Brown	Blue	Red	Yellow	Other
Summer	54.55	20.64	13.88	2.63	2.00	6.31	0.00
Autumn	53.40	30.46	9.94	0.91	1.30	0.15	3.83
Winter	37.88	42.16	7.67	4.92	2.13	4.40	0.85
Spring	55.35	8.37	26.98	0.93	0.00	6.98	1.40

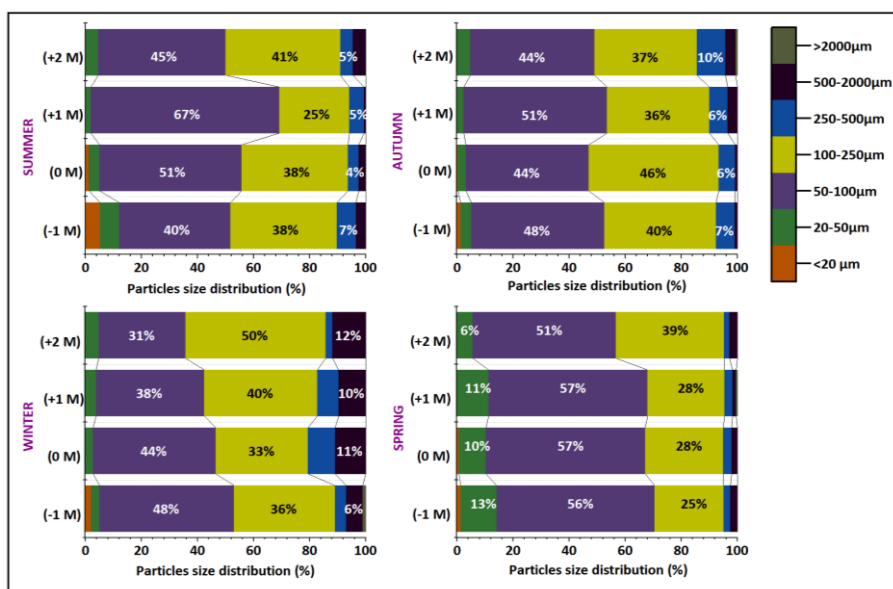**Fig. 13.** Seasonal distribution of MPs colors at different distances from the street.

3.1.2.3. Size distribution

The size distribution of MPs consistently showed a predominance of particles in the 50–100 μm size range across all seasons, with the highest average concentration observed in spring (55.26 %), followed by the 100-250 μm size range (39.82 %) in winter (Table 6). However, for the 50–100 μm size range across the distance, a high concentration of 67 % at +1 m during summer and a low concentration of 31 % at +2 m in winter were observed. The 100–250 μm size range exhibited greater variability, peaking at 50 % at +2 m in winter (Fig. 14). Notably, the 250–500 μm size range was only significant in autumn with an average of 7.33 %, whereas 500-2000 μm size range in winter (9.62 %). These results highlight the significant contribution of the 50–250 μm size range to the total MP load in the study area. While some seasonal and spatial fluctuations occur in other size ranges, the ongoing prevalence of particles within this range underscores its significance in MP pollution near roadsides.

The most significant proportion in this size range results from the fragmentation of large particles, specifically from tire wear, road surface, and other urban debris. Previous studies on tire wear particles (TWPs) reported that approximately 85 % of TWPs fall between 50 and 350 μm, with smaller particles (<50 μm) accounting for only 15 % (Z. Gao et al., 2022; Klockner et al., 2021; Kovochich et al., 2021; Kreider et al., 2010). This is consistent with the present study, where particles smaller than 50 μm made a relatively small contribution to the total MP load, with the highest average concentration (9.91 %) for the 20–50 μm size range observed in spring. These observations highlight vehicular emissions localized and significant effect on the size distribution of MPs in urban areas.

Table 6. Average values of MP size distribution (%) in respective seasons.

Seasons	<20 μm	20-50 μm	50-100 μm	100-250 μm	250-500 μm	500-200 μm	>2000 μm
Summer	1.61	4.29	50.76	35.45	5.09	2.79	0.00
Autumn	0.38	3.44	46.72	39.81	7.33	2.17	0.15
Winter	0.50	3.59	40.31	39.82	5.92	9.62	0.25
Spring	0.40	9.91	55.26	26.93	2.52	2.17	0.10

Fig. 14. Seasonal distribution of MPs size at different distances from the street.

3.1.2.4. Chemical composition of MP

The micro-FTIR spectroscopy analysis identified 10 distinct polymers in the collected MP samples: polyethylene (PE), synthetic rubber (SR), polyester (PES), polystyrene (PS), polysulfone (PSF), acrylates (ACRs), polyisoprene (PIR), polyamide (PA), polypropylene (PP), and polyvinyl chloride (PVC). The annual average analysis of MPs polymer composition revealed that PE was the most prevalent, constituting 43.13 % of the total MPs. This was followed by PIR at 18.37 %, ACRs at 17.94 %, and PES at 17.74 %. Other notable polymers included PVC at 15.80 %, PP at 14.82 %, PA at 14.45 %, SR at 13.59 %, and PS at 11.69 % (Table 7).

Table 7. Different polymers were observed in individual seasons and across all four seasons.

MPs	Average (all season), %	Seasonal highest average, %	Seasons

72

PE	43.13	69.05	Spring
PIR	18.37	35.96	winter
ACRs	17.94	28.52	summer
PES	17.74	19.50	Summer
PVC	15.80	15.80	Winter
PP	14.82	16.67	Spring
PA	14.45	21.43	Summer
SR	13.59	19.84	Summer
PS	11.69	14.29	Winter
PSF	-	9.09	Summer

The detailed seasonal and spatial distribution trends in the chemical composition of MP throughout the study campaign are presented in Fig. 15. PE is a versatile polymer frequently found in plastic bags, bottles, containers, and packing goods (Hahladakis & Iacovidou, 2018), with the highest seasonal average in spring (69.05 %), followed by PIR (35.96 %) in winter. ACRs had their highest recorded average value in summer (28.52 %), while PA, SR, PES, PP, PVC, and PS showed seasonal peaks between 21.43 % and 14.29 % across different seasons. The lowest average value was for PSF, with its highest seasonal average in summer (9.09 %) (Table 7). In summer, ACRs particles (54.55 %) dominated near the roadside (-1 m), likely from road markings and coatings that degrade under UV exposure and high temperatures (Lee et al., 2024). PE became more abundant as the distance from the street increased, reaching 33.3 % at (+2 m), followed by PES and SR (16.67 % each). PE consistently dominated in autumn and spring, where its proportion notably increased, especially in spring

(85.71 % at 0 m). The widespread presence of PE, particularly at further distances from the street, highlights its persistence in urban environments. In winter, PIR was the dominant polymer near the street (66.67 % at -1 m), but its proportion decreased with distance, while PE became more abundant at +2 m (53.33 %). PVC (17.31 %) also contributed notably at (+1 m), frequently used in consumer items and construction materials (Turner, 2019). Additionally, in spring, PES concentration increased at -1 m (28.6 %), indicating seasonal variations in polymer distribution. The highest PP concentration (22.2 %) occurred in winter near the roadside (-1 m), highlighting their widespread use in packaging materials, plastic bags, bottles, containers, disposable products, and textiles (Hahladakis & Iacovidou, 2018). These findings align with previous studies reporting PE as a dominant polymer in urban environments. For instance, (Ozen & Mutuk, 2025) reported 73 % of PE of the total MP load, while (Yang et al., 2023) found PE accounting for 30.08 % in urban environments. Similar trends were also observed in other reports (He et al., 2023; Sang et al., 2021). Other polymers also exhibited notable seasonal and spatial patterns, reflecting the urban environment's multifaceted sources of MP pollution.

TWPS are one of the significant sources of MPS, particularly PIR and SR, which are key tire components. Year-round tire wear abrasion increasingly infiltrates the urban environment, serving as a ubiquitous and constant source of MP pollution. The winter surge in PIR points to tire wear as a significant yet often overlooked contributor to MP pollution, reshaping our understanding of non-exhaust emissions. The seasonal dominance of PE, PIR, ACRs, and PES throughout the study illustrates their persistent presence in the study area, with the presence of other polymers reflecting the complex interaction between road infrastructure, non-exhaust traffic emissions, and other sources of MP pollution (Wang et al., 2024; Yang et al., 2023; Zhang et al., 2021). These findings emphasize the need for innovative mitigation strategies

for polymer-specific behaviors and seasonal variations in urban MP dynamics.
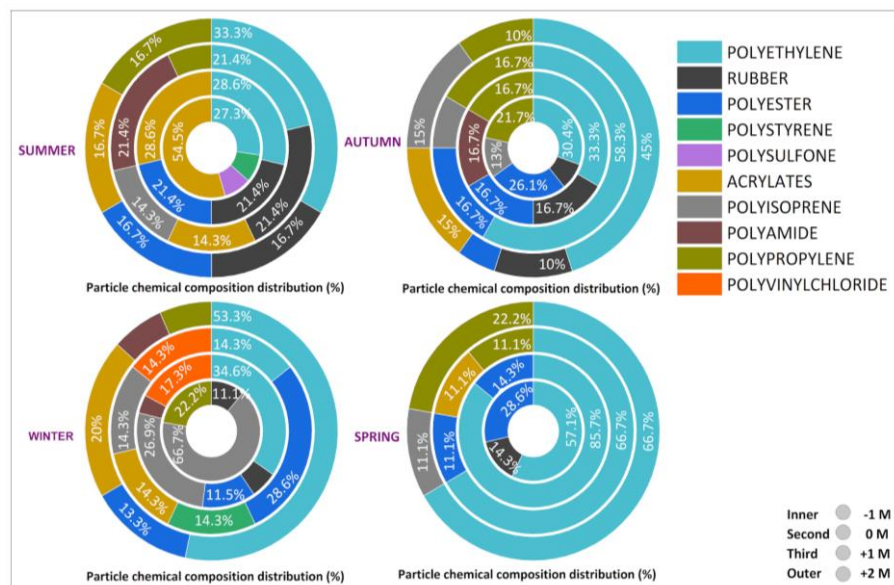

Fig. 15. Seasonal distribution of MP chemical composition (%): The innermost ring denotes -1 meter, while the outermost ring indicates +2 meters.

3.1.2.5. Vertical distribution of MP characteristics within the hedge

The concentration of fibers increases slightly at the upper part of the hedge (0.72 %) compared to the middle part (0.23 %), while fragments dominated at both levels of the hedge (Fig. 16a). Fibers are more likely to deposit at higher elevations (upper edge), around 1.5 meters, this is consistent with the previous research by (Li et al., 2020), which reported airborne fiber concentrations were higher at 1.5 meters compared to the higher altitudes. This trend indicates that fibers exhibit a slight tendency to upward transportation due to their aerodynamic properties; however, further statistical analysis is required to confirm this trend. Particles in the 50-100 µm size range were dominant at both

elevations, followed by 100-250 μm (Fig. 16c), a similar trend was observed in the horizontal distribution (Fig. 15). Black particles were abundant at both the middle and upper edges, accounting for 59.23 % and 60.10 % of the total particles, respectively (Fig. 16b). Their consistent presence, along with the dominance of the 50–100 μm size range across vertical levels, indicates a high prevalence and stability of these particles in the study area. PE was the most abundant polymer in horizontal distribution; this trend of dominance continues in the vertical distribution, with 66.66 % at the middle edge, emphasizing its prevalence in the urban environment (Ozen & Mutuk, 2025; Yang et al., 2023). Other polymers like PES 16.67 % at the middle edge and SR 17.78 % at the upper edge also highlight the presence in vertical distribution. The increase in PSF (from 0 % to 17.78 %), ACRs to (13.33 %), and PIS to (37.8 %) at the upper edge suggests that these polymers exhibit vertical transport tendencies and are deposited at higher elevations (Fig.16d). Overall, these findings highlight the relationship between particle characteristics—such as size, shape, and aerodynamic behaviors in determining particle distribution both vertically and horizontally.
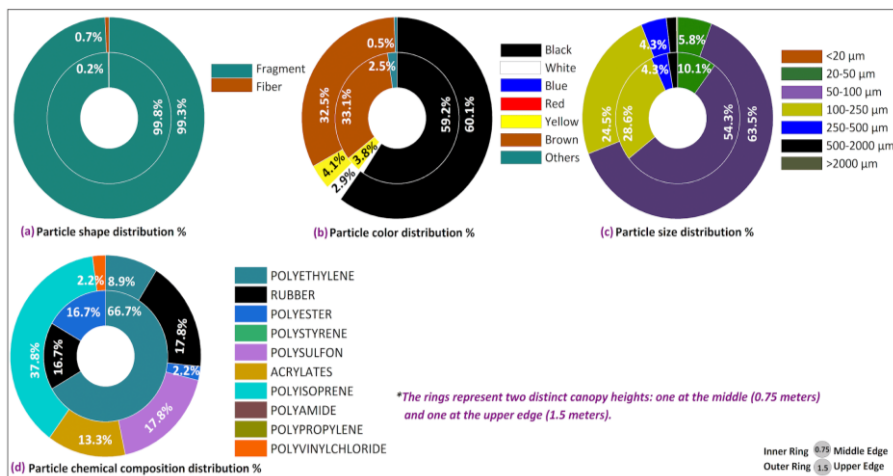
Fig. 16. Vertical profiling of MP characteristics: (a) shape, (b) color, (c) size, and (d) chemical composition at two heights: middle and upper part of the hedge.

3.1.3. Effectiveness of Urban Green Infrastructure

Thuja occidentalis hedges have proven highly effective in reducing traffic-related MP pollution, highlighting their potential as a sustainable solution. By evaluating MP removal efficiency across various particle size intervals and shapes, the study highlights the hedge's role in reducing airborne MP pollution in urban environments, where vehicular emissions and other anthropogenic activities significantly contribute to air quality degradation. The hedge achieved the highest MP removal efficiencies during summer, with 64.5 % for total MPs, 64.3 % for fragments, and 71.4 % for fibers. In contrast, the lowest efficiencies were observed in autumn, with 40.8 % for total MPs, 23.4 % for fragments, and 11.5 % for fibers (Fig. 17a). The average removal efficiencies were (54.29 % for total MPs, 50.41 % for fragments, and 44.54 % for fibers throughout the study period, which are presented in (Table 8). The hedge's ability to capture fragment particles, which are predominantly associated with vehicular activities, particularly wear and tear from tires, showcases their potential role in reducing traffic-related MP pollution. Their dense arrangement and needle-like leaves provide a large surface area favorable for trapping these particles in the urban environment. The consistently high removal efficiency for fragments and its notable performance in capturing fiber position the hedge as a valuable green infrastructure solution for reducing MP pollution. Fig. 17 b illustrates the seasonal variation in hedge removal efficiency based on particle size range. The overall mean removal efficiencies for the respective size ranges are presented in Table 7. The highest average removal efficiency was observed for the size range of (50-100 µm) at 67.25 %, with a seasonal high of 94.24 % in the spring. This was followed by 20-50 with an average of 53.29 %, with the highest value in summer reaching 81.84 %. Furthermore, in winter, the 100–250 µm size range recorded its peak efficiency at 56.86 % and the 250–500 µm range peaked at 75 % (Fig. 17b). The hedge effectively captures MP across all size ranges, with exceptionally high removal efficiency for (50-100 µm) size range

specifically in the spring season. This alignment between MP high concentration and maximum removal efficiency in spring highlights the hedge's crucial role in mitigating traffic-related MP pollution, particularly during high-emission periods. These results emphasize the effectiveness of urban green barriers in reducing exposure to airborne MPs, reinforcing the value of strategic vegetation placement in pollution control strategies. The effectiveness of UGI in reducing air pollution in the present study is further supported by the results published by (Abhijith et al., 2022; Maher et al., 2013). This highlights the hedge's capacity to mitigate pollution from vehicular emissions and its critical role in improving urban air quality, offering a powerful means to combat MP pollution in the urban environment.

Table 8. The average removal efficiency of the hedge for microplastics (MPs), as determined by their size and shape characteristics.

Size	20-50 μm	50-100μm	100-250 μm	250-500 μm
Mean value	53.29 %	67.25 %	53.18 %	50.49 %

| Shape	Total MP	Fragment	Fiber	
Mean value	54.29 %	50.41 %	44.54 %	
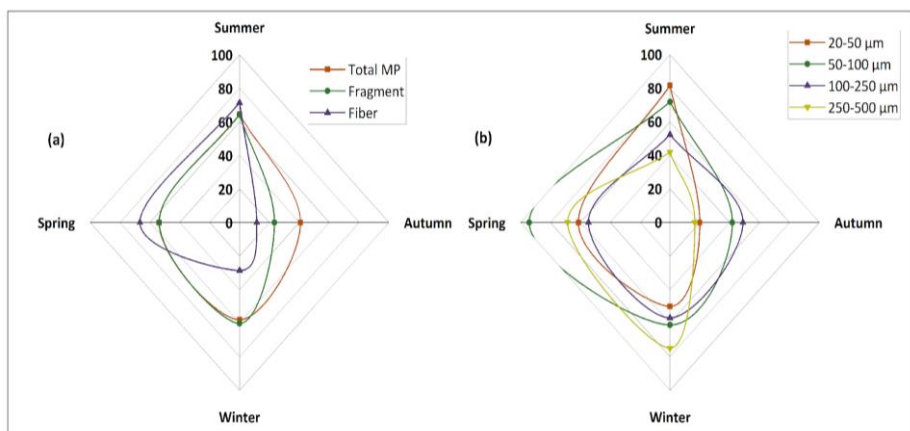
Fig. 17. Seasonal evaluation of MPs removal efficiency (%) of *Thuja occidentalis*: (a) shape-based (fragment and Fiber, (b) size-based (ranging from 20-50 µm to 250-500 µm).

3.1.4. Inhalation risk index of MPs

The MPs' inhalation risk index (IRI) was assessed at two locations during the study period. At -1 m (Roadside), where MP concentrations were higher, the IRI was also high, indicating a significant inhalation risk due to elevated exposure, primarily from vehicle emissions such as tire wear and brake dust. In contrast, at +2 m (Behind Hedge), a *Thuja occidentalis* reduced the MP exposure, lowering the IRI and inhalation risk. Across all seasons, the highest exposure to airborne MPs was observed in the spring, with an IRI of 831.1, indicating a severe inhalation risk at the roadside (Fig. 18). The lowest exposure was observed in the summer, with an IRI of 83.7, reflecting lower MP levels at the roadside. The *Thuja occidentalis* consistently demonstrated its ability to reduce inhalation risk at both locations. The degree of reduction varied from 28.8 % in autumn to 71.3 % in spring, with the highest reductions occurring in the winter (68.6 %) and spring (71.3 %) seasons. These findings suggest that the hedge is critical in filtering and trapping MPs, offering significant protection against inhalation exposure. However, the extent of the

reduction appears to be influenced by seasonal factors such as traffic volume, weather conditions, and wind patterns. In conclusion, the IRI values indicate varying levels of exposure to airborne MPs, with roadside areas generally exhibiting higher risks. The *Thuja occidentalis* effectively reduced these risks, with the most significant reduction observed in spring, followed by winter, summer, and autumn. The results emphasize the importance of urban green infrastructure, such as the *Thuja occidentalis*, in mitigating MP pollution and its associated health risks in roadside environments.
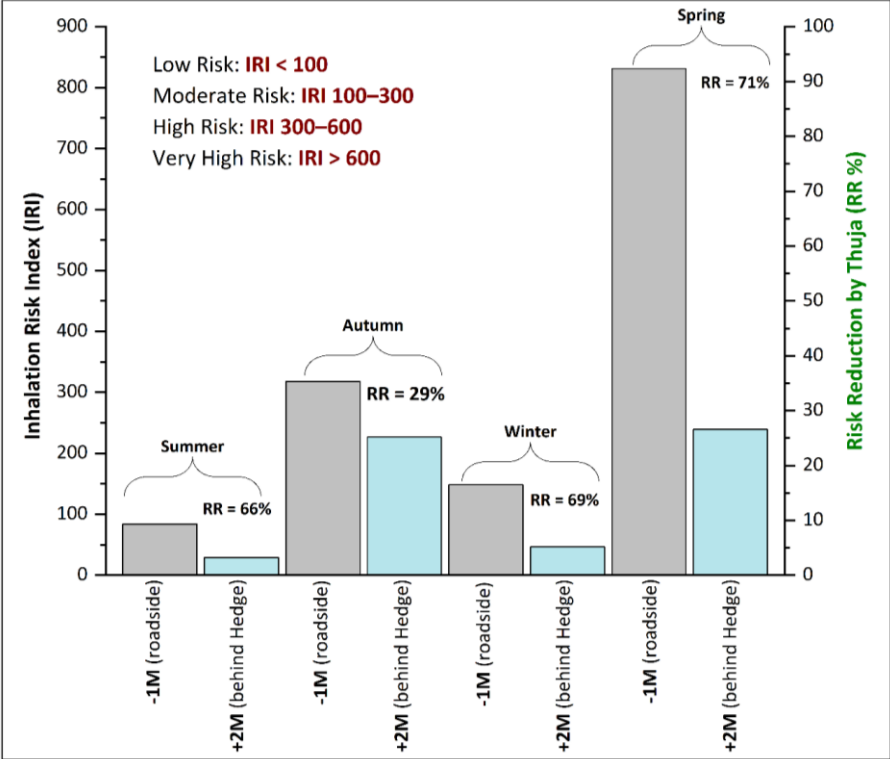

Fig. 18. Inhalation risk index and risk reduction of MPs by *Thuja occidentalis* hedge.

3.1.5. Correlation analysis of MP characteristics with distances from a street

A pairwise Pearson's correlation and a Mantel test were conducted to examine the relationships between MP concentrations and their physicochemical characteristics across different distances from the street (Fig. 19). The results indicate a spatial variation in MP attributes, which reflects both proximity to traffic sources and the influence of vegetative barriers. The area closest to the road (-1 m) showed a strong positive correlation with very small-sized MPs (<20 µm) (Mantel's r > 0.5, p ≤ 0.001) and small-sized MPs (20–50 µm) (Mantel's r > 0.5, p ≤ 0.05). This trend likely reflects direct influence from vehicular emissions, including tire and brake wear, as well as the resuspension of road dust (Sommer et al., 2018). Similar dominance of small-sized particles near traffic sources has been observed in previous studies (Ozen & Mutuk, 2025). Additionally, a significant correlation with PE was observed at this location, showing the dominant presence and resilience in the urban environment. Previous studies support these results and confirm the dominant presence of PE in road environments (Ozen & Mutuk, 2025; Yang et al., 2023). At the 0-meter distance (within the hedge), the hedge appears to be a physical barrier and a temporary sink, capturing MPs from the roadside environment through atmospheric deposition mechanisms such as interception (Kumar et al., 2022). A statistically significant accumulation of small-sized MPs (Mantel's r > 0.5, p ≤ 0.05) here suggests the potential role of the *Thuja occidentalis* hedge in trapping particles from the air. The area immediately behind the hedge (+1 m) shows a strong correlation with small size and a statistically significant presence of medium-sized MPs (50–100 µm and 100–250 µm), further supporting the influence of non-exhaust emissions in the roadside environment (Sommer et al., 2018). While further beyond the hedge (+2 m), MP concentration decreases, with no significant correlation to particle size (p > 0.05).
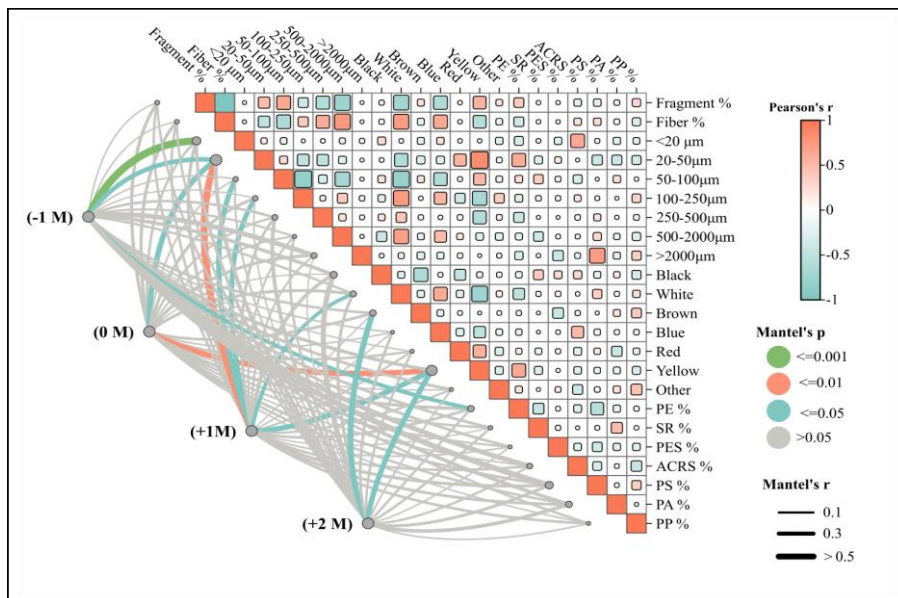
Fig. 19. Correlation of MP concentrations and physicochemical characteristics at different distances from a street.

However, significant correlations persist for MP colors, particularly brown and yellow (Mantel's r > 0.5, p ≤ 0.05). Notably, yellow remains a significant color factor at 0 m, +1 m, and +2m. The consistent appearance of yellow MPs across multiple distances (0 m to +2 m) might suggest these particles are likely to originate from multiple sources (e.g., traffic signs and road paint) (Mirabedini et al., 2020). Additionally, darker colors like brown could result from weathered particles, indicating aging processes during atmospheric transport (Schmidtmann et al., 2025). These findings highlight the spatial variability of MP characteristics influenced by traffic emissions and the mitigating role of the *Thuja occidentalis* hedge against MP pollution.

3.1.6. Chapter conclusions

Urban green infrastructure, such as *Thuja occidentalis* hedges, can significantly reduce airborne microplastic concentrations near roadways, particularly from traffic-related non-exhaust sources. The average removal efficiencies were 50 % for MP fragments and 44 % for fibers, with the highest efficiency (67 %) observed in the 50–100 µm size range, the most abundant particle class identified in the study area. A detailed size-resolved analysis demonstrated that removal efficiency peaked within the 50–100 µm size range. In comparison, particles in the 20–50 µm and 100–250 µm ranges showed similar efficiencies (53 %), while the lowest efficiency (50 %) was observed for the 250–500 µm fraction. These results suggest that mid-sized particles are more effectively captured, likely due to their aerodynamic properties and greater tendency to interact with leaf surfaces. In contrast, smaller and larger particles are less efficiently removed, possibly due to their higher mobility or lower deposition potential.

The inhalation risk index of microplastics was highest in spring, reaching a value of 831, and lowest in summer, at 84. Notably, *Thuja occidentalis* contributed to a 71 % reduction in inhalation risk during the spring, underscoring its effectiveness in mitigating airborne microplastic pollution in the urban environment. Spatial analysis revealed that smaller MPs (<20 µm) were predominantly concentrated at the roadside (-1 m), confirming that vehicular activity is a significant source of airborne MP emissions. Polymer types such as PE, PIR, ACRs, and PES accounted for 43 %, 19 %, 18 %, and 18 % of the collected samples, highlighting the complexity and diversity of MP sources in the urban environment.

3.2. Analysis of national exhaust emissions

3.2.1. Exhaust emissions trend of Lithuania from 2005 to 2020

Before investigating personal exposure to PM_S and black carbon, emissions from various sectors were analyzed to identify key sources and trends. Figure 20 illustrates the total national emissions, measured in gigagrams (Gg), from 2005 to 2020. While emissions slightly declined throughout these 15 years, their trajectory remained largely consistent. In 2020, the reported emissions of $PM_{2.5}$, PM_{10}, and BC were 6.51 Gg, 17.75 Gg, and 1.90 Gg, respectively. Compared to the baseline year 2005, these figures represent 1.26 %, 1.06 %, and 1.27 % reductions. The peak values recorded for PM_{10}, $PM_{2.5}$, and BC occurred in 2015, 2006, and 2008, reaching 19.49 Gg, 8.53 Gg, and 2.53 Gg, respectively. A notable decline in emissions was observed in 2009, attributed mainly to the global financial and economic crisis, which reduced industrial output. By 2020, the country recorded its lowest emissions levels for the three pollutants over the past 15 years. The rate of decline for $PM_{2.5}$ emissions was more pronounced, averaging a reduction of 0.10 Gg per year, whereas PM_{10} and BC each reduced at an average rate of 0.03 Gg per year. This could be related to BC being found in the PM_1 fraction. Moreover, $PM_{2.5}$ is formed from anthropogenic emissions and secondary formation (Kuang et al., 2022).

Between 2005 and 2020, $PM_{2.5}$ emissions in Lithuania experienced a notable reduction of approximately 17.2 %, declining from 8.21 kilotons in 2005 to 6.51 kilotons in 2020. This downward trend was primarily driven by a significant decrease in liquid fuel usage within the energy production sector. In 2020, total national emissions of $PM_{2.5}$ reached 6.51 gigagrams, representing a 7.6 % decrease compared to 2019 and a 20.7 % reduction relative to 2005 levels. The energy sector, including transport, was the predominant source of PM emissions, contributing 73 % of $PM_{2.5}$. In contrast, this sector accounted for only 30.1 % of PM_{10} and 1.11 % of BC emissions. Industrial Processes and Product Use (IPPU) accounted for 15.7 % of

PM$_{2.5}$ and 7.7 % of PM$_{10}$ emissions in 2020. These figures are closely linked to the widespread combustion of biomass, particularly wood burning, within the residential sector (classified as NFR 1.A.4.b). Across the European Union (EU28), PM$_{2.5}$, PM$_{10}$, and BC emissions decreased by 1.9 %, 2.2 %, and 4.4 %, respectively, between 2018 and 2019.
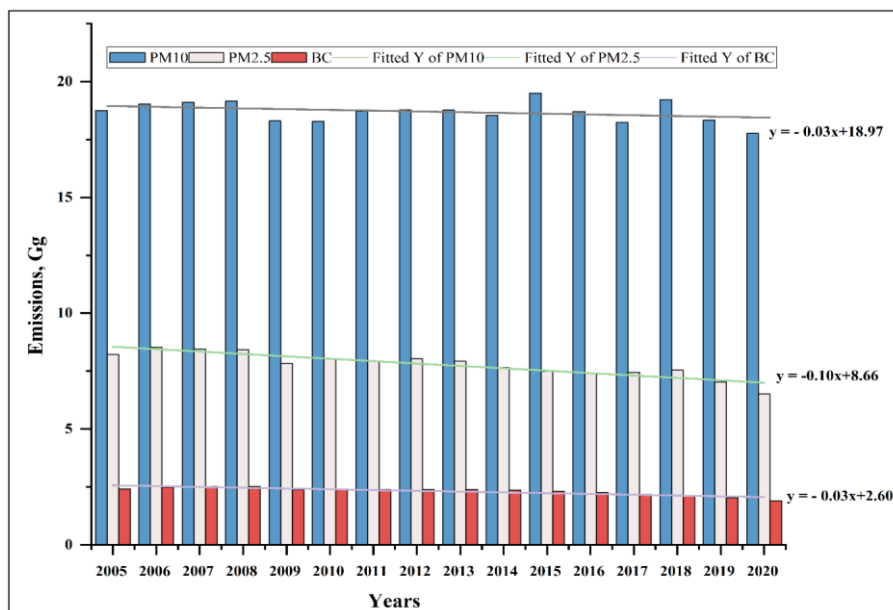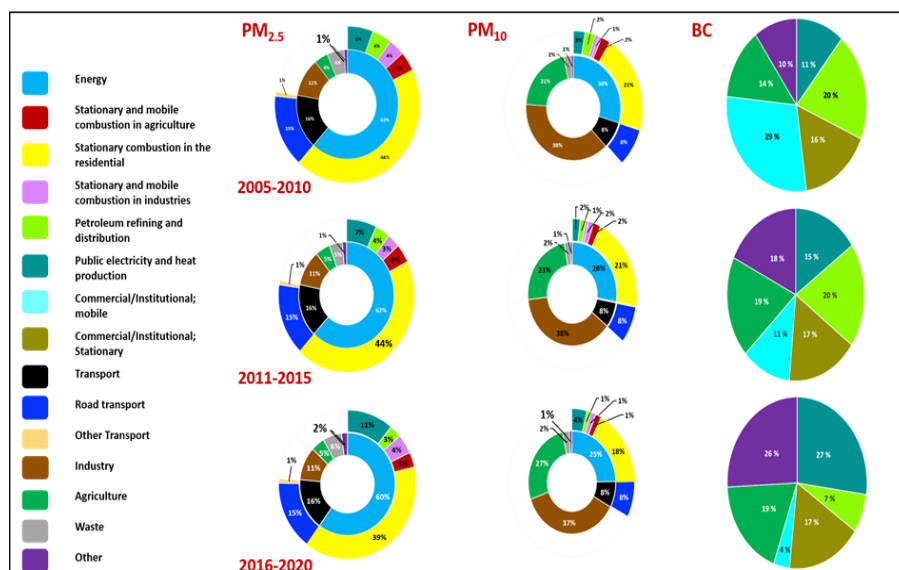

Fig. 20. Lithuania's overall national emissions of PMs and BC from 2005 to 2020.

3.2.2. Exhaust emission trends by sector

Between 2005 and 2020, the energy sector emerged as the dominant source of PM$_{2.5}$ emissions, accounting for 61.33 %. Despite this, emissions from the sector exhibited only slight reductions—0.7 % between 2010 and 2015, and 1.8 % from 2016 to 2020. Within the energy sector, stationary combustion in residential areas was the primary contributor, representing 42.33 % of emissions over the entire period. The transport and industrial sectors demonstrated comparable patterns, contributing 16 % and 11 % of PM$_{2.5}$ emissions, respectively,

without noticeable variation during the same timeframe. In contrast, PM_{10} emissions were primarily associated with industrial activities, which contributed 37.67 % of the total, followed by the energy sector at 27.67 %, over the period 2005–2020. The industrial sector has a minimal 1 % decline in PM_{10} emissions between 2016 and 2020. Meanwhile, emissions from the energy sector showed a gradual decrease of 3 % from 2005 to 2010 and an additional 5 % from 2011 to 2016. The transport sector accounted for 8 % of PM_{10} emissions.

BC emissions originating from the mobile segment of the commercial and institutional sectors experienced notable reductions, falling by 18 % from 2011 to 2015 and by a further 7 % between 2016 and 2020. However, emissions from stationary sources within the same sector remained largely unchanged. Notably, BC emissions from the public electricity and heat production sector increased by 11 % during 2016–2020, while a 13 % decline was observed in the petroleum refining and distribution sector over the same period. Other sectors reported a 16 % rise in BC emissions between 2016 and 2020 (Fig. 21).


Fig. 21. Lithuania's national emissions (%) of PM and BC from different sectors, 2005 to 2020.

3.2.3. PM mass concentrations trend in major cities of Lithuania

Both mobile and stationary sources of emissions primarily influence air quality in urban environments. The PM_{10} and $PM_{2.5}$ mass concentrations provided by the emission sources in Fig. 22 are also available for the sampling locations shown in Figs. 23 and 24. Only $PM_{2.5}$ data is available for a single site from 2005 to 2020. Emissions tend to be elevated in urban areas, specifically in high-traffic and industrial zones, making them a key focus for analyzing annual mass concentration trends, particularly in major cities and industrial hubs. Monthly average time series of PM_{10} mass concentrations were compiled for eight locations in the largest cities, and the trend is represented by a linear regression with a 95 % confidence interval, as illustrated in the figures. The trend analysis indicates a slight reduction in PM_{10} levels across all major cities, with a range of 0.38 to 0.74 µg/m³ per year, except for Klaipėda Šilutės pl., where an increase of 0.53 µg/m³ per year (representing a -0.3 % annual change) was observed. For $PM_{2.5}$, a positive trend was found, except at the Kaunas Noreikiškes and Petrašiunai sites, where negative trends of -0.50 µg/m³ (3.1 % per year) and -0.6 µg/m³ (2.7 % per year) were recorded, respectively. These negative trends at these two sites align with the observed trend in PM_{10} levels.

In the capital city of Vilnius, the smallest decrease in PM_{10} concentration was observed in Vilnius Lazdynai, where the trend showed a reduction of just 0.06 µg/m³ per year (a 14 % decrease from 2005, equivalent to a 0.9 % annual reduction). In contrast, the sharp decline was seen in Vilnius Savanorių pr., with a decrease of 0.58 µg/m³ per year (a 57 % drop from 2005, or -3.8 % annually), which also exhibited the highest concentration and percentage decline (Fig. 18). The European Union's air quality directives (2008/50/EC) and the World Health Organization's (WHO) Air Quality Guidelines (updated in 2021) set limits on key air pollutants, with national ambient air quality standards that must not be exceeded within a specified period.

These standards apply on both daily and annual scales, with the EU setting the annual PM_{10} limit at 40 μg/m³ and the WHO at 15 μg/m³. As depicted in Figs. 16 and 17, all cities significantly exceed the WHO standards for both $PM_{2.5}$ and PM_{10}. The highest annual mean concentrations were found at traffic-related sites, specifically in Vilnius Žirmūnai and Klaipėda Šilutės pl., where the levels are nearly at the EU's permissible limit for PM_{10}, in contrast to other locations.
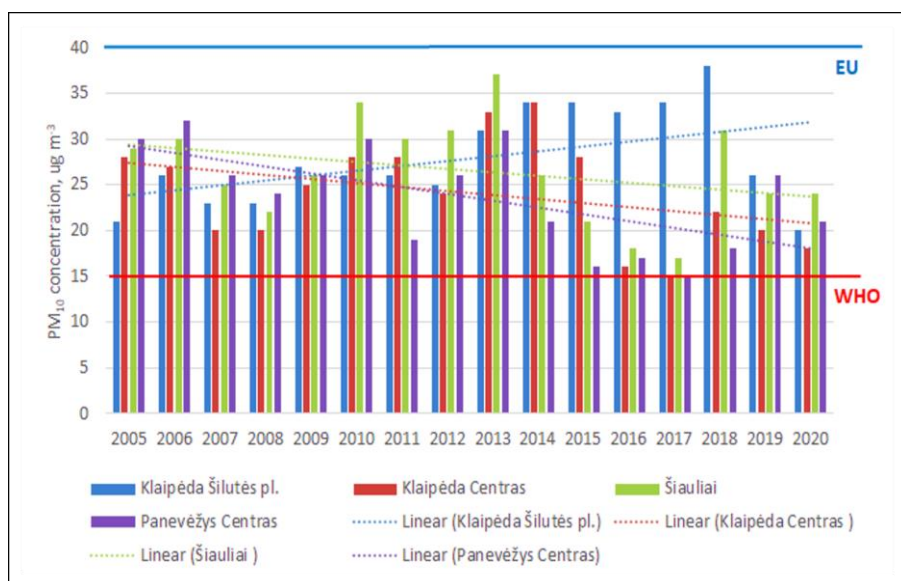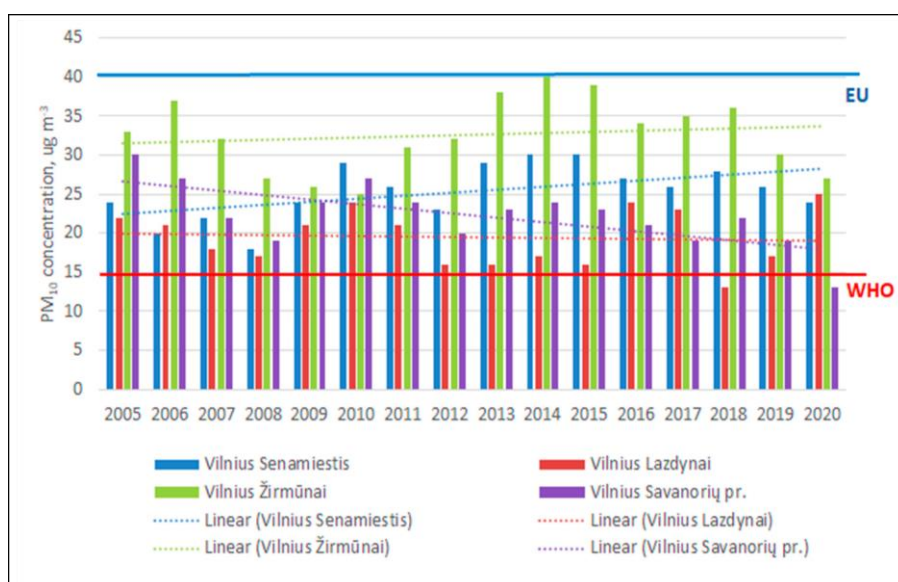

Fig. 22. Annual average PM_{10} mass concentration trends in major cities of Lithuania.
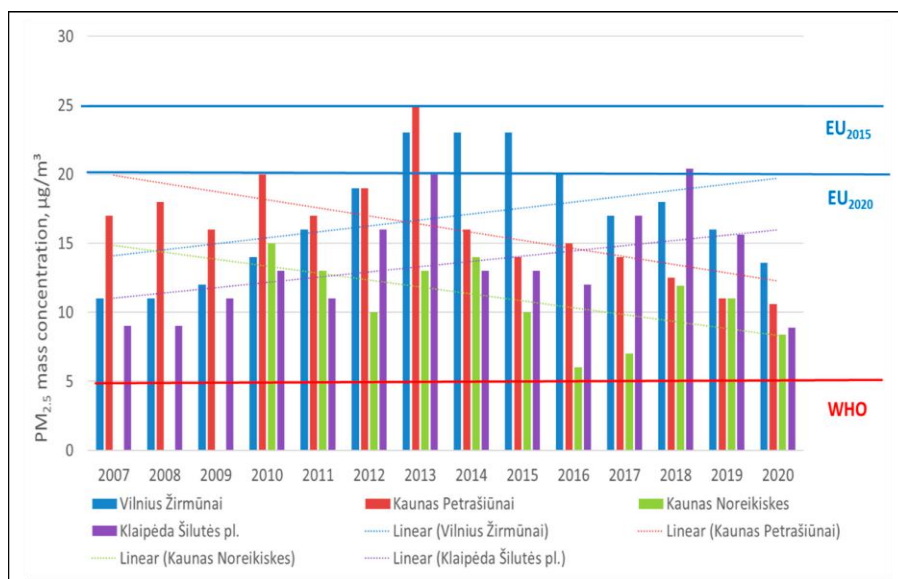
Fig. 23. Annual average PM$_{2.5}$ mass concentration and trends in major Lithuanian cities.

Fig. 24. Annual average PM$_{10}$ mass concentration at the key location in Vilnius's capital city.

### 3.2.4. Correlation analysis of emission sources and mass concentrations

An intercorrelation analysis was conducted to investigate the associations between emissions and ambient PM mass concentrations. Specifically, Pearson correlation coefficients were calculated to evaluate the relationship between annual emission levels and observed mass concentrations across all monitored sectors and locations from 2005 to 2020. In Lithuania, the dominant contributors to primary PM_{10} emissions are stationary and mobile combustion sources. As a result, most urban monitoring stations—such as Vilnius Savanorių pr.; Kaunas Petrašiūnai, Noreikiškės, and Dainava; Klaipėda city center; Šiauliai; Panevėžys center; and Jonava—exhibited a positive correlation between emissions and measured PM_{10} concentrations. Surprisingly, road transport emissions demonstrated a weak negative correlation with PM_{10} at several sites. A notable example includes the Vilnius Lazdynai station, which reflects an urban background environment and shows a negative correlation of −0.65 between total BC emissions and PM_{10} concentrations. Conversely, the Vilnius Žirmūnai site, which is influenced by traffic emissions, exhibited a positive correlation of 0.49. For $PM_{2.5}$, strong positive correlations were identified with both road transport, known to emit fine particles, and stationary combustion sources. Emissions from residential stationary combustion were significantly correlated with $PM_{2.5}$ concentrations at the Kaunas Noreikiškės (r = 0.62) and Petrašiūnai (r = 0.82) sites. These locations, interestingly, also displayed declining concentration trends, distinguishing them from other monitoring sites.

3.3. TEM and EDX analysis of BC particles during mobile measurement

Particle samples were collected inside and outside the vehicle (Fig. 25), and energy-dispersive X-ray (EDX) spectra were recorded for individual particles and larger aggregated areas. To ensure accuracy, the contribution of copper from the sampling equipment was

excluded from the EDX weight percent calculations. A typical agglomerate of BC particles was observed to consist of spherical particles fused in a chain-like formation (Fig. 30), with an approximate primary particle diameter of 30 nm. In contrast, BC agglomerates sampled inside the vehicle had diameters ranging from 300 to 400 nm. Transmission electron microscopy (TEM) images confirmed that the particles collected from the external environment were significantly larger than those found inside the vehicle, with the former reaching up to 2 µm in diameter. Additionally, the particles in the external samples exhibited a more complex compositional profile. EDX spectrum analysis revealed that carbon was the predominant element in both sets of samples, comprising 88.22 % of the outside air sample and 97.05 % of the inside air sample. However, the outside air sample also contained small proportions of sulfur (1.54 %) and silicon (0.55 %), which are typical soil constituents, as well as titanium dioxide (TiO_2) at 4.04 %, a substance commonly used in road paints.

In conclusion, the findings indicate that particles gathered from the external environment were larger and exhibited a more varied composition, including additional elements like sulfur, silicon, and titanium dioxide. These characteristics suggest that a combination of vehicle emissions, road dust, and materials such as road paint influences external particles.
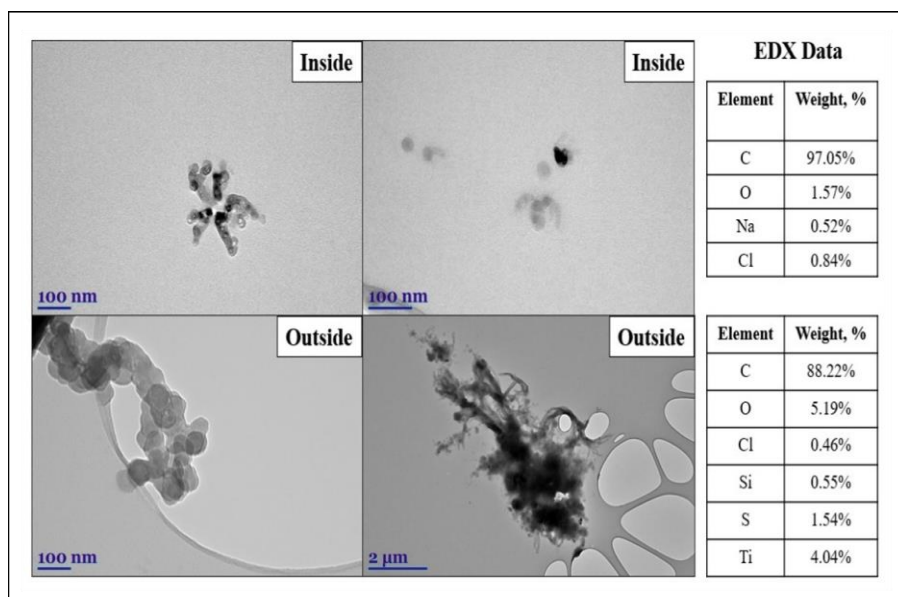
Fig. 25. Displays transmission electron microscopy (TEM) imagery and corresponding energy-dispersive X-ray spectroscopy (EDX) analyses of individual BC particles collected both inside and outside the vehicle.

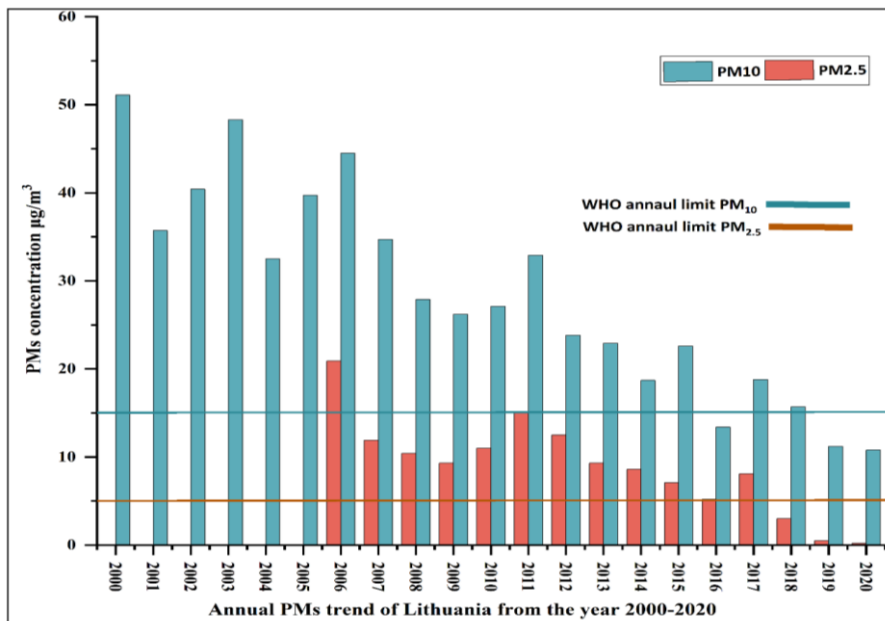### 3.3.1. Exposure to PMs mass concentration in urban environments

Over 70 % of the European Union's population lives in urban environments (Zauli-Sajani et al., 2024), where approximately 96 % are exposed to concentrations of fine PM (PM$_{2.5}$) that exceed the updated air quality guidelines established by the World Health Organization in 2021 (Table 9) (Cichowicz & Bochenek, 2024). Urban environments, characterized by dense populations and increased economic activity, are commonly associated with elevated air pollution levels, which are in turn linked to numerous adverse health outcomes, including respiratory illnesses, cardiovascular diseases, and certain forms of cancer. In Lithuania, PM concentrations have markedly declined over the past two decades. Since joining the European Union in 2004, the country has aligned with rigorous EU environmental

policies. Adopting stricter emission controls and air quality regulations has played a crucial role in reducing PM emissions across major sectors, e.g., the energy sector, industrial, petrol refining and distribution, and commercial/institutional – mobile sector. For instance, PM_{10} levels decreased from 51.1 µg/m³ in 2000 to 10.8 µg/m³, while $PM_{2.5}$ concentrations dropped from 20.9 µg/m³ in 2006 to just 0.2 µg/m³ by 2020 (Fig. 26).

Table 9. Annual and 24-hour limit values for PM_{10} and $PM_{2.5}$ as defined by the WHO and the EU.

PM_{10} standard	Protection objective	Averaging period	Value	Max number of exceedances	Date to be achieved (by and maintained thereafter)
EU limit value	Human health	1 day	50 µg/m³	35	1 January 2005
WHO limit value		1 day	45 µg/m³		22 September 2021
EU limit value	human health	1 year	40 µg/m³		1 January 2005
WHO limit value		1 year	15 µg/m³		22 September 2021
$PM_{2.5}$ standard	Protection objective	Averaging period	Value	Max number of exceedances	Date to be achieved (by and maintained thereafter)

EU target	human health	1 year 1 day	25 µg/m³ 20 µg/m³	1 January 20151 January 2020
Exposure Reductio n			Target of 20 % reduction in concentra tions at urban backgrou nd.	Between 2010 and 2020
WHO limit value		1 year	5 µg/m³	22 Septembe r 2021
WHO limit value		1 day	15 µg/m³	

Fig. 26. Urban population exposed to PMs concentrations above selected EU air quality standards, EU-27.

### 3.3.2. Personal exposure to BC and PM in urban microenvironments

3.3.3. BC measurement campaign summary

The results from (Figure 27) summarize BC mass concentrations, their source-specific contributions, and aerosol particle number and mass concentrations recorded in March 2022 at the urban background monitoring site. The average monthly total aerosol particle number concentration (N_{total}), measured within the 10–430 nm size range, was 9820 particles per cubic centimeter (SD: 6410 #/cm³). The hourly concentrations ranged from a minimum of 740 #/cm³ to a peak of 38,370 #/cm³. The corresponding aerosol mass concentrations (M_{total}) exhibited substantial temporal variability, with values spanning from 0.3 to 33.4 µg/m³ and a mean of 6.2 µg/m³ (SD: 5.3 µg/m³). During the targeted experimental period (17–18 March), the average M_{total} concentrations reached 11.3 and 12.7 µg/m³, aligning with the monthly distribution's upper quartile (Q3). Hourly BC mass concentrations across March ranged between 0.30 and 9.01 µg/m³, with a mean value of 1.94 µg/m³ (SD: 1.80 µg/m³), as illustrated in (Fig. 27). The traffic-related fraction of BC (BC_{tr}) closely mirrored the overall BC concentration (correlation coefficient r = 0.98) and constituted approximately 66 % of the total BC mass. BC_{tr} was predominantly observed during daytime hours (08:00–18:00 LT), while the biomass-burning-related fraction (BC_{wb}) accounted for the remaining 34 % and showed elevated contributions during the night, peaking at 42 % around 04:00 LT. These diurnal variations in BC concentrations reflected the combined influence of meteorological conditions, vehicular activity patterns, and domestic biomass burning for heating. A strong positive correlation (r = 0.83) was found between BC mass concentrations and N_{total}, suggesting a notable impact of BC emission sources on the total particle number concentration within the sub-430 nm range. In contrast, the correlation between M_{total} and BC was moderate (r = 0.68), indicating that BC plays a comparatively

minor role in contributing to PM_1 mass than particle number concentrations.

New particle formation (NPF) events occurred predominantly in two daily windows—between 07:00 and 08:00 and 18:00 and 20:00 LT—with peak particle concentrations reaching up to 49,200 #/cm³. Daytime concentrations were lower, averaging around 3890 #/cm³, likely due to enhanced atmospheric dispersion, reduced traffic emissions, and a higher boundary layer, as noted by (Byčenkienė et al., 2023). During the initial field experiment (FTMC1–FTMC2), all size modes exhibited their lowest number concentrations. However, particle sizes below 100 nm showed distinctly different trends, potentially influenced by a higher mixing layer during daytime. The morning segment of the FTMC1–Home route displayed the highest nucleation mode concentration, reaching 8960 #/cm³. In contrast, the evening trip along the same route was characterized by a dominance of particles around 70 nm in diameter, with concentrations up to 3000 #/cm³. Normalized distributions of particle number (dN) and mass (dM), shown in Fig. 28, revealed a clear shift in morning profiles, with increased dN values for particles smaller than 70 nm compared to larger modes at other times of the day. These findings underscore the frequent occurrence of NPF events in urban background environments. The mobile measurement period, coinciding with NPF events on March 17 and 18, is depicted in Fig. 28.
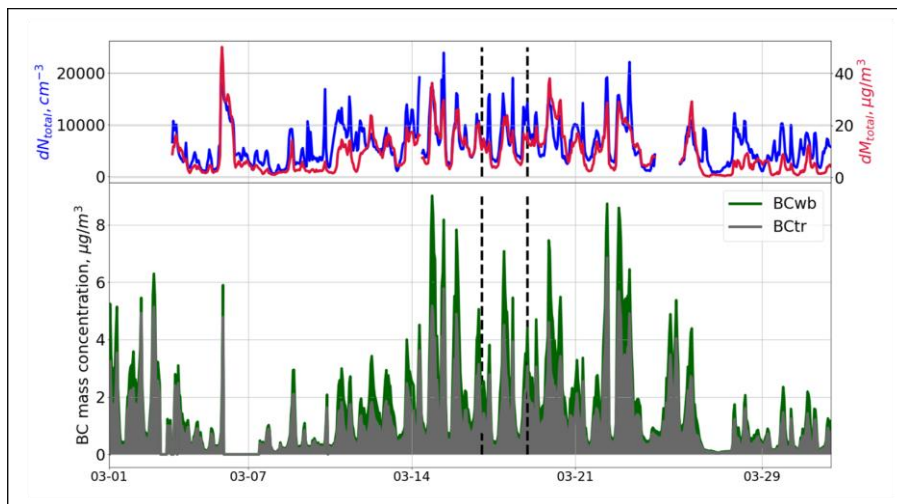
Fig. 27. Temporal resolution of (N_{total}) and (M_{total}) for aerosol particles within the 10–430 nm size range, as measured by the (SMPS) at the urban background monitoring site (FTMC1) during March 2022. Black dashed lines mark periods corresponding to mobile measurement campaigns.

The particle number size distribution was categorized into distinct modes based on aerodynamic diameter: total particles (10–430 nm, represented by the blue line), accumulation mode (100–430 nm, red line), Aitken mode (25–100 nm, green line), and nucleation mode (particles smaller than 25 nm, yellow line). As illustrated in Fig. 29, the average particle number concentration exhibited considerable temporal variation throughout the commuting periods, with values during the morning trip reaching up to five times higher than those recorded at midday. The most pronounced fluctuations were observed in the nucleation mode, where concentrations varied by as much as a factor of twelve (Table 10). The particle distribution was predominantly composed of Aitken mode particles, which accounted for approximately 45–62 % of the total number concentration, in line with findings from previous urban aerosol studies (Byčenkienė et al., 2014).
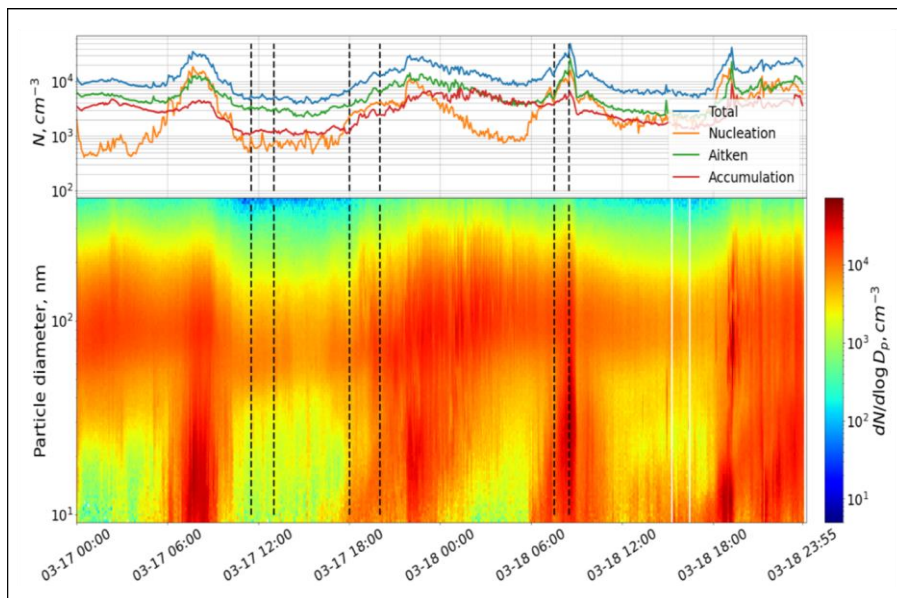
Fig. 28. Presents the particle number concentration and size distribution of aerosol particles within the 10–430 nm range observed during the March 17–18 event days. Black dashed lines indicate the time intervals corresponding to mobile measurement activities.

Table 10. Particle number concentrations at the urban background during field experiments for particle size modes.

Field experiment date and time	Number concentration (SD), $\#/cm^3$			
	Nucleation	Aitken	Accumulation	Total
17/03/2022 11:30-13:00	700 (140)	3170 (180)	1210 (50)	5080 (310)
17/03/2022 18:00-20:00	3210 (600)	5130 (1330)	2210 (550)	10550 (2360)

| 18/03/2022 7:30-8:30	8700 (2310)	11020 (4120)	4700 (600)	24420 (6800)
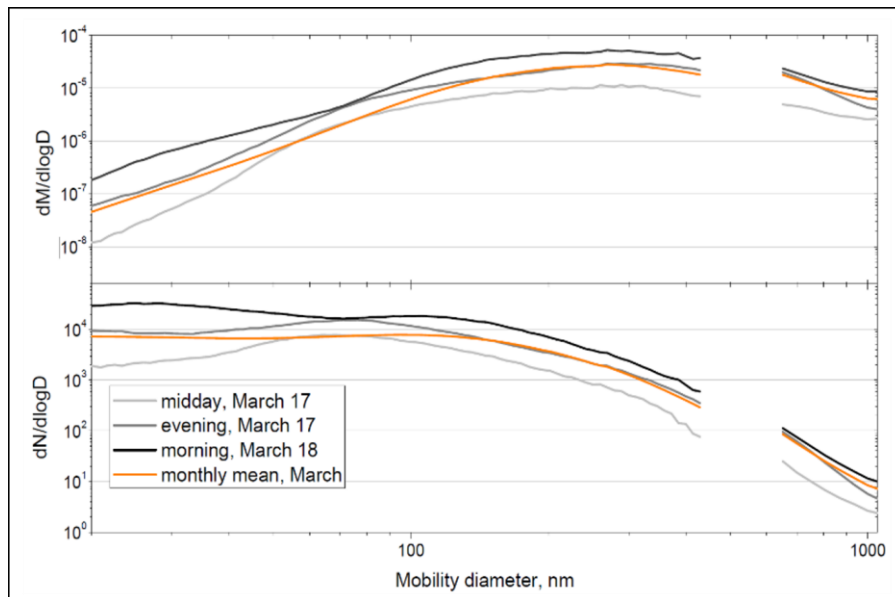
Fig. 29. Normalized size distributions of particle number and mass concentrations recorded during the field experiments conducted on March 17–18, along with the corresponding distributions for March 2022.

3.3.4. PM measurement campaign summary

In March 2022, the mean daily air temperature was recorded at 1.4 °C, with an average relative humidity (RH) of 59.7 %. On the 17th and 18th of March, the diurnal maximum temperatures ranged from 5.5 °C to 7.0 °C during midday to early afternoon hours (2:00–5:00 p.m.), while the minimum values, between −4.5 °C and −4.0 °C, were observed in the early morning (6:00–7:00 a.m.). During these two days, RH fluctuated from 24 % to 66 % (Fig. 30). Average daily concentrations of nitrogen oxides (NOx) during the field experiment were measured at 33.2 μg/m³ and 32.1 μg/m³, closely aligning with the monthly mean for March, which was 33.3 μg/m³. These NOx levels indicate an absence of major pollution episodes (e.g., wildfires) on 17

and 18 March. Moreover, NOx concentrations demonstrated strong positive correlations with PM fractions—specifically PM_1, $PM_{2.5}$, and PM_{10}—with correlation coefficients of 0.72, 0.74, and 0.70, respectively, throughout the measurement period. Regarding aerosol particles within the 0.5–20 µm size range, the highest observed daily mean number concentration during the campaign reached 260 particles per cm³, whereas the lowest was 30 particles per cm³. Throughout March, particle number concentrations varied from 5 to 500 particles per cm³, with a monthly mean total number concentration (N_{total}) of 85 ± 80 particles per cm³.
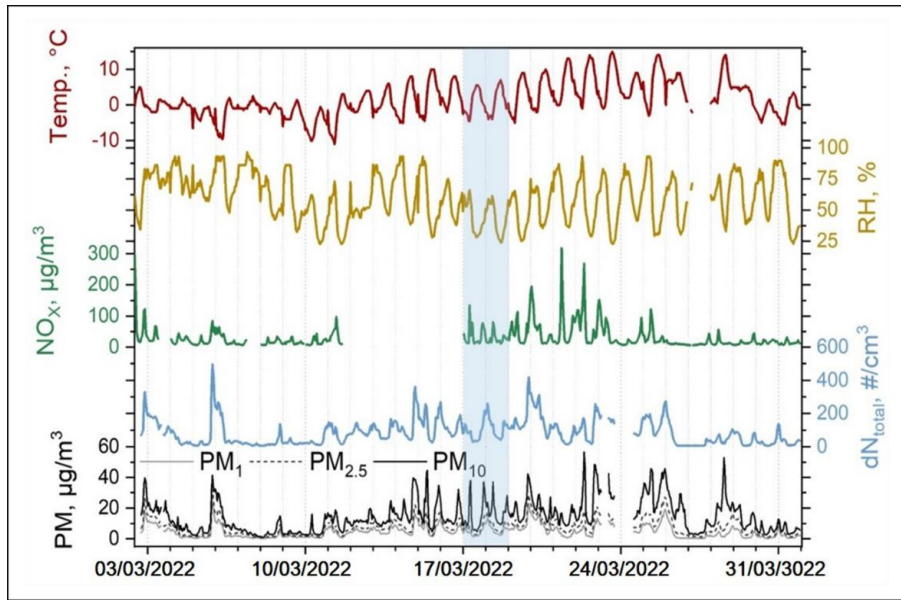
Fig. 30. Presents monitoring data for various meteorological and air quality parameters in March 2022. Field experiment days are highlighted in the blue rectangle.

The mean concentrations of PM_1, $PM_{2.5}$, and PM_{10} across the entire month were 4.7 ± 4.2, 7.5 ± 5.6, and 14.5 ± 10.4 µg/m³, respectively. For the specific dates of the field measurements, the corresponding daily mean concentrations were slightly elevated: 5.2 ± 2.9 µg/m³ for PM_1, 7.8 ± 4.0 µg/m³ for $PM_{2.5}$, and

$15.8 \pm 8.9\ \mu g/m^3$ for PM_{10}. These findings confirm that the fieldwork was conducted under typical atmospheric conditions without interfering with anomalous pollution events. Notably, $PM_{2.5}$ concentrations in the urban background exceeded the World Health Organization (WHO) annual guideline of $5\ \mu g/m^3$ during approximately 50 % of the sampling period (Fig. 31). In comparison, the WHO's 24-hour threshold of $15\ \mu g/m^3$ was surpassed on about 10 % of the measured days.
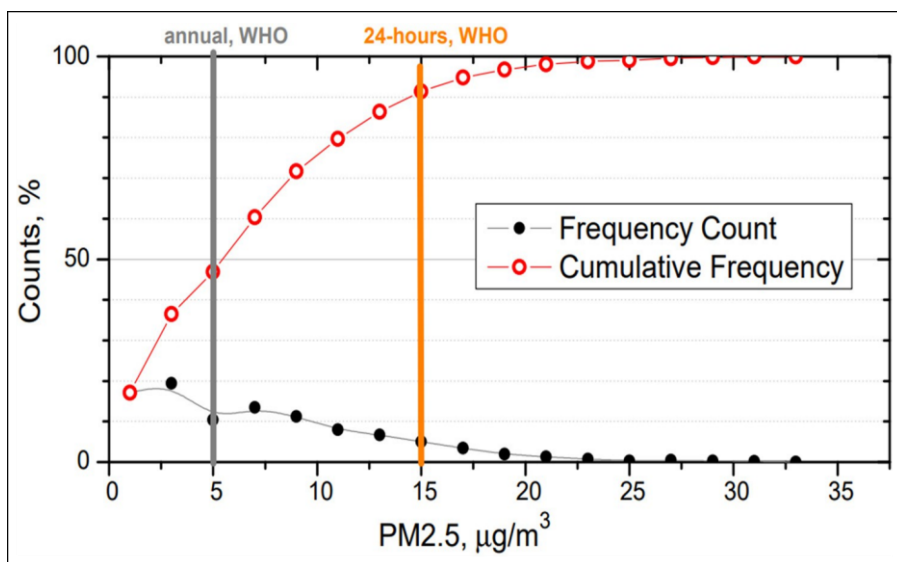
Fig. 31. Distribution and cumulative frequency of $PM_{2.5}$ concentrations recorded in March 2022 at an urban monitoring station in Vilnius.

Three mobile monitoring campaigns were conducted at different times of the day and along two distinct travel routes to assess PM mass concentrations within the vehicle cabin and the surrounding outdoor environment. The initial monitoring route covered the distance between the main premises of FTMC (FTMC1) and its laboratory facilities (FTMC2), while the subsequent two routes connected the researcher's residence and FTMC1. During outbound trips, PM_1, $PM_{2.5}$, and PM_{10} mass concentrations were recorded inside the vehicle.

101

In contrast, return trips were used to measure PM levels in the outdoor air (Fig. 32). The highest recorded PM mass concentration occurred during the morning commute, with PM_{10} levels reaching $36.9\ \mu g/m^3$, likely attributable to increased vehicular traffic during rush hour. In contrast, the lowest concentration of PM_{10}, measured at $5.7\ \mu g/m^3$, was observed during the midday journey along the FTMC1–FTMC2–FTMC1 route.
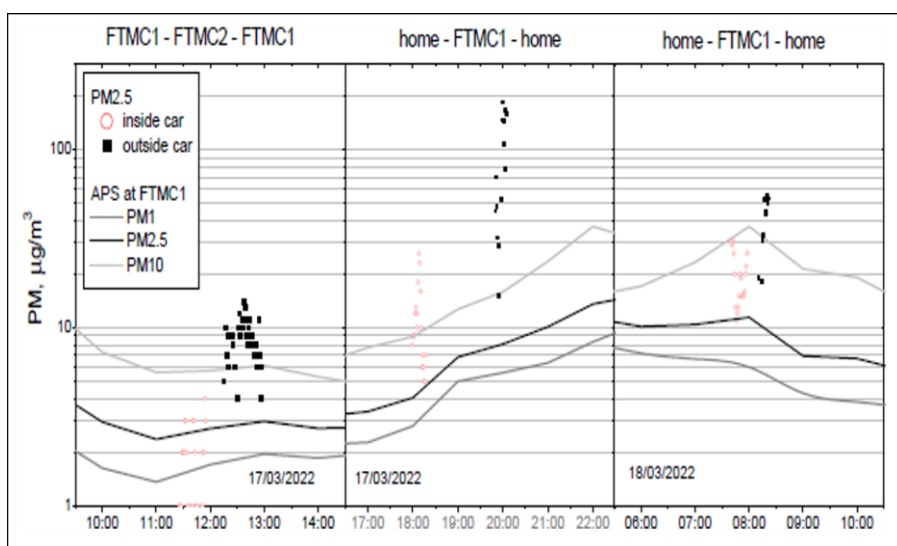
Fig. 32. Schedule of mobile field measurements and the corresponding $PM_{2.5}$ concentrations measured both inside the vehicle and in the ambient air outside the car.

3.3.5. Total and regional deposition dose of BC in the human airways

To evaluate personal exposure and the associated deposition dose BC and PM_1 in an individual's lungs during mobile monitoring and while stationed at the urban background site (FTMC1), mean mass concentrations of BC and PM_1 were analyzed. The temporal variation in mass concentrations, both outside and within the vehicle cabin, is presented in Fig. 33. During the three in-vehicle journeys, the mean BC concentrations were recorded as 2.42 ± 1.77, 1.67 ± 0.66, and

102

7.14 ± 4.42 µg/m³, respectively. Corresponding PM_1 concentrations were 3.36 ± 1.32, 15.26 ± 5.16, and 8.53 ± 4.78 µg/m³. In contrast, the mean concentrations within the office environment were significantly lower, with PM_1 at 1.3 ± 0.45 µg/m³ and BC at 0.08 ± 0.4 µg/m³. A strong positive correlation (r = 0.92) was observed between the mass concentrations of BC and PM_1 across all environments.
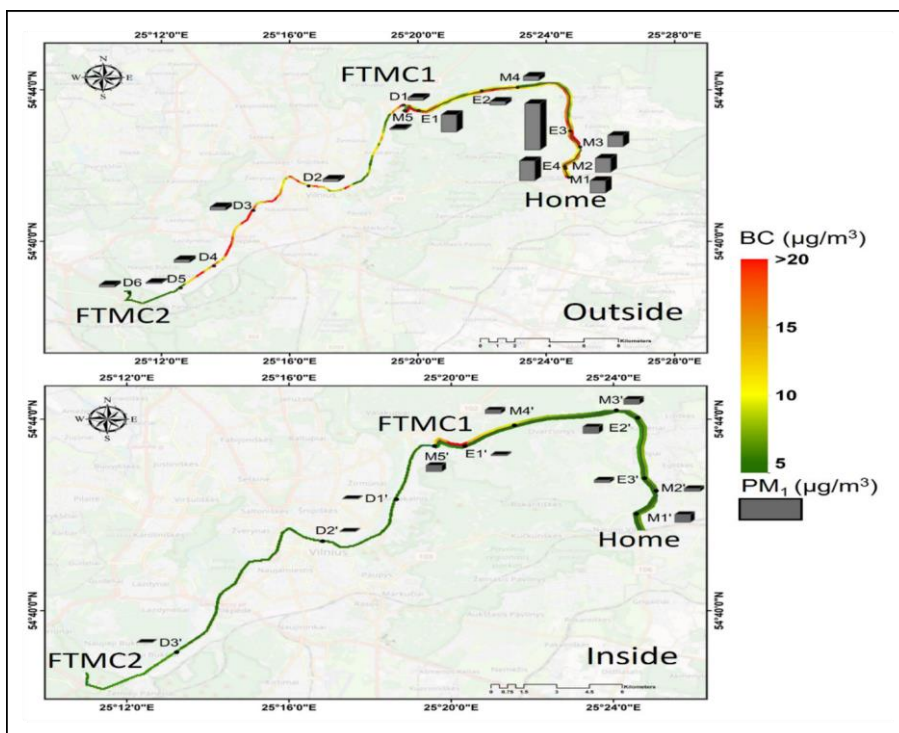
Fig. 33. Mass concentrations of BC and PM_1 were recorded during mobile measurements.

Deposition dose (DD) experiments were conducted on a sedentary male participant. The average indoor BC concentration during this phase was 1700 ng/m³. The DD corresponding to the five-minute averaged inhaled BC concentration was estimated at 38 ± 5 % (Fig. 9). The participant's minute ventilation (MV) rate was calculated to be 19.1 L/min (Fig. 8), which exceeds the typical upper limit range (8.8–16.1 L/min) reported for a seated male (Madueno et al., 2019).

Using Equation (7), the modeled mass deposition dose of BC (MDDBC) during commuting in Vilnius was found to vary between 19 and 53 ng/min inside the vehicle, with the highest values recorded in suburban residential areas. For outdoor exposures, MDDBC ranged from 74 to 125 ng/min, peaking near a central viaduct (Savanoriai traffic ring). On average, in-vehicle MDDBC was two to four times lower than that recorded outside. The lowest MDDBC values were associated with the office/laboratory microenvironment.

When comparing BC levels measured during the commutes to those recorded at the FTMC1 background station, concentrations were generally higher throughout most commuting periods, with the lowest values approaching background levels. Inside the vehicle, BC concentrations typically ranged from background levels up to 9 μg/m³ (Q3), whereas outside measurements reached up to 20 μg/m³ (Q3) (Fig. 34(D)). Notably, BC concentrations measured inside the vehicle did not consistently correspond with those recorded outside, which is attributed to the presence of a vehicular ventilation system that effectively limits indoor particle penetration (Fig. 34(B), (D)). During morning commutes, in-cabin BC levels were frequently equal to or lower than those outside the vehicle (Fig. 34(B)). A comparison of median BC concentrations inside and outside the vehicle during trips 1 and 2 revealed disparities of up to twofold and fivefold, respectively. It is worth noting that elevated background BC levels during trip 2 may have contributed to this variation. Compared to concentrations in the vehicle and outdoors, background BC concentrations measured at the FTMC1 site were generally lower. As shown in Figures 34(A) and 34(C), the contribution of background levels to MDDBC was estimated to constitute up to 25 % of the on-road dose and as much as 60 % of the in-cabin dose. Figure 34(C) illustrates the estimated BC mass deposited in the respiratory tract across all microenvironments throughout a workday, encompassing commuting and office hours. The highest MDDBC values were observed during the morning commute (53 ng/min) and evening (26 ng/min), reflecting significant

exposure to traffic-derived ultrafine particles. Conversely, the lowest MDDBC during commuting (13 ng/min) occurred during a midday trip between FTMC1 and FTMC2, likely due to improved atmospheric dispersion conditions and reduced traffic intensity. The distinction in exposure doses between indoor and commuting environments was substantial. During travel, individuals are typically exposed to emissions from nearby vehicles, with influencing factors such as traffic density, time of travel (rush vs. off-peak hours), and urban layout (residential, commercial, or industrial zones). In contrast, indoor settings, particularly offices with mechanical ventilation systems, can significantly limit BC exposure. The MDDBC measured in the office environment was 11 ng/min, approximately 4.8 times lower than the morning in-vehicle dose (53 ng/min). This reduction is attributed to efficient air filtration systems (e.g., F7–F9 filters), effectively mitigating airborne particulate infiltration. Considering an average commuting time of 40 minutes per day and an 8-hour workday, the ratio of BC deposition doses between the office and commuting environments was calculated as DD_{office} / DD_{trip} = (0.011×8) / $(0.052 \times 2/3)$ = 2.5. This suggests that commuting could contribute up to one-third of a person's total daily BC exposure related to work activities, contingent upon workplace air quality and travel duration. Variations in modelled MDDBC across microenvironments reached up to a fourfold difference. The regional deposition within the human respiratory system peaked in the pulmonary region, ranging from 5.1 ng/min during office occupancy to 19.9 ng/min during the morning commute (Fig. 34C).

The average BC mass concentration measured across all commuting routes and within the office environment was utilized as input for calculating the deposition fraction (DF) using the Multiple-Path Particle Dosimetry (MPPD) model. Although DF is primarily influenced by the aerodynamic diameter of inhaled particles rather than their ambient concentration (J. Gao et al., 2022), the concentration becomes relevant when DF is estimated across a spectrum of particle

sizes. This is due to temporal variability in particle size distribution, which ultimately affects the calculated deposition pattern. As a result, the fractional deposition across different regions of the respiratory tract can fluctuate. When DF was calculated for BC particles within the size range of 10 to 1000 nm, the average distribution of deposited particles across respiratory regions was as follows: 33.6 % in the upper respiratory tract (URT), 26.8 % in the tracheobronchial (TB) region, and 39.2 % in the alveolar or pulmonary (PU) region, as depicted in Figure 33(A). Variations in deposition fraction across different segments of the respiratory tract during the monitored trips ranged between 2.5 % and 5 %, indicating modest shifts depending on the exposure scenario.
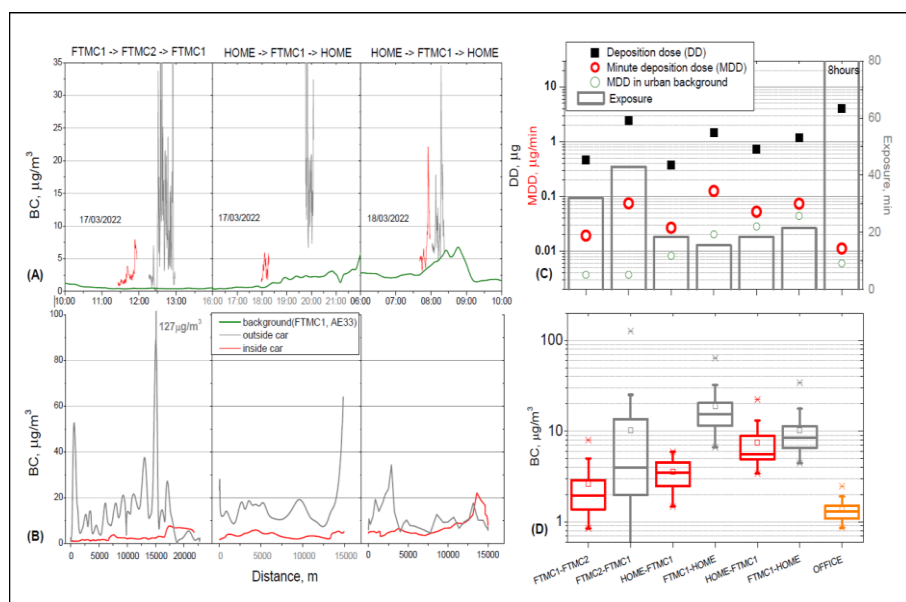
Fig. 34. BC concentrations and deposition doses from three commuting scenarios: (A) time-resolved BC concentrations inside and outside the vehicle, including urban background levels (in green); (B) BC concentrations measured along travel routes; (C) cumulative respiratory deposition dose; (D) statistical distribution of BC concentrations.

3.3.6. Total and regional deposition dose of PM in the human airways

The results (Figs. 35-36) illustrate the estimated mass of PM deposited in the respiratory tract during office hours and while driving along various routes, as well as the minute deposition dose (MDD) across different regions of the respiratory system. Based on model simulations, the deposition fraction (DF) is influenced solely by the aerodynamic diameter of particles, rather than their ambient concentration. Consequently, DF values for PM remain consistent between indoor (office) and in-vehicle environments when comparing particles of identical aerodynamic size. As shown in Figure 35, the overall DFs for particles smaller than 1 μm (PM<1), between 1 and 2.5 μm (PM$_{1-2.5}$), and between 2.5 and 10 μm (PM$_{2.5-10}$) are approximately 38 %, 90 %, and 98 %, respectively. Coarser particles primarily deposit in the upper respiratory pathways (head region), whereas finer fractions penetrate deeper, reaching the lower airways.
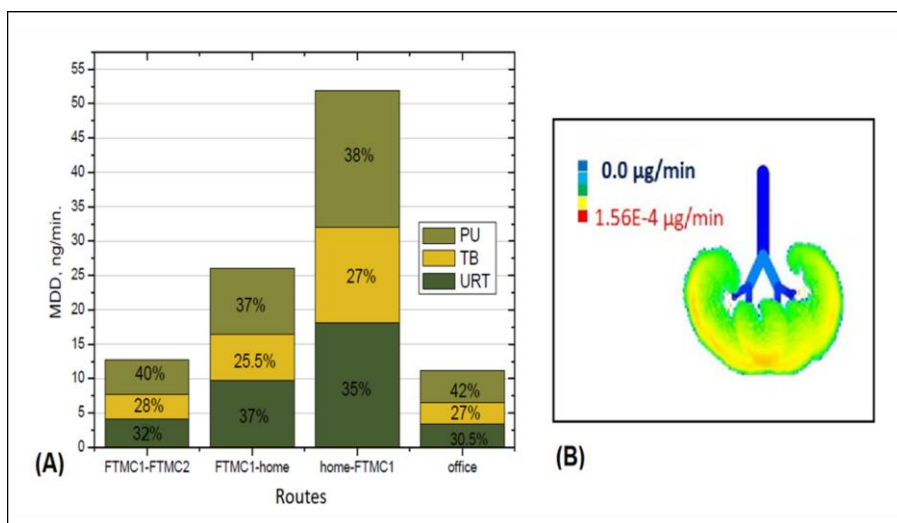

Fig. 35. Subfigure (A) shows the minute deposition dose of black carbon (BC) during various commuting scenarios in Vilnius, while subfigure (B) illustrates the minute BC deposition dose throughout the human respiratory tract.

When applying equation 6 (refer to the Methods section), the total DFs for PM_1, $PM_{2.5}$, and PM_{10} were calculated as roughly 38 %, 56 %, and 65 %, respectively, with a slight inter-series variation of about 3 %. The lowest MDD values were observed during the midday route between FTMC1 and FTMC2, which coincided with the lowest recorded urban background PM levels during the monitoring period. In contrast, higher exposure levels during peak traffic hours are likely due to increased emissions and possibly influenced by reduced atmospheric mixing height and elevated vehicle density. This assessment assumed normal respiratory parameters and nasal breathing for estimating particle deposition, although DF can vary substantially with different breathing patterns. For instance, research conducted in Hungary demonstrated a decreasing trend in PM_1 deposition in the extra-thoracic region (head) from 26 % during sleep to 9.4 % during intense physical activity, accompanied by an increase in alveolar deposition from 14.7 % to 34 % under the same conditions (Salma et al., 2015). Other studies have revealed considerable variability in deposition depending on demographic factors such as age and gender, with adults typically showing deposition fractions ranging from 17 % to 45 %, compared to 10 % to 23 % in children (Salma et al., 2015). In our scenario, the modeled DF for a seated, middle-aged male yielded 26 % in the head region and 8 % in the alveolar region. The lower alveolar DF relative to the aforementioned Hungarian study may be attributed to differences in particle size distribution. Furthermore, our model might underestimate PM_1 deposition since calculations were based on a fixed particle diameter of 1 µm rather than a continuous size distribution.

Marked differences between deposition doses in indoor office settings and those experienced while driving were identified. Indoor PM levels were similar to in-vehicle concentrations observed during midday travel, when urban background pollution is relatively low, but were significantly lower than levels measured during rush hour. Specifically, during rush hour, deposition doses for drivers were 8 to

14 times greater than those measured in the office for PM_1 and PM_{10}, respectively. This discrepancy likely reflects the more efficient air filtration systems in FTMC1 office spaces, which help maintain lower PM exposure for occupants compared to on-road conditions. When accounting for time spent in each environment—approximately 40 minutes commuting and 8 hours in the office—the total PM_1 inhalation dose (calculated as MDD multiplied by time spent) becomes comparable:$(0.006×8)/(0.072+0.039)×1/3≈48/37≈1.3$. This suggests that under these conditions, daily PM_1 exposure indoors may slightly exceed exposure while driving, depending on the proportion of time spent commuting. Despite occupying less than 10 % of the total time assessed, commuting can contribute up to 80 % of the total PM_1 exposure, particularly during rush hour conditions. During periods with high urban background concentrations ($PM_{2.5} ≈ 10$ µg/m³), the MDD for drivers reached levels approximately 14 times higher than those recorded in office environments. Conversely, during times of low pollution, in-vehicle concentrations were observed to be roughly half of the concurrent urban background levels. This unexpected result may reflect the technical limitations of the mobile monitoring equipment.
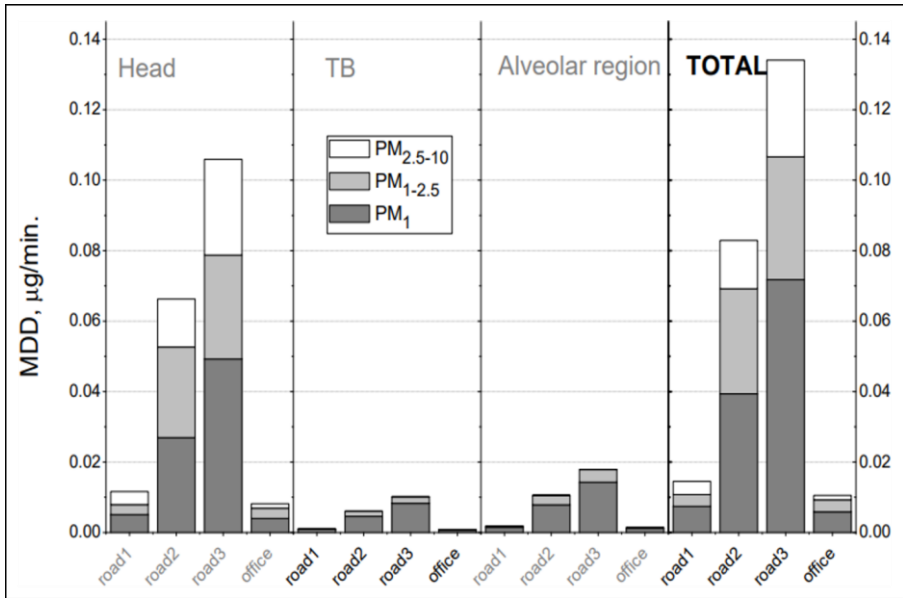
Fig. 36. Relative contributions of PM sub-fractions (PM$_1$ µm, PM$_{1-2.5}$ µm, and PM$_{2.5-10}$ µm) to the total deposition dose within the upper respiratory tract using the MPPD model.
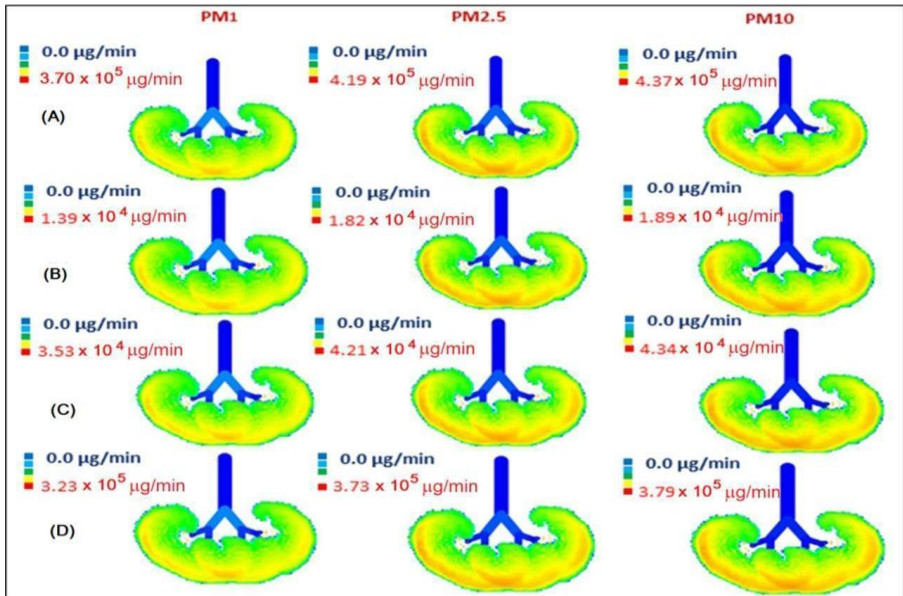
Fig. 37. Spatial distribution of the size-segregated mass deposition rates of PM in the human respiratory tract for multiple scenarios: (A)

midday travel between FTMC1 and FTMC2, (B) evening commute from FTMC1 to home, (C) morning rush hour commute from home to FTMC1, and (D) indoor exposure in the FTMC1 office building.

Finally, Fig. 37 visualizes the mass deposition rates of size-segregated PM across the human respiratory tract for both office and driving environments. The graphical representation emphasizes the stark contrast in MDD distribution between these settings. Notably, PM_1 exerts the most significant influence, with deposition concentrated in the alveolar region—the deepest and most sensitive part of the respiratory system.

3.3.7. Chapter conclusions

Peak particle number and mass concentrations for BC, PM_1, and $PM_{2.5}$ occur during morning commute hours (7:00–8:00 LT), which are linked to high traffic intensity and specific meteorological conditions. These factors lead to increased deposition doses on human lungs. Personal exposure to PM_1, $PM_{2.5}$, and black carbon is significantly higher during commuting than in a well-ventilated office. On-road $PM_{2.5}$ concentrations were 4 to 10 times higher than those at urban background stations, and in-vehicle PMs concentrations accounted for up to 80 % of total daily exposure, despite driving representing less than 10 % of total time. Similarly, BC deposition dose was considerably higher in vehicles (53 ng/min) compared to offices (11 ng/min).

Office environments exhibited lower PM and BC concentrations than outdoor and in-vehicle measurements due to an effective filtration system. Nevertheless, particle infiltration still resulted in minimal deposition doses over time. BC from transport (BCtr) accounted for 66 % of the total BC mass, whilst roadside $PM_{2.5}$ levels exceeded WHO limits, confirming that vehicle emissions are the primary source during commutes.

The prevalence of PM_1 particles in vehicles and on-road environments further highlights the toxicity of exhaust-emitted particles. Low-cost environmental sensors have proven useful for assessing exposure in mobile and indoor spaces. However, certain limitations exist, particularly under conditions of low background pollution, which can lead to underestimations of actual in-vehicle concentrations.

MAIN CONCLUSIONS

1. Fragment-shaped microplastics dominate airborne non-exhaust emissions near urban street environments, with the highest seasonal proportion observed in spring (98 %). Microplastics within the 50–100 µm size range constituted the majority across all seasons, accounting for up to 55 % of the total microplastic load, indicating a consistent prevalence of particles within the inhalable size fraction at breathing height. Color and polymer composition analysis revealed that traffic-related sources are the principal contributors, with black-colored microplastics, primarily linked to tire wear, reaching up to 71 % in summer. Polyethylene was the most abundant polymer across all samples (43 % on average), peaking at 69 % in spring, highlighting its widespread presence and persistence in the urban atmosphere.

2. The *Thuja occidentalis* hedge significantly reduced airborne non-exhaust microplastic pollution in an urban street environment. The hedge achieved an average microplastic removal efficiency of 54 % throughout all seasons, with the highest seasonal efficiency recorded in summer (65 % total MPs, 71 % fibers). Size-specific removal efficiency was most pronounced for particles in the 50–100 µm range, averaging 67 % and peaking at 94 % in spring. The hedge resulted in a 50 % reduction in microplastic concentration at +1 meter behind the hedge (4.59 particles cm^{-2} day^{-1}) compared to the control (9.2 particles cm^{-2} day^{-1}). Furthermore, *Thuja occidentalis* lowered the exposure risk by 71 % in spring when the inhalation risk index was highest, at 831, confirming the potential role of urban green infrastructure in mitigating traffic-related airborne MPs.

3. Personal exposure to PM_1, $PM_{2.5}$, and BC was significantly higher during commuting than in indoor office environments. PMs exposure accounted for up to 80 % of daily exposure,

despite commuting comprising less than 10 % of daily time. Although office environments with mechanical ventilation reduced PM and BC exposure, infiltration still contributed to a measurable deposition dose of BC (11 ng/min), which is 4.8 times lower than the deposition dose in the vehicle (53 ng/min). Additionally, 39 % of the inhaled BC mass was deposited in the lower part of the lung, the alveolar region.

4. Traffic-related black carbon is the primary source of personal exposure during commuting in urban environments. During this period, 66 % of the total BC mass concentration was attributed to traffic-related emissions, significantly increasing the deposition dose of inhaled particles in the human respiratory tract. The most significant impact was observed during morning rush hours, when the modelled BC deposition dose in the alveolar region reached 19.9 ng/min, compared to 5.1 ng/min in the office environment. This indicates that, despite shorter exposure durations, transport microenvironments contribute disproportionately to the respiratory deposition load, particularly in the lower regions of the respiratory system, where fine particles are deposited most efficiently.

SANTRAUKA

ĮVADAS

Aktualumas

Aplinkos oro tarša yra viena iš pagrindinių aplinkos sveikatos grėsmių. Ypač reikšmingą poveikį visuomenės sveikatai daro kietosios dalelės (KD), kurios prisideda prie kvėpavimo ir širdies bei kraujagyslių ligų paplitimo (de Bont ir kt., 2022). Pasaulio sveikatos organizacijos (PSO) duomenimis, oro tarša kasmet nulemia apie 7 milijonus priešlaikinių mirčių visame pasaulyje (Chen ir kt., 2024). Pagrindiniu šios visuotinės sveikatos naštos veiksniu laikoma blogėjanti oro kokybė urbanizuotose teritorijose, kuriose, kaip teigiama, apie 99 % gyventojų gyvena esant oro teršalų koncentracijoms, viršijančioms PSO nustatytas gaires (Chen ir kt., 2024; Karthick Raja Namasivayam ir kt., 2024).

Urbanizuotose aplinkose kietųjų dalelių tarša kyla iš įvairių šaltinių, kurie dažniausiai klasifikuojami į išmetamąsias ir neišmetamąsias emisijų kategorijas. Išmetamosios kietosios dalelės, tokios kaip aerozolio juodoji anglis (JA), daugiausia susidaro dėl nepilno iškastinio kuro ir biomasės deginimo. Šios aerozolio dalelės daro reikšmingą poveikį klimatui absorbuodamos saulės spinduliuotę, taip pat kelia rimtą grėsmę žmonių sveikatai (Chowdhury ir kt., 2022; Sharma ir kt., 2024). Priešingai, neišmetamosios emisijos apima daleles, atsirandančias dėl transporto priemonių stabdžių nusidėvėjimo, padangų dilimo, kelio dangos erozijos ir pakartotinio kelio dulkių pakilimo. Dėl savo sintetinės polimerinės sudėties ir mažo dydžio šios dalelės vis dažniau klasifikuojamos kaip ore esantys mikroplastikai (Sangkham ir kt., 2022). Ore esantys MP kelia ypatingą susirūpinimą dėl galimo įkvėpimo ir galimos žalos sveikatai, įskaitant kvėpavimo sistemos ligas bei neurologinius sutrikimus (Winiarska ir kt., 2024). Skaičiuojama, kad kasmet į atmosferą patenka apie šeši milijonai tonų MP, atsirandančių dėl padangų ir kelio dangos nusidėvėjimo,, todėl šis šaltinis laikomas vienu reikšmingiausių ore esančių MP taršos šaltinių mieste (Lee ir kt., 2024; Liao ir kt., 2021).

Aplinkos oro kokybės vertinimas dažniausiai grindžiamas fiksuotų stebėjimo stočių duomenimis. Tačiau toks metodas dažnai neatskleidžia individualaus poveikio dinamikos skirtingose mikroaplinkose, kuriose teršalų koncentracijos gali reikšmingai kisti net per trumpus laiko ir erdvės intervalus. Dėl šios priežasties asmenys nėra vienodai veikiami aplinkos oro taršos – jų įkvėptą teršalų dozę lemia artumas iki emisijos šaltinių, poveikio trukmė bei laikas, praleistas konkrečiose mikroaplinkose. Urbanizuotose teritorijose gyvenantys asmenys vidutiniškai praleidžia beveik 90 % savo kasdienio laiko patalpose, o dar 4–7 % – transporto priemonėse (Matz ir kt., 2018). Nepaisant šių mikroaplinkų svarbos, jos dažnai neįtraukiamos į sveikatos rizikos vertinimus, kurie dažnai remiasi fiksuotų stočių duomenimis, neatspindinčiais individualaus poveikio rizikos.

Atsižvelgiant į šiuos iššūkius, miesto žalioji infrastruktūra (MŽI) vis dažniau vertinama kaip perspektyvi priemonė mažinant oro taršos mažinimui, ypač tankiai apgyvendintose urbanizuotose teritorijose, pasižyminčiose intensyviu transporto srautu (Kwak ir kt., 2019). Tokie MŽI elementai kaip žaliosios sienos, gatvių medžiai ir kelkraščio gyvatvorės yra rekomenduojami dėl jų gebėjimo gerinti oro kokybę sulaikant KD, mažinant teršalų sklaidą ir gerinant mikroklimato sąlygas (Lafortezza ir kt., 2018). Nepaisant augančio susidomėjimo MŽI, jos veiksmingumas mažinant individualų KD poveikį vis dar nėra pakankamai ištirtas, ypač kalbant apie teršalus, nesusijusius su vidaus degimo proceso emisijomis. Be to, MŽI gebėjimas filtruoti įvairių dydžių ir formų KD taip pat išlieka nepakankamai išanalizuotas, o esami duomenys rodo, kad jos teikiama nauda gali būti ribota arba priklausyti nuo specifinių aplinkos sąlygų. Atsižvelgiant į didėjančią teršalų, atsirandančių dėl stabdymo, padangų ir kelio dangos dėvėjimosi reikšmę urbanizuotose aplinkose, tampa itin aktualu kompleksiškai vertinti MŽI veiksmingumą mažinant tiek su vidaus degimo proceso emisijomis susijusių, tiek su jomis nesusijusių aerozolio dalelių poveikį.

Problemos formulavimas

     Nors urbanizuotose aplinkose buvo atlikta nemažai tyrimų apie KD poveikį, dabartinis individualaus poveikio dinamikos supratimas vis dar turi reikšmingų trūkumų. Visų pirma, nepakankamas integruojamas tiek išmetamųjų ir neišmetamųjų emisijų indėlis į bendrą KD taršą miestuose. Daugelis tyrimų daugiausia dėmesio skiria emisijoms, susijusioms su vidaus degimo varikliu veikla, dažnai nepakankamai įvertindami neišmetamuosius šaltinius, tokius kaip stabdžių nusidėvėjimas, padangų dilimas ir kelio dangos dulkės. Šių šaltinių svarba išlieka arba net didėja, transporto priemonėms pereinant prie švaresnių technologijų ir mažinant išmetamųjų teršalų emisijas. Antra, dauguma poveikio vertinimų vis dar grindžiami aplinkos oro kokybės stebėsenos duomenimis arba apibendrintais poveikio įverčiais, kurie neatsižvelgia į individualaus poveikio erdvinį ir laikiną kintamumą. Toks kintamumas gali būti nulemtas tokių veiksnių kaip kelkraščio taršos židiniai (karštosios vietos) bei individualūs judėjimo modeliai skirtingose mikroaplinkose. Trečia, MŽI veiksmingumas mažinant KD poveikį, ypač neišmetamųjų emisijų kontekste, vis dar yra nepakankamai ištirtas, nepaisant įrodymų apie jos potencialą mažinti išmetamųjų emisijųjų teršalų skeltą taršą. Šiame darbe siekiama užpildyti minėtas žinių spragas, įvertinant tiek su variklio emisijomis susijusių kietųjų dalelių, tiek neišmetamųjų mikroplastiko dalelių šaltinių įtaką individualiam poveikiui urbanizuotoje aplinkoje. Tyrime integruojami asmens lygmens poveikio duomenys, apimantys skirtingas mikroaplinkas, bei analizuojamas miesto žaliosios infrastruktūros veiksmingumas, vertinant ją kaip tvarią, gamta pagrįstą oro taršos mažinimo strategiją.

Pagrindinis tyrimo tikslas

     Šio tyrimo tikslas – ištirti asmeninę ekspoziciją kietųjų dalelių taršai, kylančiai tiek iš išmetamųjų, susijusių su variklio degimo procesais, tiek iš neišmetamųjų, šaltinių, tokių kaip stabdžių ir padangų dėvėjimasis bei kelio dangos dėvėjimosi, mieste.

Tyrimas bus sutelktas į miesto žaliosios infrastruktūros vaidmenį mažinant oro taršą mikroplastiku bei kasdienius žmonių veiklos modelius, ypač kelionės į darbą ir darbo valandų metu.

Uždaviniai

1. Įvertinti ore esančio mikroplastiko dalelių savybes ir sklaidą šalia intensyvaus eismo gatvės, nustatant morfologines (forma, dydis, spalva) ir chemines (sudėtis) charakteristikas.
2. Įvertinti miesto žaliosios infrastruktūros efektyvumą mažinant mikroplastiko ore kiekį ir asmeninę ekspoziciją.
3. Įvertinti asmeninę ekspoziciją išmetamosioms juodosios anglies ir kietųjų dalelių frakcijoms įvairių kasdienių veiklų metu, ypatingą dėmesį skiriant kelionėms į darbą bei buvimui mechaniškai ventiliuojamuose energiją taupančiuose pastatuose.

Mokslinis naujumas

Tyrimo mokslinis naujumas pasireiškia keliomis kryptimis. Kompleksiškai įvertinta transporto sukeltos mikroplastiko taršos apimtis ir miesto žaliosios infrastruktūros vaidmuo, siekiant sumažinti jo koncentraciją ore. Tyrimas išsiskiria sisteminiu požiūriu, apjungiančiu taršos šaltinių identifikavimą, mikroplastiko savybių analizę ir gamta pagrįstų sprendimų taikymą oro kokybės gerinimui, įgyvendinant „nuo taršos iki sprendimo" paradigmą.

Ginamieji teiginiai

1. Šalia intensyvaus eismo miesto kelių ore aptinkamos mikroplastiko dalelės daugiausia yra polietileno sudėties, juodos spalvos fragmentai, kurių gausa ir pasiskirstymas reikšmingai priklauso nuo sezoninių veiksnių bei atstumo iki neišmetamųjų transporto taršos šaltinių, tokių kaip stabdžių, padangų ir kelio dangos nusidėvėjimas.

2. *Thuja occidentalis* efektyvumas mažinant oro taršą mikroplastiku priklauso nuo sezono ir dalelių dydžio. Fragmentų formos mikroplastiko dalelės 50–100 µm dydžio intervale pasižymi didesniu šalinimo efektyvumu.
3. Asmens ekspozicija PM_1 frakcijos kietosioms dalelėms mieste daugiausia susikaupia kasdienių veiklų metu, ypač kelionės į darbą laikotarpiu, ir sudaro iki 80 % visos paros ekspozicijos.
4. Transporto kilmės juodoji anglis sudaro iki 66 % visos BC masės koncentracijos kelionių į/iš darbą metu ir yra pagrindinis veiksnys, didinantis dalelių nusėdimo dozes plaučiuose, ypač rytinio piko metu.

Autoriaus indėlis

Aktyviai dalyvavo mobiliojo matavimo eksperimente Vilniuje. Buvo atsakingas už surinktų duomenų apdorojimą, formalųjį analizavimą, validavimą ir vizualizavimą. Mokslinius rezultatus pristatė nacionalinėse bei tarptautinėse konferencijose.

METODAI

Skyriuje pristatomi metodai, taikyti tiriant asmeninę ekspoziciją teršalams, susijusiems su variklio degimo procesais, ir, kylantiems dėl stabdžių, padangų bei kelio dangos dėvėjimosi mieste. Tyrimas buvo struktūruotas dviem pagrindinėmis kryptimis: (1) mikroplastiko dalelių ore įvertinimą šalia intensyvaus eismo kelių, ypatingą dėmesį skiriant miesto žaliosios infrastruktūros vaidmeniui mažinant taršą, ir (2) asmeninės ekspozicijos juodajai angliai, kuri yra viena pagrindinių su išmetamaisiais teršalais susijusių kietųjų dalelių sudedamoji dalis, vertinimą skirtingose miesto mikroaplinkose.

Ore sklandančių mikroplastiko dalelių prie intensyvaus eismo gatvės vertinimas

Tyrimas buvo atliktas Kauno mieste, Lietuvoje (geografinės koordinatės: 54°51'00.7"N, 24°01'46.5"E), pasirinkus reprezentatyvų miesto žaliosios infrastruktūros elementą – *Thuja occidentalis* gyvatvorę. Gyvatvorės apie 0,6 m pločio, 1,5 m aukščio ir 19 m ilgio (38 pav.), įrengta tarp važiuojamosios kelio dalies ir šalia esančių gyvenamųjų pastatų. Tyrimo vieta pasirinkta tikslingai, siekiant įvertinti MŽI potencialą mažinant mikroplastiko dalelių taršą, kylančią dėl transporto priemonių judėjimo, ypač padangų nusidėvėjimo. Mikroplastiko dalelių nusėdimo tyrimui buvo taikytas pasyvus ėminių surinkimo metodas, naudoti 8 cm skersmens stiklo pluošto filtrus, įdėtus į Petri lėkšteles. Šie ėmikliai buvo išdėstyti keturiose skirtingose vietose, atsižvelgiant į atstumą nuo gyvatvorės:

(i)   -1 m – tiesiai prie kelio krašto, tikintis užfiksuoti didžiausią MP koncentraciją;

(ii)   0 m   – tiesiai po gyvatvore, žemės lygyje;

(iii)   +1 m – vienas metras už gyvatvorės;

(iv)   +2 m – du metrai už gyvatvorės, toliau nuo tiesioginio emisijos šaltinio.

Kiekvienas filtras buvo laikomas nejudinant ant žemės 24 valandas, kad būtų užtikrintas natūralus ore esančių dalelių nusėdimas.

Tyrimas buvo vykdomas visais metų laikais siekiant įvertinti sezoniškumo poveikį MP nusėdimui: vasarą (2023 m. birželį), rudenį (2023 m. spalį), žiemą (2024 m. vasarį) ir pavasarį (2024 m. kovą). Iš viso surinkti 22 ėminiai. Kiekvienos sezono metu kiekvienu atstumu buvo surinkta po keturis ėminius, iš viso gauta 16 ėminių. Papildomai, 2024 m. pavasarį buvo surinkti keturi lyginamieji ėminiai tose pačiose keturiose pozicijose, bet atviroje vietoje, kur nebuvo gyvatvorės, siekiant įvertinti gyvatvorės poveikį MP nusėdimui.

Siekiant papildomai įvertinti mikroplastiko dalelių vertikalų pasiskirstymą gyvatvorėje, buvo surinkti du papildomi ėminiai skirtingame gyvatvorės aukštyje: vienas – vidurinėje dalyje (apie 0,75 m aukštyje), kitas – viršutinėje dalyje (apie 1,5 m aukštyje). Pasibaigus ėminių rinkimui, filtrai buvo kruopščiai uždaryti, kad būtų išvengta užteršimo ir dalelių praradimo, ir transportuoti į laboratoriją detaliai analizei. Kiekvienas filtras buvo kruopščiai uždarytas, siekiant išvengti antrinio užteršimo bei dalelių praradimo, ir transportuotas į laboratoriją analizei.

Mikroplastiko dalelių laboratorinė analizė

Ant stiklo pluošto filtrų susikaupusios dalelės buvo atsargiai nuplautos į atskirus, iš anksto išvalytus stiklo indelius, naudojant distiliuotą vandenį. Siekiant pašalinti organines priemaišas, mėginiai buvo veikiami 30 % vandenilio peroksido (H_2O_2) tirpalu (Sigma-Aldrich, Vokietija), ir paliekami 24 valandoms. Siekiant atskirti mikroplastiko daleles nuo kitų likusių dalelių buvo taikytas tankio skirtumo metodas, panaudojant prisotintą cinko chlorido ($ZnCl_2$) tirpalą, kurio tankis siekė 1,6–1,8 g/cm³ (Crutchett & Bornt, 2024; Konechnaya et al., 2020; Rodrigues et al., 2020). Mėginiai buvo supilti į separavimo piltuvą su $ZnCl_2$ tirpalu ir palikti kelioms valandoms, kad mažesnio tankio dalelės, dažniausiai mikroplastiko, iškilų į paviršių, o sunkesnės nusėstų į dugną. Vėliau paviršiuje susikaupusios frakcijos buvo filtruojamos per stiklo pluošto filtrus („Branchia", 50 mm skersmens, 1,6 µm porų dydžio). Filtrai buvo džiovinami orkaitėje 60 °C temperatūroje 24 valandas, kad būtų paruošti cheminei analizei. Mėginiai buvo tiriami ir apibūdinami naudojant skaitmeninį optinį mikroskopą su 200× didinimo objektyvu. Kiekviena aptikta dalelė buvo įvertinta ir klasifikuota pagal morfologinius požymius, įskaitant dydį, formą ir spalvą. Ilgiausias dalelės ašies ilgis buvo matuojamas naudojant vaizdų analizės programinę įrangą „Motic Images Plus 3.0". Pagal dydį dalelės buvo suskirstytos į šiuos intervalus: <20 µm, 20–50 µm, 50–100 µm, 100–250 µm, 250–500 µm, 500–2000 µm ir >2000

μm. Pagal struktūrinius ypatumus MP dalelės buvo toliau klasifikuojamos į dvi pagrindines morfologines kategorijas – pluoštą ir fragmentus. Taip pat buvo įvertinta kiekvienos dalelės spalva, kuri pagal vizualinius kriterijus buvo priskiriama vienai iš spalvų grupių: juoda, ruda, balta, mėlyna, raudona, geltona ir kita.

Siekiant nustatyti MP dalelių polimerinę sudėtį, mėginiai buvo perkeliami ant aliuminio oksido (Al$_2$O$_3$) filtro ir tiriami mikro-Fourier transformacijos infraraudonųjų spindulių (μ-FTIR) spektroskopijos metodu, naudojant LUMOS II spektrometrą (Bruker, Vokietija). Spektrai buvo registruojami 4000–1200 cm^{-1} intervale, naudojant 4 nuskaitymus vienam taškui. Kiekvienos dalelės spektrinis signalas buvo lyginamas su prietaiso referencine polimerų biblioteka. Dalelė buvo identifikuojama kaip mikroplastikas, jei jos spektrinis atitikimas su referenciniu polimeru viršijo 70 %.

Juodosios anglies tyrimai miesto mikroaplinkose

Antrasis tyrimas skirtas asmeninės ekspozicijos kietosioms dalelėms ir juodajai angliai vertinimui darbo valandomis bei kelionėse į darbą ir iš jo, siekiant nustatyti įkvėpiamų teršalų nusėdimo dozę kvėpavimo takuose. Tyrimas buvo atliktas Vilniuje, Lietuvos sostinėje, turinčioje apie 600 000 gyventojų, kur urbanizacijos lygis, transporto intensyvumas ir sezoniniai veiksniai lemia reikšmingą oro taršos kintamumą. Kaip ir daugelyje sostinių, oro tarša Vilniuje pasižymi reikšmingu erdviniu nevienodumu, priklausomai nuo transporto intensyvumo, reljefo bei mikroklimato sąlygų. Miestui būdingas vidutinių platumų žemyninis klimatas, pasižymintis šiltomis vasaromis ir šaltomis žiemomis. Šalčiausias mėnuo yra sausis (vidutinė temperatūra –4 °C), o šilčiausias – liepa (vidutinė temperatūra 17 °C), metinė vidutinė oro temperatūra siekia 6,6 °C. Kasmet iškrenta vidutiniškai 688 mm kritulių. Eksperimento metu, 2022 m. kovo mėn. Lietuvoje vidutinė oro temperatūra buvo 1,5 °C, t. y. 0,8 °C aukštesnė nei daugiametis vidurkis. Vyraujanti vėjo kryptis tuo laikotarpiu buvo pietų. Matavimo metu užfiksuota maksimali oro

temperatūra siekė 17,7 °C, o minimali –14,5 °C. Kritulių kiekis buvo labai mažas, vidutiniškai apie 1,9 mm, todėl meteorologinės sąlygos buvo palankios dalelių akumuliacijai.

Mobiliesiems matavimams buvo pasirinkti iš anksto nustatyti maršrutai, apimantys skirtingo funkcinio pobūdžio miesto zonas – gyvenamuosius ir komercinius rajonus, taip pat vietas prie centrinės ir vietinės reikšmės kelių. Matavimai apėmė keliones tiek iš namų į darbą, tiek tarp darbo filialų (žr. 39 pav.). Kelionėms į darbą buvo pasirinkti trys pagrindiniai maršrutai: FTMC1-Namai, FTMC1-FTMC2 ir Namai-FTMC1, kurie atspindėjo tipiškus kasdienius judėjimo modelius urbanizuotoje aplinkoje.

Vidutinis oro taršos lygis matavimo dienomis buvo apskaičiuotas siekiant įvertinti, ar pasirinktos dienos atspindi tipiškas šaltojo sezono sąlygas. Matavimai buvo atlikti referenciniame miesto fono taške, įrengtame ant Fizinių ir technologijos mokslų centro (FTMC1, www.ftmc.lt, prieiga 2025 m. gegužės 29 d.) stogo. Šis taškas yra nutolęs apie 6–7 km į šiaurės rytus nuo miesto centro ir yra apsaugotas miško masyvu nuo dviejų judrių gatvių. Viena jų, pagrindinė, pasižymi apie 8400 transporto priemonių eismu per dieną, kita mažesnio intensyvumo, su maždaug 6200 transporto priemonių per dieną (https://portal.sisp.lt/portal/home/ žiūrėta 2025 m. gegužės 29 d.).

REZULTATAI
Mikroplastiko dalelių mažinimas miesto žaliąja infrastruktūra
Mikroplastiko dalelių koncentracijos apžvalga

Išsami MP dalelių koncentracijos analizė tyrimo laikotarpiu pateikta 11 pav. Eksperimento metu MP dalelės buvo aptiktos visuose mėginių ėmimo taškuose (–1, 0, +1 ir +2 metrai) palei miesto gatvę visais metų sezonais, o bendra jų koncentracija svyravo nuo 0,20 iki 5,95 dalelių cm^{-2} per dieną. Didžiausia MP koncentracija (5,95 dalelės cm^2 per dieną) buvo nustatyta pavasarį –1 m atstumu nuo gyvatvorės (iš gatvės pusės). Antroji pagal kiekį koncentracija tuo pačiu sezonu

buvo užfiksuota vidinėje (0 m) gyvatvorės pusėje, ir sudarė 4,84 daleles cm² per dieną.

Priešingai nei pavasarį, mažiausia MP koncentracija buvo užfiksuota vasarą 2 m atstumu nuo gyvatvorės (+2 m) ir siekė 0,20 dalelės cm² per dieną. MP koncentracijų sezoniniai svyravimai atspindi meteorologinių sąlygų, taršos šaltinių intensyvumo bei atmosferos dinamikos sąveiką, lemiančią MP dalelių sklaidą (Hee et al., 2023; Lee et al., 2024). Vasarą, aukštesnis planetos ribinis sluoksnis ir sustiprėjęs vertikalus atmosferos maišymasis gali skatinti dalelių išsisklaidymą aukštesniuose atmosferos sluoksniuose, dėl ko sumažėja jų koncentracijos (Su et al., 2018). Be to, sumažėjęs transporto intensyvumas vasaros atostogų laikotarpiu, taip pat gali prisidėti prie emisijų mažėjimo, o tai dar labiau veikia MP lygį vasaros metu.

Siekiant įvertinti miesto žaliosios infrastruktūros, šiuo atveju – gyvatvorės, vaidmenį mažinant ore esančių MP dalelių koncentraciją, pavasario sezono rezultatai buvo analizuojami tiek eksperimentinėje aplinkoje (su gyvatvore), tiek kontrolinėje aplinkoje (be gyvatvorės) (40 pav.). Palyginimui buvo pasirinktas (+1 metro) atstumas kaip atskaitos taškas, leidžiantis įvertinti gyvatvorės efektyvumą mažinant MP taršą artimoje aplinkoje.

Šis palyginimas suteikia vertingų įžvalgų apie žaliosios infrastruktūros, tokios kaip tujų gyvatvorė, efektyvumą mažinant transporto kilmės MP koncentracijas miesto gatvėse. Pavasario sezono rezultatai atskleidė ryškius skirtumus tarp eksperimentinės ir kontrolinės aplinkų. Ypač reikšmingas skirtumas nustatytas +1 m atstumu už gyvatvorės ribų: eksperimentinėje aplinkoje MP koncentracija siekė 4,59 dalelės cm² per dieną, o kontrolinėje – net 9,20 dalelės cm² per dieną. Tai atitinka 50,11 % sumažėjimą ir pabrėžia gyvatvorės gebėjimą riboti MP dalelių sklaidą į tolimesnes zonas, ypač vėjo pusėje nuo taršos šaltinio, taip prisidedant prie oro kokybės gerinimo. Pastebėta, kad MP lygiai buvo aukštesni arčiau gatvės (−1 m) nei toliau nuo jos (+2 m), o tai rodo, gyvatvorės veiksmingumą kaip

fizinio barjero, gebančio sulaikyti ir kaupti ore esančias MP daleles (Blanuša et al., 2020; Kumar et al., 2022; Redondo-Bermudez et al., 2021).

Didžiausi mikroplastiko koncentracijos sumažėjimai buvo nustatyti toliau nuo gyvatvorės, o tai rodo, kad jos poveikis oro kokybei peržengia tiesioginę aplinkos ribą, sudarydamas efektyvią apsauginę zoną, pasižyminčią mažesne oro tarša. Toks rezultatas leidžia daryti prielaidą, kad žalioji infrastruktūra, pavyzdžiui, tankios gyvatvorės, gali veiksmingai sumažinti transporto emisijų sukeltą oro taršą ne tik artimoje aplinkoje, bet ir platesniuose miesto erdvių kontekstuose. Šie rezultatai pabrėžia žaliosios infrastruktūros integravimo į miesto planavimą svarbą kaip tvarų sprendimą mažinti eismo sukeliamą MP taršą ir gerinti visuomenės sveikatą, ypač teritorijose, tiesiogiai paveiktose intensyvios transporto taršos.

Miesto želdinių veiksmingumas mažinant taršą

Thuja occidentalis gyvatvorės pasirodė esančios itin efektyvios mažinant transporto eismo sukeltą mikroplastiko taršą, pabrėžiant jų potencialą kaip tvarų sprendimą oro kokybės gerinimui. Įvertinus MP sulaikymo efektyvumą atsižvelgiant į skirtingus dydžio intervalus ir morfologines formas, tyrimas atskleidė reikšmingą gyvatvorės vaidmenį mažinant ore esančių MP dalelių koncentracijas miesto aplinkoje. Tai ypač aktualu teritorijose, kur transporto išmetimai ir kiti antropogeniniai šaltiniai daro didelį poveikį oro kokybei ir visuomenės sveikatai.
Didžiausias MP sulaikymo efektyvumas buvo nustatytas vasarą (64,5 % visų MP dalelių, iš jų 64,3 % fragmentų ir 71,4 % pluošto. Priešingai, mažiausias efektyvumas fiksuotas rudenį – atitinkamai 40,8 %, 23,4 % ir 11,5 % (žr. 41 pav. a). Apskaičiuotas vidutinis MP dalelių sulaikymo efektyvumas viso tyrimo laikotarpiu sudarė 54,29 % visų MP dalelių, iš jų 50,41 % fragmentų ir 44,54 % pluošto (žr. 7 lentelę).

Tanki augalų struktūra ir adatėlių formos lapai užtikrina didelį paviršiaus plotą, palankų ore esančioms dalelėms kauptis ir sulaikyti.

Nuosekliai aukštas MP dalelių sulaikymas pozicionuoja *Thuja occidentalis* gyvatvorę kaip vertingą žaliąją infrastruktūrą, galinčią prisidėti prie tvaresnės oro taršos valdymo strategijos. Miestuose. Paveikslas 41 b iliustruoja sezoniškai kintantį MP dalelių sulaikymo efektyvumą pagal skirtingus dydžio intervalus. Apibendrinti vidutiniai sulaikymo efektyvumo rodikliai pagal dydžio intervalus pateikti 7 lentelėje. Aukščiausias vidutinis MP sulaikymo efektyvumas buvo nustatytas 50–100 μm dydžio dalelėms – 67,25 %, o pavasarį šis rodiklis pasiekė net 94,24 %. Antroje vietoje pagal efektyvumą buvo 20–50 μm intervalas, kurio vidutinis sulaikymo lygis siekė 53,29 %, o vasarą – net 81,84 %. Žiemos sezono metu didžiausias efektyvumas pasiektas 100–250 μm dydžių intervale (56,86 %) bei 250–500 μm intervale (75 %) (41 pav. b). Miesto želdinių veiksmingumą mažinant oro taršą šiame tyrime taip pat patvirtina kitų autorių (Abhijith ir kt., 2022; Maher ir kt., 2013) rezultatai.

Asmeninė ekspozicija juodajai angliai ir kietosioms dalelėms miesto mikroaplinkose
Juodosios anglies matavimai

Rezultatai, pateikti 42 paveiksle, apibūdina juodajai angliai būdingas masės koncentracijas, jų šaltinių indėlius bei aerozolio dalelių skaitines koncentracijas, fiksuotas 2022 m. kovo mėn. miesto fono stebėjimo vietoje. Vidutinė mėnesinė bendro aerozolių dalelių skaičiaus koncentracija (N_{total}), matuota 10–430 nm dydžio diapazone, siekė 9820 dalelių #/cm³ (SD: 6410 #/cm³). Valandinės bendro aerozolio dalelių skaičiaus koncentracijos svyravo nuo 740 #/cm³ iki 38 370 #/cm³. Atitinkamai, bendra aerozolio dalelių masės koncentracija (M_{total}) rodė reikšmingą laiko kintamumą – nuo 0,3 iki 33,4 μg/m³, vidurkis , vidutinė reikšmė siekė 6,2 μg/m³ (SD: 5,3 μg/m³). Eksperimento metu (kovo 17–18 d.) vidutinės M_{total} koncentracijos siekė 11,3 ir 12,7 μg/m³, atitinkančios mėnesio pasiskirstymo aukštesnį kvartilį (Q3). Valandinės juodosios anglies masės koncentracija 2022 m. kovo mėnesį svyravo nuo 0,30 iki 9,01

μg/m³, o vidutinė reikšmė siekė 1,94 μg/m³ (SD: 1,80 μg/m³), kaip parodyta 42 paveiksle. Su eismu susijusios juodosios anglies dalis (BC$_{tr}$) labai stipriai koreliavo su bendra BC koncentracija (r = 0,98) ir sudarė apie 66 % visos BC masės koncentracijos. Didžiausiai transporto kilmės juodosios anglies indėlis daugiausia buvo fiksuojamas dienos metu (08:00–18:00), o biomasės deginimo kilmės juodosios anglies (BC$_{wb}$) indėlis sudarė likusius 34 % ir buvo ryškesnis nakties valandomis, pasiekdamas piką apie 04:00 vietos laiku – 42 % visos koncentracijos. Paros BC koncentracijos kitimas atspindi bendrą meteorologinių sąlygų, transporto srautų modelių ir biomasės deginimo namų šildymui bendrą poveikį. Tarp BC masės koncentracijos ir aerozolio dalelių skaitinės koncentraciios N$_{total}$ nustatyta stipri teigiama koreliacija (r = 0,83), rodanti reikšmingą BC emisijos šaltinių indėlį bendram dalelių skaičiui <430 nm dydžio intervale. Tuo tarpu koreliacija tarp bendros aerozolio dalelių masės koncentracijos M$_{total}$ ir BC buvo vidutinė (r = 0,68), kas rodo, kad BC mažiau prisideda prie PM$_1$ masės koncentracijos palyginti su indėliu dalelių skaičiaus koncentracijai.

Juodosios anglies nusėdimo dozės žmogaus kvėpavimo takuose vertinimas

Norint įvertinti asmeninę ekspoziciją bei su tuo susijusią juodosios anglies bei PM$_1$ nusėdimo dozę žmogaus kvėpavimo takuose mobiliųjų matavimų metu bei miesto fono sąlygomis (FTMC1), buvo analizuojamos vidutinės BC ir PM$_1$ masės koncentracijos. Laikinasis masės koncentracijų kitimas tiek lauke, tiek transporto priemonės viduje pateikta 43 pav. Trijų kelionių automobiliu metu vidutinės BC koncentracijos siekė 2,42 ± 1,77, 1,67 ± 0,66 ir 7,14 ± 4,42 μg/m³, atitinkamai, o PM$_1$ koncentracijos siekė 3,36 ± 1,32, 15,26 ± 5,16 ir 8,53 ± 4,78 μg/m³. Tuo tarpu patalpose vidutinės koncentracijos buvo ženkliai mažesnės – PM$_1$ 1,3 ± 0,45 μg/m³ ir BC 0,08 ± 0,4 μg/m³. Visose aplinkose nustatyta stipri teigiama koreliacija (r = 0,92) tarp BC ir PM$_1$ masės koncentracijų.

Juodosios anglies nusėdimo dozės (DD) vertinimas buvo atliktas remiantis eksperimentu, kurio metu tiriamasis asmuo sėdėjo patalpoje. Šio eksperimento metu vidutinė juodosios anglies koncentracija patalpoje siekė 1700 ng/m³. Penkių minučių laikotarpiui apskaičiuota BC nusėdimo dozė sudarė 38 ± 5 % įkvėptos koncentracijos (9 pav.). Tiriamojo minutinis ventiliacijos (MV) apskaičiuotas rodiklis 19,1 L/min (8 pav.), o tai viršijo įprastą sėdinčio vyro kvėpavimo normos viršutię ribą (8,8–16,1 L/min) (Madueno ir kt., 2019). Remiantis lygtimi [7], buvo sumodeliuota BC masės koncentracijos nusėdimo dozė kelionės į/iš darbo metu Vilniaus mieste. Gauti rezultatai svyravo nuo 19 iki 53 ng/min automobilio viduje, didžiausios reikšmės užfiksuotos važiuojant priemiesčių gyvenamosiose teritorijose. Tuo tarpu lauke svyravo nuo 74 iki 125 ng/min, o didžiausias pikas fiksuotas prie centrinio viaduko (Savanorių transporto žiedas). Vidutiniškai nusėdimo dozė automobilio viduje buvo 2–4 kartus mažesnė nei lauke. Mažiausios reikšmės buvo siejamos su biuro/laboratorijos mikroaplinka.

Lyginamoji analizė tarp juodosios anglies koncentracijų, matuotų mobiliosios stebėsenos metu transporto priemonėje, ir miesto fono reikšmėmis atskleidė, kad daugumos kelionių laikotarpiais BC koncentracijos buvo žymiai aukštesnės. Automobilio salone fiksuotos BC koncentracijos dažniausiai svyravo nuo fono reikšmių iki 9 µg/m³ (Q3 kvantilis), o tuo tarpu lauke šios koncentracijos siekė iki 20 µg/m³ (Q3) (44 pav. D). Šie rezultatai atskleidžia reikšmingą transporto aplinkos indėlį į asmeninę BC ekspoziciją, viršijantį miesto fonines sąlygas, ypač intensyvaus eismo ar riboto oro cirkuliavimo sąlygomis.

Pastebėta, kad BC koncentracijos automobilyje ne visada atitiko lauko vertes, ką lėmė efektyvi ventiliacijos sistema, ribojanti dalelių patekimą į vidų (44 pav. B, D). Ypač ryški ši tendencija buvo ryto kelionių metu, kai salone fiksuotos vidinės BC koncentracijos dažnai buvo panašios arba netgi mažesnės nei lauke (44 pav. B). Lyginant vidutines BC koncentracijas automobilyje ir lauke pirmosios ir antrosios kelionių metu, nustatyti reikšmingi skirtumai, kurie siekė iki

2 ir 5 kartų, atitinkamai. Svarbu paminėti, kad padidėjęs miesto fono BC lygis antrosios kelionės metu galėjo reikšmingai prisidėti prie šių skirtumų. Palyginus automobilyje ir lauke fiksuotas koncentracijas su miesto fono BC koncentracijomis, paaiškėjo, kad pastarosios dažniausiai buvo žemesnės. Kaip parodyta 44 paveiksle (A ir C), fono juodosios anglies koncentracijos indėlis nusėdimo dozei sudarė iki 25 % kelionės metu ir iki 60 % kabinoje gaunamos dozės. Be to, 44 paveiksle (C) pateiktas BC masės nusėdimo vertinimas visuose kvėpavimo takuose įvairiose mikroaplinkose darbo dienos metu, apimančiose tiek keliones, tiek darbo laiką biure. Didžiausios modeliuotos juodosios anglies masės nusėdimo dozės reikšmės buvo fiksuotos rytinės kelionės metu (53 ng/min) ir vakare (26 ng/min), atspindinčios reikšmingą asmeninę ekspoziciją transporto kilmės itin smulkioms dalelėms. Tuo tarpu mažiausia nusėdimo dozės reikšmė kelionės metu (13 ng/min) nustatyta vidurdienio maršrute tarp FTMC1 ir FTMC2. Šį sumažėjimą tikėtina lėmė palankesnės išsklaidymo atmosferoje sąlygos bei sumažėjęs transporto intensyvumas.

T yrimo rezultatai atskleidė reikšmingą skirtumą tarp juodosios anglies nusėdimo dozių skirtingose mikroaplinkose – patalpose ir kelionių metu. Kelionės į/iš darbą metu asmenys dažniausiai yra veikiami šalia esančių transporto priemonių išmetamųjų teršalų, kurių įtaką lemia eismo intensyvumas, kelionės laikas (piko ar ne piko valandos) ir miesto planavimas (gyvenamosios, komercinės ar pramoninės zonos). Priešingai, patalpose, ypač biuruose su mechaninėmis ventiliacijos sistemomis, BC ekspozicija gali būti reikšmingai mažesnė. Pavyzdžiui, biure apskaičiuota vidutinė nusėdimo dozė siekė 11 ng/min, t. y. maždaug šešis kartus mažiau nei didžiausia nustatyta dozė rytinės kelionės automobiliu metu (53 ng/min). Šis skirtumas daugiausia siejamas su efektyviu oro filtravimu, kurį užtikrina aukšto efektyvumo filtrai (pvz., F7–F9 filtrams), ženkliai mažinantys ore esančių smulkiųjų dalelių patekimą į patalpas.

Įvertinus vidutinį dienos laiką, praleidžiamą kelionėse (~40 min) ir standartinę 8 valandų darbo dieną, juodosios anglies nusėdimo

dozių santykis tarp biuro ir kelionės aplinkų siekė 2,5: DD_{office} / DD_{trip} = (0,011 × 8) / (0,052 × 2/3) = 2,5. Šis rezultatas rodo, kad kelionės, nors ir trumpesnės trukmės gali lemti iki trečdalio bendros dienos asmeninės ekspozicijos, susijusios su darbo veikla. , priklausomai nuo darbo vietos oro kokybės ir kelionės trukmės.

Modeliuotos juodosios anglies masės nusėdimo dozės kintamumas tarp skirtingų mikroaplinkų siekė iki keturių kartų skirtumą. Vertinant nusėdimą žmogaus kvėpavimo takuose, didžiausias nusėdimo intensyvumas buvo nustatytas plaučių (alveoliniame) regione, kur dozė kito nuo 5,1 ng/min darbo metu biure iki 19,9 ng/min rytinės kelionės metu (44 pav. C).

Vidutinės juodosios anglies masės koncentracijos, išmatuotos visuose kelionių maršrutuose ir biure, buvo naudojamos kaip įvesties duomenys nusėdimo frakcijos (DF) skaičiavimui, taikant daugiafazės kvėpavimo takų dalelių dozimetrijos modelį (MPPD). Nors DF reikšmės daugiausiai priklauso nuo įkvėptų dalelių aerodinaminio skersmens, o ne nuo aplinkos koncentracijos (J. Gao ir kt., 2022), koncentracija tampa svarbi įvertinant dalelių dydžių pasiskirstymą, kuris lemia realų lnusėdimo efektyvumą. Laiko eigoje kintantis dalelių dydžio pasiskirstymas tiesiogiai veikia skirtingų kvėpavimo takų regionų nusėdimo modeliavimo rezultatus. Todėl depozicijos frakcijos įvairiose kvėpavimo takų dalyse (nosies, trachėjos–bronchų bei alveoliniame regione) gali reikšmingai svyruoti priklausomai nuo mikroaplinkos sąlygų ir aerodinaminių parametrų dinamikos. Skaičiuojant nusėdimo frakciją juodosios anglies dalelėms 10–1000 nm dydžių intervale, vidutinis modeliuotas dalelių paskirstymas žmogaus kvėpavimo takų regionuose pasiskirstė taip: 33,6 % nusėdo viršutiniuose kvėpavimo takuose (URT), 26,8 % – tracheobronchų (TB) regione ir 39,2 % – alveolinėjee arba plaučių (PU) dalyje. Stebėtas nusėdimo frakcijos kintamumas tarp kvėpavimo takų segmentų skirtingų kelionių metu svyravo nuo 2,5 % iki 5 %, o tai rdo, kad tik nežymius skirtumus, priklausančius nuo konkretaus nusėdimo scenarijaus. Tokie rezultatai leidžia teigti, kad, nepaisant

mikroaplinkos pokyčių, dalelių nusėdimo proporcijos kvėpavimo sistemoje išlieka palyginti pastovios, kai vertinamos panašaus dydžio BC dalelės.

IŠVADOS

1. Miesto aplinkoje, šalia intensyvaus eismo kelių, oro mėginiuose vyrauja fragmentinės formos mikroplastiko dalelės, o didžiausias jų kiekis fiksuojamas pavasarį (iki 98 %). Visais sezonais daugumą MP sudaro 50–100 µm dydžio frakcija, kuri siekia iki 55 % viso aptikto kiekio, o tai rodo įkvėpuojamo dydžio dalelių paplitimą žmogaus kvėpavimo takų aukštyje. Spalvinė analizė parodė, kad juodos spalvos dalelės, dažniausiai siejamos su padangų nusidėvėjimu, vasaros metu sudarė iki 71 % visų MP, pabrėžiant kelių transporto reikšmę kaip pagrindinį MP taršos šaltinį. Polimerinė sudėtis atskleidė, kad visuose mėginiuose vyraujantis polimeras yra polietilenas, vidutiniškai sudaręs 43 % visų aptiktų MP, o pavasarį jo kiekis išauga iki 69 %, kas patvirtina šio plastiko plačią naudojimo sritį ir jo ilgalaikį išsilaikymą miesto atmosferoje.

2. *Thuja occidentalis* gyvatvorė, kaip žaliųjų miesto infrastruktūrų elementas, yra veiksminga priemonė oro mikroplastiko taršai mažinti šalia intensyvaus eismo gatvių. Visų metų sezonų analizė atskleidė, kad bendras mikroplastiko sulaikymo efektyvumas siekė 54 %, o vasaros metu šis rodiklis padidėjo iki 65 %, kai kartu buvo fiksuotas ir didžiausias pluošto formos dalelių sulaikymas (71 %). Pagal dalelių dydį, didžiausias sulaikymo efektyvumas buvo nustatytas 50–100 µm dydžio frakcijai – vidutiniškai 67 %, o pavasarį pasiekė net 94 %, atspindint sezoninį medžių paviršiaus savybių ir dalelių sedimentacijos sąlygų poveikį. Erdvinė analizė parodė, kad MP koncentracija ženkliai sumažėjo jau 1 metro atstumu nuo gyvatvorės – nuo 9,2 iki 4,59 dalelės cm^{-2} per dieną, t. y. 50 % mažiau nei kontroliniame taške be apsauginio barjero. Tai patvirtina, kad fizinė augalo struktūra efektyviai veikia kaip dalelių kaupimo paviršius, mažinantis MP sklaidą ore. Sveikatos rizikos vertinimas parodė, kad gyvatvorė taip pat

mažina potencialią įkvėpimo riziką, kuri pavasarį sumažėjo net 71 %, kai buvo nustatytas didžiausias rizikos indeksas – 831.

3. Asmeninė ekspozicija PM_1, $PM_{2.5}$ dalelėms ir juodajai angliai (BC) buvo žymiai didesnė kelionių metu nei biuro vidaus aplinkoje. Nors kelionės sudarė mažiau nei 10 % paros trukmės, PM_1 ekspozicija šiuo laikotarpiu sudarė iki 80 % bendros dienos ekspozicijos. Biuro aplinkos, aprūpintos mechaninėmis vėdinimo sistemomis, veiksmingai mažino PM ir BC koncentracijas; tačiau dalelių infiltracija vis tiek lėmė reikšmingą BC nusėdimo dozę – 11 ng/min, kuri buvo 4,8 karto mažesnė nei nusėdimo dozė transporto priemonėje (53 ng/min). Be to, modeliavimas parodė, kad 39 % įkvėptos juodosios anglies masės nusėdo alveoliniame regione, pabrėžiant trumpalaikės, bet intensyvios ekspozicijos transporto mikroaplinkose svarbą žmogaus sveikatai.

4. Iškastinio kuro (arba transporto) kilmės juodoji anglis yra pagrindinis asmeninės ekspozicijos šaltinis kelionių į/iš darbą metu urbanizuotoje aplinkoje. Kelionių laikotarpiu net 66 % visos BC masės koncentracijos sudaro transporto kilmės juodoji anglis, o tai reikšmingai padidina įkvepiamų dalelių nusėdimo dozes žmogaus kvėpavimo takuose. Didžiausias poveikis nustatytas rytinių piko valandų metu – tuomet modeliuota BC nusėdimo dozė alveoliniame regione siekė iki 19,9 ng/min, palyginti su vos 5,1 ng/min esant biure. Tai rodo, kad nepaisant trumpesnės buvimo trukmės, transporto mikroaplinkos lemia didesnį kvėpavimo takų apkrovimą, ypač apatinėse kvėpavimo sistemos dalyse, kur smulkiosios dalelės efektyviausiai nusėda.

REFERENCES

Abdel-Shafy, H. I., & Mansour, M. S. M. (2016). A review on polycyclic aromatic hydrocarbons: Source, environmental impact, effect on human health and remediation. *Egyptian Journal of Petroleum, 25*(1), 107-123. https://doi.org/10.1016/j.ejpe.2015.03.011

Abhijith, K. V., Kukadia, V., & Kumar, P. (2022). Investigation of air pollution mitigation measures, ventilation, and indoor air quality at three schools in London. *Atmospheric Environment, 289*. https://doi.org/10.1016/j.atmosenv.2022.119303

Baensch-Baltruschat, B., Kocher, B., Stock, F., & Reifferscheid, G. (2020, Sep 1). Tyre and road wear particles (TRWP) - A review of generation, properties, emissions, human health risk, ecotoxicity, and fate in the environment. *Sci Total Environ, 733*, 137823. https://doi.org/10.1016/j.scitotenv.2020.137823

Ballent, A., Corcoran, P. L., Madden, O., Helm, P. A., & Longstaffe, F. J. (2016, Sep 15). Sources and sinks of microplastics in Canadian Lake Ontario nearshore, tributary and beach sediments. *Mar Pollut Bull, 110*(1), 383-395. https://doi.org/10.1016/j.marpolbul.2016.06.037

Blanuša, T., Qadir, Z. J., Kaur, A., Hadley, J., & Gush, M. B. (2020). Evaluating the Effectiveness of Urban Hedges as Air Pollution Barriers: Importance of Sampling Method, Species Characteristics and Site Location. *Environments, 7*(10). https://doi.org/10.3390/environments7100081

Bouza, E., Vargas, F., Alcazar, B., Alvarez, T., Asensio, A., Cruceta, G., Gracia, D., Guinea, J., Gil, M. A., Linares, C., Munoz, P., Pastor, P., Pedro-Botet, M. L., Querol, X., Tovar, J., Urrutia, I., Villar, F., & Palomo, E. (2022, Aug). Air pollution and health prevention: A document of reflection. *Rev Esp Quimioter, 35*(4), 307-332. https://doi.org/10.37201/req/171.2021

Brugge, D., Durant, J. L., & Rioux, C. (2007, Aug 9). Near-highway pollutants in motor vehicle exhaust: a review of epidemiologic evidence of cardiac and pulmonary health risks. *Environ Health, 6*, 23. https://doi.org/10.1186/1476-069X-6-23

Butt, E. W., Turnock, S. T., Rigby, R., Reddington, C. L., Yoshioka, M., Johnson, J. S., Regayre, L. A., Pringle, K. J., Mann, G. W., & Spracklen, D. V. (2017). Global and regional trends in particulate air pollution and attributable health burden over the past 50 years. *Environmental Research Letters, 12*(10). https://doi.org/10.1088/1748-9326/aa87be

Byčenkienė, S., Gill, T., Khan, A., Kalinauskaitė, A., Ulevicius, V., & Plauškaitė, K. (2023). Estimation of Carbonaceous Aerosol Sources under Extremely Cold Weather Conditions in an Urban Environment. *Atmosphere, 14*(2). https://doi.org/10.3390/atmos14020310

Byčenkienė, S., Plauškaitė, K., Dudoitis, V., & Ulevicius, V. (2014). Urban background levels of particle number concentration and sources in Vilnius, Lithuania. *Atmospheric Research, 143*, 279-292. https://doi.org/10.1016/j.atmosres.2014.02.019

Cai, Z., Li, F., Rong, M., Lin, L., Yao, Q., Huang, Y., Chen, X., & Wang, X. (2019). Introduction. In *Novel Nanomaterials for Biomedical, Environmental and Energy Applications* (pp. 1-36). https://doi.org/10.1016/b978-0-12-814497-8.00001-1

Calvo, A. I., Alves, C., Castro, A., Pont, V., Vicente, A. M., & Fraile, R. (2013). Research on aerosol sources and chemical composition: Past, current and emerging issues. *Atmospheric Research, 120-121*, 1-28. https://doi.org/10.1016/j.atmosres.2012.09.021

Capotorti, G., Bonacquisti, S., Abis, L., Aloisi, I., Attorre, F., Bacaro, G., Balletto, G., Banfi, E., Barni, E., Bartoli, F., Bazzato, E., Beccaccioli, M., Braglia, R., Bretzel, F., Brighetti, M. A., Brundu, G., Burnelli, M., Calfapietra, C., Cambria, V. E., Caneva, G., Canini, A., Caronni, S., Castello, M., Catalano, C.,

Celesti-Grapow, L., Cicinelli, E., Cipriani, L., Citterio, S., Concu, G., Coppi, A., Corona, E., Del Duca, S., Del, V. E., Di Gristina, E., Domina, G., Faino, L., Fano, E. A., Fares, S., Farris, E., Farris, S., Fornaciari, M., Gaglio, M., Galasso, G., Galletti, M., Gargano, M. L., Gentili, R., Giannotta, A. P., Guarino, C., Guarino, R., Iaquinta, G., Iiriti, G., Lallai, A., Lallai, E., Lattanzi, E., Manca, S., Manes, F., Marignani, M., Marinangeli, F., Mariotti, M., Mascia, F., Mazzola, P., Meloni, G., Michelozzi, P., Miraglia, A., Montagnani, C., Mundula, L., Muresan, A. N., Musanti, F., Nardini, A., Nicosia, E., Oddi, L., Orlandi, F., Pace, R., Palumbo, M. E., Palumbo, S., Parrotta, L., Pasta, S., Perini, K., Poldini, L., Postiglione, A., Prigioniero, A., Proietti, C., Raimondo, F. M., Ranfa, A., Redi, E. L., Reverberi, M., Roccotiello, E., Ruga, L., Savo, V., Scarano, P., Schirru, F., Sciarrillo, R., Scuderi, F., Sebastiani, A., Siniscalco, C., Sordo, A., Suanno, C., Tartaglia, M., Tilia, A., Toffolo, C., Toselli, E., Travaglini, A., Ventura, F., Venturella, G., Vincenzi, F., & Blasi, C. (2020). More nature in the city. *Plant Biosystems - An International Journal Dealing with all Aspects of Plant Biology, 154*(6), 1003-1006. https://doi.org/10.1080/11263504.2020.1837285

Chauhan, B. V. S., Corada, K., Young, C., Smallbone, K. L., & Wyche, K. P. (2024). Review on Sampling Methods and Health Impacts of Fine (PM2.5, ≤2.5 μm) and Ultrafine (UFP, PM0.1, ≤0.1 μm) Particles. *Atmosphere, 15*(5). https://doi.org/10.3390/atmos15050572

Chen, F., Zhang, W., Mfarrej, M. F. B., Saleem, M. H., Khan, K. A., Ma, J., Raposo, A., & Han, H. (2024, Jul 15). Breathing in danger: Understanding the multifaceted impact of air pollution on health impacts. *Ecotoxicol Environ Saf, 280*, 116532. https://doi.org/10.1016/j.ecoenv.2024.116532

Chowdhury, S., Pozzer, A., Haines, A., Klingmuller, K., Munzel, T., Paasonen, P., Sharma, A., Venkataraman, C., & Lelieveld, J. (2022, Jan 15). Global health burden of ambient PM(2.5) and the contribution of anthropogenic black carbon and organic aerosols. *Environ Int, 159*, 107020. https://doi.org/10.1016/j.envint.2021.107020

Cichowicz, R., & Bochenek, A. D. (2024). Assessing the effects of urban heat islands and air pollution on human quality of life. *Anthropocene, 46.* https://doi.org/10.1016/j.ancene.2024.100433

Corley, R. A., Kuprat, A. P., Suffield, S. R., Kabilan, S., Hinderliter, P. M., Yugulis, K., & Ramanarayanan, T. S. (2021, Aug 3). New Approach Methodology for Assessing Inhalation Risks of a Contact Respiratory Cytotoxicant: Computational Fluid Dynamics-Based Aerosol Dosimetry Modeling for Cross-Species and In Vitro Comparisons. *Toxicol Sci, 182*(2), 243-259. https://doi.org/10.1093/toxsci/kfab062

Crutchett, T. W., & Bornt, K. R. (2024, Jun). A simple overflow density separation method that recovers >95 % of dense microplastics from sediment. *MethodsX, 12*, 102638. https://doi.org/10.1016/j.mex.2024.102638

Darquenne, C. (2014, Jun). Aerosol deposition in the human lung in reduced gravity. *J Aerosol Med Pulm Drug Deliv, 27*(3), 170-177. https://doi.org/10.1089/jamp.2013.1079

Davuliene, L., Khan, A., Semcuk, S., Minderyte, A., Davtalab, M., Kandrotaite, K., Dudoitis, V., Uoginte, I., Skapas, M., & Bycenkiene, S. (2022, Jul 21). Evaluation of Work-Related Personal Exposure to Aerosol Particles. *Toxics, 10*(7). https://doi.org/10.3390/toxics10070405

de Bont, J., Jaganathan, S., Dahlquist, M., Persson, A., Stafoggia, M., & Ljungman, P. (2022, Jun). Ambient air pollution and cardiovascular diseases: An umbrella review of systematic

reviews and meta-analyses. *J Intern Med, 291*(6), 779-800. https://doi.org/10.1111/joim.13467

Deevi, R., & Lu, M. (2024). In-Vehicle Air Pollutant Exposures from Daily Commute in the San Francisco Bay Area, California. *Atmosphere, 15*(9). https://doi.org/10.3390/atmos15091130

Dias, D., & Tchepel, O. (2018, Mar 20). Spatial and Temporal Dynamics in Air Pollution Exposure Assessment. *Int J Environ Res Public Health, 15*(3). https://doi.org/10.3390/ijerph15030558

Eklund, A. G., Chow, J. C., Greenbaum, D. S., Hidy, G. M., Kleinman, M. T., Watson, J. G., & Wyzga, R. E. (2014, Nov). Public health and components of particulate matter: the changing assessment of black carbon. *J Air Waste Manag Assoc, 64*(11), 1221-1231. https://doi.org/10.1080/10962247.2014.960218

Faria, T., Cunha-Lopes, I., Pilou, M., Housiadas, C., Querol, X., Alves, C., & Almeida, S. M. (2022, Jun 1). Children's exposure to size-fractioned particulate matter: Chemical composition and internal dose. *Sci Total Environ, 823*, 153745. https://doi.org/10.1016/j.scitotenv.2022.153745

Fussell, J. C., Franklin, M., Green, D. C., Gustafsson, M., Harrison, R. M., Hicks, W., Kelly, F. J., Kishta, F., Miller, M. R., Mudway, I. S., Oroumiyeh, F., Selley, L., Wang, M., & Zhu, Y. (2022, Jun 7). A Review of Road Traffic-Derived Non-Exhaust Particles: Emissions, Physicochemical Characteristics, Health Risks, and Mitigation Measures. *Environ Sci Technol, 56*(11), 6813-6835. https://doi.org/10.1021/acs.est.2c01072

Gao, J., Qiu, Z., Cheng, W., & Gao, H. O. (2022, Mar 1). Children's exposure to BC and PM pollution, and respiratory tract deposits during commuting trips to school. *Ecotoxicol Environ Saf, 232*, 113253. https://doi.org/10.1016/j.ecoenv.2022.113253

Gao, Z., Cizdziel, J. V., Wontor, K., Clisham, C., Focia, K., Rausch, J., & Jaramillo-Vogel, D. (2022). On airborne tire wear particles along roads with different traffic characteristics using

passive sampling and optical microscopy, single particle SEM/EDX, and μ-ATR-FTIR analyses. *Frontiers in Environmental Science, 10*. https://doi.org/10.3389/fenvs.2022.1022697

Gehrke, I., Schlafle, S., Bertling, R., Oz, M., & Gregory, K. (2023, Dec 15). Review: Mitigation measures to reduce tire and road wear particles. *Sci Total Environ, 904*, 166537. https://doi.org/10.1016/j.scitotenv.2023.166537

González-Flórez, C., Klose, M., Alastuey, A., Dupont, S., Escribano, J., Etyemezian, V., Gonzalez-Romero, A., Huang, Y., Kandler, K., Nikolich, G., Panta, A., Querol, X., Reche, C., Yus-Díez, J., & Pérez García-Pando, C. (2023). Insights into the size-resolved dust emission from field measurements in the Moroccan Sahara. *Atmospheric Chemistry and Physics, 23*(12), 7177-7212. https://doi.org/10.5194/acp-23-7177-2023

Grazuleviciute-Vileniske, I., Zaleskiene, E., Baltrusaityte, G., & Rubikaite, L. (2015). Urbanization Influence on the Relicts of Soviet Rural Landscape. *Sage Open, 5*(3). https://doi.org/10.1177/2158244015601718

Hahladakis, J. N., & Iacovidou, E. (2018, Jul 15). Closing the loop on plastic packaging materials: What is quality and how does it affect their circularity? *Sci Total Environ, 630*, 1394-1400. https://doi.org/10.1016/j.scitotenv.2018.02.330

He, B., Shi, C., Chen, B., Wu, H., Goonetilleke, A., & Liu, A. (2023, Oct 5). Occurrence and risk associated with urban road-deposited microplastics. *J Hazard Mater, 459*, 132012. https://doi.org/10.1016/j.jhazmat.2023.132012

Hee, Y. Y., Hanif, N. M., Weston, K., Latif, M. T., Suratman, S., Rusli, M. U., & Mayes, A. G. (2023). Atmospheric microplastic transport and deposition to urban and pristine tropical locations in Southeast Asia. *Science of The Total Environment, 902*. https://doi.org/10.1016/j.scitotenv.2023.166153

Jahandari, A. (2023). Microplastics in the urban atmosphere: Sources, occurrences, distribution, and potential health implications. *Journal of Hazardous Materials Advances, 12*. https://doi.org/10.1016/j.hazadv.2023.100346

Janssen, N. A., Hoek, G., Simic-Lawson, M., Fischer, P., van Bree, L., ten Brink, H., Keuken, M., Atkinson, R. W., Anderson, H. R., Brunekreef, B., & Cassee, F. R. (2011, Dec). Black carbon as an additional indicator of the adverse health effects of airborne particles compared with PM10 and PM2.5. *Environ Health Perspect, 119*(12), 1691-1699. https://doi.org/10.1289/ehp.1003369

Jarlskog, I., Stromvall, A. M., Magnusson, K., Galfi, H., Bjorklund, K., Polukarova, M., Garcao, R., Markiewicz, A., Aronsson, M., Gustafsson, M., Norin, M., Blom, L., & Andersson-Skold, Y. (2021, Jun 20). Traffic-related microplastic particles, metals, and organic pollutants in an urban area under reconstruction. *Sci Total Environ, 774*, 145503. https://doi.org/10.1016/j.scitotenv.2021.145503

Jiang, Y., Han, J., Na, J., Fang, J., Qi, C., Lu, J., Liu, X., Zhou, C., Feng, J., Zhu, W., Liu, L., Jiang, H., Hua, Z., Pan, G., Yan, L., Sun, W., & Yang, Z. (2022, Nov). Exposure to microplastics in the upper respiratory tract of indoor and outdoor workers. *Chemosphere, 307*(Pt 3), 136067. https://doi.org/10.1016/j.chemosphere.2022.136067

Johansson, K. O., Dillstrom, T., Monti, M., El Gabaly, F., Campbell, M. F., Schrader, P. E., Popolan-Vaida, D. M., Richards-Henderson, N. K., Wilson, K. R., Violi, A., & Michelsen, H. A. (2016, Jul 26). Formation and emission of large furans and oxygenated hydrocarbons from flames. *Proc Natl Acad Sci U S A, 113*(30), 8374-8379. https://doi.org/10.1073/pnas.1604772113

Johnson, P. R., & Graham, J. J. (2005, Sep). Fine particulate matter national ambient air quality standards: public health impact on populations in the northeastern United States. *Environ Health Perspect, 113*(9), 1140-1147. https://doi.org/10.1289/ehp.7822

Jones, E. R., Laurent, J. G. C., Young, A. S., MacNaughton, P., Coull, B. A., Spengler, J. D., & Allen, J. G. (2021, Aug). The Effects of Ventilation and Filtration on Indoor PM(2.5) in Office Buildings in Four Countries. *Build Environ, 200*. https://doi.org/10.1016/j.buildenv.2021.107975

Karthick Raja Namasivayam, S., Priyanka, S., Lavanya, M., Krithika Shree, S., Francis, A. L., Avinash, G. P., Arvind Bharani, R. S., Kavisri, M., & Moovendhan, M. (2024, Aug). A review on vulnerable atmospheric aerosol nanoparticles: Sources, impact on the health, ecosystem and management strategies. *J Environ Manage, 365*, 121644. https://doi.org/10.1016/j.jenvman.2024.121644

Khalid, N., Aqeel, M., & Noman, A. (2020, Dec). Microplastics could be a threat to plants in terrestrial systems directly or indirectly. *Environ Pollut, 267*, 115653. https://doi.org/10.1016/j.envpol.2020.115653

Khomenko, S., Cirach, M., Pereira-Barboza, E., Mueller, N., Barrera-Gomez, J., Rojas-Rueda, D., de Hoogh, K., Hoek, G., & Nieuwenhuijsen, M. (2021, Mar). Premature mortality due to air pollution in European cities: a health impact assessment. *Lancet Planet Health, 5*(3), e121-e134. https://doi.org/10.1016/S2542-5196(20)30272-2

Klockner, P., Seiwert, B., Weyrauch, S., Escher, B. I., Reemtsma, T., & Wagner, S. (2021, Sep). Comprehensive characterization of tire and road wear particles in highway tunnel road dust by use of size and density fractionation. *Chemosphere, 279*, 130530. https://doi.org/10.1016/j.chemosphere.2021.130530

Knight, L. J., Parker-Jurd, F. N. F., Al-Sid-Cheikh, M., & Thompson, R. C. (2020, May). Tyre wear particles: an abundant yet widely unreported microplastic? *Environ Sci Pollut Res Int, 27*(15), 18345-18354. https://doi.org/10.1007/s11356-020-08187-4

Kole, P. J., Lohr, A. J., Van Belleghem, F., & Ragas, A. M. J. (2017, Oct 20). Wear and Tear of Tyres: A Stealthy Source of Microplastics in the Environment. *Int J Environ Res Public Health, 14*(10). https://doi.org/10.3390/ijerph14101265

Konechnaya, O., Luchtrath, S., Dsikowitzky, L., & Schwarzbauer, J. (2020, Feb). Optimized microplastic analysis based on size fractionation, density separation and mu-FTIR. *Water Sci Technol, 81*(4), 834-844. https://doi.org/10.2166/wst.2020.173

Kousis, I., Manni, M., & Pisello, A. L. (2022). Environmental mobile monitoring of urban microclimates: A review. *Renewable and Sustainable Energy Reviews, 169*. https://doi.org/10.1016/j.rser.2022.112847

Kovochich, M., Liong, M., Parker, J. A., Oh, S. C., Lee, J. P., Xi, L., Kreider, M. L., & Unice, K. M. (2021, Feb 25). Chemical mapping of tire and road wear particles for single particle analysis. *Sci Total Environ, 757*, 144085. https://doi.org/10.1016/j.scitotenv.2020.144085

Kreider, M. L., Panko, J. M., McAtee, B. L., Sweet, L. I., & Finley, B. L. (2010, Jan 1). Physical and chemical characterization of tire-related particles: comparison of particles generated using different methodologies. *Sci Total Environ, 408*(3), 652-659. https://doi.org/10.1016/j.scitotenv.2009.10.016

Kuang, B., Zhang, F., Shen, J., Shen, Y., Qu, F., Jin, L., Tang, Q., Tian, X., & Wang, Z. (2022, Dec 10). Chemical characterization, formation mechanisms and source apportionment of PM(2.5) in north Zhejiang Province: The importance of secondary formation and vehicle emission. *Sci Total Environ, 851*(Pt 2), 158206. https://doi.org/10.1016/j.scitotenv.2022.158206

Kumar, P., Zavala-Reyes, J. C., Tomson, M., & Kalaiarasan, G. (2022, Jan). Understanding the effects of roadside hedges on the horizontal and vertical distributions of air pollutants in street canyons. *Environ Int, 158*, 106883. https://doi.org/10.1016/j.envint.2021.106883

Kwak, M. J., Lee, J., Kim, H., Park, S., Lim, Y., Kim, J. E., Baek, S. G., Seo, S. M., Kim, K. N., & Woo, S. Y. (2019). The Removal Efficiencies of Several Temperate Tree Species at Adsorbing Airborne Particulate Matter in Urban Forests and Roadsides. *Forests, 10*(11). https://doi.org/10.3390/f10110960

Lafortezza, R., Chen, J., van den Bosch, C. K., & Randrup, T. B. (2018, Aug). Nature-based solutions for resilient landscapes and cities. *Environ Res, 165*, 431-441. https://doi.org/10.1016/j.envres.2017.11.038

Lee, J. Y., Chia, R. W., Veerasingam, S., Uddin, S., Jeon, W. H., Moon, H. S., Cha, J., & Lee, J. (2024, Oct 10). A comprehensive review of urban microplastic pollution sources, environment and human health impacts, and regulatory efforts. *Sci Total Environ, 946*, 174297. https://doi.org/10.1016/j.scitotenv.2024.174297

Li, Y., Shao, L., Wang, W., Zhang, M., Feng, X., Li, W., & Zhang, D. (2020, Feb 25). Airborne fiber particles: Types, size and concentration observed in Beijing. *Sci Total Environ, 705*, 135967. https://doi.org/10.1016/j.scitotenv.2019.135967

Liao, Z., Ji, X., Ma, Y., Lv, B., Huang, W., Zhu, X., Fang, M., Wang, Q., Wang, X., Dahlgren, R., & Shang, X. (2021, Sep 5). Airborne microplastics in indoor and outdoor environments of a coastal city in Eastern China. *J Hazard Mater, 417*, 126007. https://doi.org/10.1016/j.jhazmat.2021.126007

Lindén, J., Gustafsson, M., Uddling, J., Watne, Å., & Pleijel, H. (2023). Air pollution removal through deposition on urban vegetation: The importance of vegetation characteristics.

Urban   Forestry   &   Urban   Greening,   81.
https://doi.org/10.1016/j.ufug.2023.127843

Liu, B., Ma, X., Ma, Y., Li, H., Jin, S., Fan, R., & Gong, W. (2022). The relationship between atmospheric boundary layer and temperature inversion layer and their aerosol capture capabilities. *Atmospheric   Research,   271*. https://doi.org/10.1016/j.atmosres.2022.106121

Liu, X., Zhao, D., Niu, Z., Zhao, G., Ding, D., Chen, Y., & Liu, H. (2024). Aircraft observations of aerosol and BC during the East Asian dust storm event: Vertical profiles, size distribution and mixing   state.   *Atmospheric   Environment,   327*. https://doi.org/10.1016/j.atmosenv.2024.120492

Londahl, J., Moller, W., Pagels, J. H., Kreyling, W. G., Swietlicki, E., & Schmid, O. (2014, Aug). Measurement techniques for respiratory tract deposition of airborne nanoparticles: a critical review. *J Aerosol Med Pulm Drug Deliv, 27*(4), 229-254. https://doi.org/10.1089/jamp.2013.1044

Long, C. M., Nascarella, M. A., & Valberg, P. A. (2013, Oct). Carbon black vs. black carbon and other airborne materials containing elemental carbon: physical and chemical distinctions. *Environ Pollut,   181*,   271-286. https://doi.org/10.1016/j.envpol.2013.06.009

Luo, X., Wang, Z., Yang, L., Gao, T., & Zhang, Y. (2022, Jul 1). A review of analytical methods and models used in atmospheric microplastic research. *Sci Total Environ, 828*, 154487. https://doi.org/10.1016/j.scitotenv.2022.154487

Ly, A., & El-Sayegh, Z. (2023). Tire Wear and Pollutants: An Overview of Research. *Archives of Advanced Engineering Science,   1*(1),   2-10. https://doi.org/10.47852/bonviewAAES32021329

Madueno, L., Kecorius, S., Londahl, J., Muller, T., Pfeifer, S., Haudek, A., Mardonez, V., & Wiedensohler, A. (2019, May). A new method to measure real-world respiratory tract deposition of

inhaled ambient black carbon. *Environ Pollut, 248*, 295-303. https://doi.org/10.1016/j.envpol.2019.02.021

Maher, B. A., Ahmed, I. A., Davison, B., Karloukovski, V., & Clarke, R. (2013, Dec 3). Impact of roadside tree lines on indoor concentrations of traffic-derived particulate matter. *Environ Sci Technol, 47*(23), 13737-13744. https://doi.org/10.1021/es404363m

Manigrasso, M., Guerriero, E., & Avino, P. (2015). Ultrafine Particles in Residential Indoors and Doses Deposited in the Human Respiratory System. *Atmosphere, 6*(10), 1444-1461. https://doi.org/10.3390/atmos6101444

Matz, C. J., Stieb, D. M., Egyed, M., Brion, O., & Johnson, M. (2018). Evaluation of daily time spent in transportation and traffic-influenced microenvironments by urban Canadians. *Air Qual Atmos Health, 11*(2), 209-220. https://doi.org/10.1007/s11869-017-0532-6

McDonald, A. G., Bealey, W. J., Fowler, D., Dragosits, U., Skiba, U., Smith, R. I., Donovan, R. G., Brett, H. E., Hewitt, C. N., & Nemitz, E. (2007). Quantifying the effect of urban tree planting on concentrations and depositions of PM10 in two UK conurbations. *Atmospheric Environment, 41*(38), 8455-8467. https://doi.org/10.1016/j.atmosenv.2007.07.025

Miller, F. J., Asgharian, B., Schroeter, J. D., & Price, O. (2016). Improvements and additions to the Multiple Path Particle Dosimetry model. *Journal of Aerosol Science, 99*, 14-26. https://doi.org/10.1016/j.jaerosci.2016.01.018

Minderytė, A., Pauraite, J., Dudoitis, V., Plauškaitė, K., Kilikevičius, A., Matijošius, J., Rimkus, A., Kilikevičienė, K., Vainorius, D., & Byčenkienė, S. (2022). Carbonaceous aerosol source apportionment and assessment of transport-related pollution. *Atmospheric Environment, 279*. https://doi.org/10.1016/j.atmosenv.2022.119043

Mirabedini, S. M., Zareanshahraki, F., & Mannari, V. (2020). Enhancing thermoplastic road-marking paints performance using sustainable rosin ester. *Progress in Organic Coatings, 139*. https://doi.org/10.1016/j.porgcoat.2019.105454

Muresan, A. N., Sebastiani, A., Gaglio, M., Fano, E. A., & Manes, F. (2022). Assessment of air pollutants removal by green infrastructure and urban and peri-urban forests management for a greening plan in the Municipality of Ferrara (Po river plain, Italy). *Ecological Indicators, 135*. https://doi.org/10.1016/j.ecolind.2022.108554

Nawab, A., Ahmad, M., Khan, M. T., Nafees, M., Khan, I., & Ihsanullah, I. (2024). Human exposure to microplastics: A review on exposure routes and public health impacts. *Journal of Hazardous Materials Advances, 16*. https://doi.org/10.1016/j.hazadv.2024.100487

Nie, X., Yu, L., Mao, Q., & Zhang, X. (2025). Study on global atmospheric aerosol type identification from combined satellite and ground observations. *Atmospheric Environment, 347*. https://doi.org/10.1016/j.atmosenv.2025.121100

Niranjan, R., & Thakur, A. K. (2017). The Toxicological Mechanisms of Environmental Soot (Black Carbon) and Carbon Black: Focus on Oxidative Stress and Inflammatory Pathways. *Front Immunol, 8*, 763. https://doi.org/10.3389/fimmu.2017.00763

Oliveira, M., Slezakova, K., Delerue-Matos, C., Pereira, M. C., & Morais, S. (2019, Mar). Children environmental exposure to particulate matter and polycyclic aromatic hydrocarbons and biomonitoring in school environments: A review on indoor and outdoor exposure levels, major sources and health impacts. *Environ Int, 124*, 180-204. https://doi.org/10.1016/j.envint.2018.12.052

Oxley, T., ApSimon, H. M., & de Nazelle, A. (2015). Investigating the sensitivity of health benefits to focussed PM2.5 emission

abatement strategies. *Environmental Modelling & Software, 74*, 268-283. https://doi.org/10.1016/j.envsoft.2015.07.011

Ozdemir, H. (2019, Apr 1). Mitigation impact of roadside trees on fine particle pollution. *Sci Total Environ, 659*, 1176-1185. https://doi.org/10.1016/j.scitotenv.2018.12.262

Ozen, H. A., & Mutuk, T. (2025, Feb 15). The influence of road vehicle tyre wear on microplastics in a high-traffic university for sustainable transportation. *Environ Pollut, 367*, 125536. https://doi.org/10.1016/j.envpol.2024.125536

Palle, S. N. R., Tandule, C. R., Kalluri, R. O. R., Gugamsetty, B., Kotalo, R. G., Thotli, L. R., Akkiraju, B., & Lingala, S. S. R. (2021). The Impact of Lockdown on eBC Mass Concentration over a Semi-arid Region in Southern India: Ground Observation and Model Simulations. *Aerosol and Air Quality Research, 21*(11). https://doi.org/10.4209/aaqr.210101

Pauraite, J., Mainelis, G., Kecorius, S., Minderytė, A., Dudoitis, V., Garbarienė, I., Plauškaitė, K., Ovadnevaite, J., & Byčenkienė, S. (2021). Office Indoor PM and BC Level in Lithuania: The Role of a Long-Range Smoke Transport Event. *Atmosphere, 12*(8). https://doi.org/10.3390/atmos12081047

Pichelstorfer, L., Winkler-Heil, R., & Hofmann, W. (2013). Lagrangian/Eulerian model of coagulation and deposition of inhaled particles in the human lung. *Journal of Aerosol Science, 64*, 125-142. https://doi.org/10.1016/j.jaerosci.2013.05.007

Pruss-Ustun, A., Wolf, J., Corvalan, C., Neville, T., Bos, R., & Neira, M. (2017, Sep 1). Diseases due to unhealthy environments: an updated estimate of the global burden of disease attributable to environmental determinants of health. *J Public Health (Oxf), 39*(3), 464-475. https://doi.org/10.1093/pubmed/fdw085

Radney, J. G., You, R., Ma, X., Conny, J. M., Zachariah, M. R., Hodges, J. T., & Zangmeister, C. D. (2014, Mar 18). Dependence of soot optical properties on particle morphology:

measurements and model comparisons. *Environ Sci Technol,*
48(6), 3169-3176. https://doi.org/10.1021/es4041804

Rawat, N., & Kumar, P. (2023, Feb 1). Interventions for improving
indoor and outdoor air quality in and around schools. *Sci Total*
Environ, *858*(Pt 2), 159813.
https://doi.org/10.1016/j.scitotenv.2022.159813

Redondo-Bermudez, M. D. C., Gulenc, I. T., Cameron, R. W., &
Inkson, B. J. (2021, Nov 1). 'Green barriers' for air pollutant
capture: Leaf micromorphology as a mechanism to explain
plants capacity to capture particulate matter. *Environ Pollut,*
288, 117809. https://doi.org/10.1016/j.envpol.2021.117809

Riemer, N., West, M., Zaveri, R., & Easter, R. (2010). Estimating
black carbon aging time-scales with a particle-resolved aerosol
model. *Journal of Aerosol Science, 41*(1), 143-158.
https://doi.org/10.1016/j.jaerosci.2009.08.009

Rodrigues, M. O., Goncalves, A. M. M., Goncalves, F. J. M., &
Abrantes, N. (2020). Improving cost-efficiency for MPs
density separation by zinc chloride reuse. *MethodsX, 7*,
100785. https://doi.org/10.1016/j.mex.2020.100785

Sadrizadeh, S., Yao, R., Yuan, F., Awbi, H., Bahnfleth, W., Bi, Y.,
Cao, G., Croitoru, C., de Dear, R., Haghighat, F., Kumar, P.,
Malayeri, M., Nasiri, F., Ruud, M., Sadeghian, P., Wargocki,
P., Xiong, J., Yu, W., & Li, B. (2022). Indoor air quality and
health in schools: A critical review for developing the roadmap
for the future school environment. *Journal of Building*
Engineering, 57. https://doi.org/10.1016/j.jobe.2022.104908

Salma, I., Füri, P., Németh, Z., Balásházy, I., Hofmann, W., & Farkas,
Á. (2015). Lung burden and deposition distribution of inhaled
atmospheric urban ultrafine particles as the first step in their
health risk assessment. *Atmospheric Environment, 104*, 39-49.
https://doi.org/10.1016/j.atmosenv.2014.12.060

Sandradewi, J., Prévôt, A. S. H., Weingartner, E., Schmidhauser, R., Gysel, M., & Baltensperger, U. (2008). A study of wood burning and traffic aerosols in an Alpine valley using a multi-wavelength Aethalometer. *Atmospheric Environment, 42*(1), 101-112. https://doi.org/10.1016/j.atmosenv.2007.09.034

Sang, W., Chen, Z., Mei, L., Hao, S., Zhan, C., Zhang, W. B., Li, M., & Liu, J. (2021, Feb 10). The abundance and characteristics of microplastics in rainwater pipelines in Wuhan, China. *Sci Total Environ, 755*(Pt 2), 142606. https://doi.org/10.1016/j.scitotenv.2020.142606

Sangkham, S., Faikhaw, O., Munkong, N., Sakunkoo, P., Arunlertaree, C., Chavali, M., Mousazadeh, M., & Tiwari, A. (2022, Aug). A review on microplastics and nanoplastics in the environment: Their occurrence, exposure routes, toxic studies, and potential effects on human health. *Mar Pollut Bull, 181*, 113832. https://doi.org/10.1016/j.marpolbul.2022.113832

Schmidtmann, J., Weishaupl, H. K., Hopp, L., Meides, N., & Peiffer, S. (2025, Mar 7). UV-weathering affects heteroaggregation and subsequent sedimentation of polystyrene microplastic particles with ferrihydrite. *Environ Sci Process Impacts*. https://doi.org/10.1039/d4em00666f

Schraufnagel, D. E. (2020, Mar). The health effects of ultrafine particles. *Exp Mol Med, 52*(3), 311-317. https://doi.org/10.1038/s12276-020-0403-3

Sebastiani, A., Buonocore, E., Franzese, P. P., Riccio, A., Chianese, E., Nardella, L., & Manes, F. (2021). Modeling air quality regulation by green infrastructure in a Mediterranean coastal urban area: The removal of PM10 in the Metropolitan City of Naples (Italy). *Ecological Modelling, 440*. https://doi.org/10.1016/j.ecolmodel.2020.109383

Selmi, W., Weber, C., Rivière, E., Blond, N., Mehdi, L., & Nowak, D. (2016). Air pollution removal by trees in public green spaces

in Strasbourg city, France. *Urban Forestry & Urban Greening, 17*, 192-201. https://doi.org/10.1016/j.ufug.2016.04.010

Shaddick, G., Thomas, M. L., Mudu, P., Ruggeri, G., & Gumy, S. (2020). Half the world's population is exposed to increasing air pollution. *npj Climate and Atmospheric Science, 3*(1). https://doi.org/10.1038/s41612-020-0124-2

Sharma, R., Kurmi, O. P., Hariprasad, P., & Tyagi, S. K. (2024). Health implications due to exposure to fine and ultra-fine particulate matters: a short review. *International Journal of Ambient Energy, 45*(1). https://doi.org/10.1080/01430750.2024.2314256

Sommer, F., Dietze, V., Baum, A., Sauer, J., Gilge, S., Maschowski, C., & Gieré, R. (2018). Tire Abrasion as a Major Source of Microplastics in the Environment. *Aerosol and Air Quality Research, 18*(8), 2014-2028. https://doi.org/10.4209/aaqr.2018.03.0099

Sridharan, S., Kumar, M., Singh, L., Bolan, N. S., & Saha, M. (2021, Sep 15). Microplastics as an emerging source of particulate air pollution: A critical review. *J Hazard Mater, 418*, 126245. https://doi.org/10.1016/j.jhazmat.2021.126245

Sturm, R. (2012). Modeling the deposition of bioaerosols with variable size and shape in the human respiratory tract – A review. *Journal of Advanced Research, 3*(4), 295-304. https://doi.org/10.1016/j.jare.2011.08.003

Su, T., Li, Z., & Kahn, R. (2018). Relationships between the planetary boundary layer height and surface pollutants derived from lidar observations over China: regional pattern and influencing factors. *Atmospheric Chemistry and Physics, 18*(21), 15921-15935. https://doi.org/10.5194/acp-18-15921-2018

Tanaka, K., & Takada, H. (2016, Sep 30). Microplastic fragments and microbeads in digestive tracts of planktivorous fish from urban coastal waters. *Sci Rep, 6*, 34351. https://doi.org/10.1038/srep34351

Toledano, C., Cachorro, V. E., de Frutos, A. M., Torres, B., Berjón, A., Sorribas, M., & Stone, R. S. (2009). Airmass Classification and Analysis of Aerosol Types at El Arenosillo (Spain). *Journal of Applied Meteorology and Climatology, 48*(5), 962-981. https://doi.org/10.1175/2008jamc2006.1

Torres-Agullo, A., Karanasiou, A., Moreno, T., & Lacorte, S. (2021, Dec 15). Overview on the occurrence of microplastics in air and implications from the use of face masks during the COVID-19 pandemic. *Sci Total Environ, 800*, 149555. https://doi.org/10.1016/j.scitotenv.2021.149555

Wagner, S., Huffer, T., Klockner, P., Wehrhahn, M., Hofmann, T., & Reemtsma, T. (2018, Aug 1). Tire wear particles in the aquatic environment - A review on generation, analysis, occurrence, fate and effects. *Water Res, 139*, 83-100. https://doi.org/10.1016/j.watres.2018.03.051

Wang, D., Li, Z., Wang, Y., Wei, T., Hou, Y., Zhao, X., & Ding, Y. (2024, Apr 1). Exploring particle concentrations and inside-to-outside ratios in vehicles: A real-time road test study. *Sci Total Environ, 919*, 170783. https://doi.org/10.1016/j.scitotenv.2024.170783

Wang, X., Heald, C. L., Sedlacek, A. J., de Sá, S. S., Martin, S. T., Alexander, M. L., Watson, T. B., Aiken, A. C., Springston, S. R., & Artaxo, P. (2016). Deriving brown carbon from multiwavelength absorption measurements: method and application to AERONET and Aethalometer observations. *Atmospheric Chemistry and Physics, 16*(19), 12733-12752. https://doi.org/10.5194/acp-16-12733-2016

Watson, A. Y., & Valberg, P. A. (2001, Mar-Apr). Carbon black and soot: two different substances. *AIHAJ, 62*(2), 218-228. https://doi.org/10.1080/15298660108984625

Weingartner, E., Saathoff, H., Schnaiter, M., Streit, N., Bitnar, B., & Baltensperger, U. (2003). Absorption of light by soot particles: determination of the absorption coefficient by means of aethalometers. *Journal of Aerosol Science, 34*(10), 1445-1463. https://doi.org/10.1016/s0021-8502(03)00359-8

Winiarska, E., Jutel, M., & Zemelka-Wiacek, M. (2024, Jun 15). The potential impact of nano- and microplastics on human health: Understanding human health risks. *Environ Res, 251*(Pt 2), 118535. https://doi.org/10.1016/j.envres.2024.118535

Wong, Y. K., Liu, K. M., Yeung, C., Leung, K. K. M., & Yu, J. Z. (2022). Measurement report: Characterization and source apportionment of coarse particulate matter in Hong Kong: insights into the constituents of unidentified mass and source origins in a coastal city in southern China. *Atmospheric Chemistry and Physics, 22*(7), 5017-5031. https://doi.org/10.5194/acp-22-5017-2022

Xie, Y., Li, Y., Feng, Y., Cheng, W., & Wang, Y. (2022, Apr). Inhalable microplastics prevails in air: Exploring the size detection limit. *Environ Int, 162*, 107151. https://doi.org/10.1016/j.envint.2022.107151

Yang, C., Niu, S., Xia, Y., & Wu, J. (2023). Microplastics in urban road dust: Sampling, analysis, characterization, pollution level, and influencing factors. *TrAC Trends in Analytical Chemistry, 168*. https://doi.org/10.1016/j.trac.2023.117348

Yli-Juuti, T., Nieminen, T., Hirsikko, A., Aalto, P. P., Asmi, E., Hõrrak, U., Manninen, H. E., Patokoski, J., Dal Maso, M., Petäjä, T., Rinne, J., Kulmala, M., & Riipinen, I. (2011). Growth rates of nucleation mode particles in Hyytiälä during 2003−2009: variation with particle size, season, data analysis method and ambient conditions. *Atmospheric Chemistry and Physics, 11*(24), 12865-12886. https://doi.org/10.5194/acp-11-12865-2011

Zauli-Sajani, S., Thunis, P., Pisoni, E., Bessagnet, B., Monforti-Ferrario, F., De Meij, A., Pekar, F., & Vignati, E. (2024, May 3). Reducing biomass burning is key to decrease PM(2.5) exposure in European cities. *Sci Rep, 14*(1), 10210. https://doi.org/10.1038/s41598-024-60946-2

Zhang, L., Ou, C., Magana-Arachchi, D., Vithanage, M., Vanka, K. S., Palanisami, T., Masakorala, K., Wijesekara, H., Yan, Y., Bolan, N., & Kirkham, M. B. (2021, Oct 21). Indoor Particulate Matter in Urban Households: Sources, Pathways, Characteristics, Health Effects, and Exposure Mitigation. *Int J Environ Res Public Health, 18*(21). https://doi.org/10.3390/ijerph182111055

Zotter, P., Herich, H., Gysel, M., El-Haddad, I., Zhang, Y., Močnik, G., Hüglin, C., Baltensperger, U., Szidat, S., & Prévôt, A. S. H. (2017). Evaluation of the absorption Ångström exponents for traffic and wood burning in the Aethalometer-based source apportionment using radiocarbon measurements of ambient aerosol. *Atmospheric Chemistry and Physics, 17*(6), 4229-4249. https://doi.org/10.5194/acp-17-4229-2017

CURRICULUM VITAE

Abdullah Khan

Peshawar, Pakistan

<u>*Education:*</u>

Department of Environmental Sciences,	*2013-2017*
University of Peshawar, Pakistan	

<u>*Bachelor of Science in Environmental Sciences*</u>

Sustainable Development Study Center,	*2018-2021*
Government College University Lahore, Pakistan	

<u>*Master of Science in Environmental Sciences*</u>

Department of Environmental Research	*2021-2025*
Center for Physical Sciences and Technology (FTMC), Lithuania	

<u>*PhD studies*</u>

<u>*Professional career:*</u>

Department of Environmental Research	*2023-2025*
Center for Physical Sciences and Technology (FTMC), Lithuania	

<u>*Junior researcher*</u>

ACKNOWLEDGEMENTS

been the emotional bedrock of this entire process. In moments of doubt and exhaustion, your support reminded me of my strength and purpose.

The more I understand, the less I know; the more I know, the less I understand.
In chasing the universe, I find no answers—only deeper questions wrapped in wonder.
Knowledge builds the path, but it is humility that lights the way.

(Abdullah Khan)

FOR NOTES

FOR NOTES